NBSIR 84-2940

Phase Equilibria of Stored Chemical Energy Reactants

L. P. Cook
E. R. Plante
R. S. Roth
J. W. Hastie

U.S. DEPARTMENT OF COMMERCE
National Bureau of Standards
Center for Materials Science
Gaithersburg, MD 20899

September 1984

Prepared for
Department of the Navy
Office of Naval Research
Arlington, VA 22217

NBSIR 84-2940

PHASE EQUILIBRIA OF STORED CHEMICAL ENERGY REACTANTS

L. P. Cook
E. R. Plante
R. S. Roth
J. W. Hastie

U.S. DEPARTMENT OF COMMERCE
National Bureau of Standards
Center for Materials Science
Gaithersburg, MD 20899

September 1984

Prepared for
Department of the Navy
Office of Naval Research
Arlington, VA 22217

U.S. DEPARTMENT OF COMMERCE, Malcolm Baldrige, *Secretary*
NATIONAL BUREAU OF STANDARDS, Ernest Ambler, *Director*

Phase Equilibria of Stored Chemical Energy Reactants

Annual Report

For the Period May 25, 1983 - May 25, 1984

L. P. Cook, E. R. Plante, R. S. Roth and J. W. Hastie

Inorganic Materials Division
Center for Materials Science
National Bureau of Standards
Gaithersburg, Md 20899

July 25, 1984

Prepared for the Department of the Navy
Office of Naval Research
Arlington, VA 22217

Under Contract No. N00014-83-F-0117

Phase Equilibria of Stored Chemical Energy Reactants

Table of Contents

Abstract..... 1

I. Background and Review of Li-Al-O-H System..... 2
A. Objective of Study..... 2
B. Phases Reported in Li-Al-O-H System..... 3
C. Thermodynamic Analysis..... 4

II. Sample Preparation and Materials Handling of Li_2O/Al_2O_3 Mixtures... 6

III. DTA Experiments in the System Li_2O-$LiAlO_2$..... 7
A. Experimental Method..... 7
B. Results..... 8
C. Interpretation..... 9

IV. Quench Experiments and Crystallographic Studies in the Li_2O-Al_2O_3 System..... 10
A. Previous Studies..... 10
B. The High-Alumina Portion of the System..... 12
C. Neutron Diffraction Study of $LiAl_5O_8$..... 13
D. The High-Lithia Portion of the System..... 14

V. Mass Spectrometric Vapor Pressure Measurements in the System Li_2O-Al_2O_3..... 15
A. Literature Survey..... 15
B. Mass Spectrometric Method..... 17
C. Thermodynamic Treatment..... 18
D. Vaporization of $LiAlO_2$-$LiAl_5O_8$..... 21
E. Li and O_2 Pressure Data..... 24
F. Vaporization of $LiAl_5O_8$-Al_2O_3..... 24
G. Discussion..... 26

VI. Solution and Phase Equilibria Models for the Li_2O-Al_2O_3 System.... 29
A. Basis of the Model..... 29
B. Thermodynamic Data Base 31
C. Results..... 32

VII. Needs for Future Research in the Li-Al-O-H System..... 33

VIII. References Cited..... 35

IX. Appendix 1. Modeling of Viscosities in Multiphase Mixtures..... 38

X. Appendix 2. Literature Search on the System Li-Al-O-H..... 40

XI. Tables..... 60

XII. Figures..... 78

XIII. Distribution.....104

Abstract

The reaction of lithium aluminum alloy with water at high temperature is considered in terms of phase equilibria in the system Li-Al-O-H. A thermodynamic analysis of the system reveals the potential importance of lithium hydride as a reaction product. Major needs for experimental phase equilibria data are outlined, and a determination of the Li_2O-Al_2O_3 phase diagram is given top priority.

Experimental methods for preparation and handling of atmospherically sensitive Li_2O/Al_2O_3 mixtures are given. DTA investigation of the system Li_2O-$LiAlO_2$ has yielded information on equilibrium melting behavior, and the lower limit of melting in the system appears to be 1055° ± 10 °C, with the eutectic located near $(Li_2O)_{75}$ $(Al_2O_3)_{25}$ (mole %).

Quenching experiments with x-ray crystallographic analysis for the high lithia portion of the system have been inconclusive, possibly due to non-quenchable, rapidly reversible solid-state phase transitions. DTA data suggest appreciable solid solution of alumina in Li_2O, yet there is no direct evidence of this from the x-ray powder diffraction patterns. Also the α/β transition in Li_5AlO_4 has been particularly difficult to locate consistently.

On the high alumina end of the system Li_2O-Al_2O_3, experiments in sealed Mo capsules have shown that the eutectic temperature is near 1630 °C, that $LiAlO_2$ melts congruently near 1750 °C, and that $LiAl_5O_8$ melts incongruently near 1750 °C. Neutron diffraction analysis of $LiAl_5O_8$, cooled rapidly from 1600 °C, shows a 1:3 ordering of Li:Al in the octahedral sites, with extra peaks of undetermined origin.

Mass Spectrometrically determined vapor pressure data are reported for mixtures of $LiAlO_2$-$LiAl_5O_8$ and $LiAl_5O_8$-Al_2O_3. The results are in reasonable agreement with literature values, but indicate the need for more information on solid solution limits. Heats of reaction for the vaporization processes are reported. A preliminary thermodynamic model for prediction of solid-liquid-vapor equilibria has been developed and tested by comparison with the experimental data.

Needs for future research in the systems Li_2O-Al_2O_3 and Li-Al-Li_2O-Al_2O_3 are outlined. The utility of such research in understanding the combustion of mixtures in the Li-Al-O-H system is emphasized. Two Appendices describe the modeling of viscosities in multiphase mixtures, and the results of a computerized literature search on the system Li-Al-O-H.

I. Background and Review of Li-Al-O-H System (L.P Cook)

A. Objective of Study

Among the stored chemical energy propulsion systems currently under consideration those using lithium as a reactant, or lithium alloyed with other light metals such as aluminum, appear to offer the most promise in terms of energy release per unit mass (1). One such system under development is actually a two stage process (2):

$$2Li(\ell) + H_2O(g) \longrightarrow Li_2O(c) + H_2(g) \qquad [1]$$

$$H_2(g) + 1/2\ O_2(g) \longrightarrow H_2O(g). \qquad [2]$$

Both reactions release substantial heat. A variant of this scheme uses a lithium aluminum alloy as the reactant and, in place of reaction [1], the reaction is:

$$LiAl(\ell) + 2H_2O(g) \longrightarrow LiAlO_2(c) + 2H_2(g). \qquad [3]$$

This reaction produces a higher enthalpy yield owing to the high stability of $LiAlO_2(c)$.

During the testing of prototype combustors based on these reactions, it has become apparent that a detailed knowledge of the chemistry for all phases is needed for optimum design and operation. Factors which must be accommodated include heat flow associated with phase separation and the build up of solid products, and the transport of volatile species between regions in the combustor. The aim of this project is to provide fundamental chemical data pertaining to the oxidation of lithium aluminum alloy by water.

B. Phases Reported in Li-Al-O-H System

The phase equilibrium chemistry of reaction [3] is potentially complex. However, as written the phases in this reaction contain three components, LiAl, H and O, and can be plotted on a triangular diagram, as in figure 1-a. A somewhat more convenient representation is figure 1-b, which is actually a truncated, distorted version of figure 1-a, with oxygen plotting at infinity in the compositional plane. The possible production of other phases is apparent in figure 2 where the reaction plane has been plotted in the quaternary reciprocal system Li-Al-H-Li_2O-Al_2O_3-H_2O. Table 1

lists phases reported in this system. Of these phases only the ones having stability at temperatures near combustor operation (e.g., ~ 1100 K) have been plotted in figure 2. The lithium aluminum hydrides, for example, apparently dissociate at relatively low temperatures.

Figure 2 may be visualized as a triangular prism in which the edges are binary systems and the sides are ternaries. Phase diagrams have been published for the Li-LiH portion of the Li-H binary (3) and for the Li-Al, and Al-Al_2O_3 binaries (4,5). The solubility of oxygen in lithium metal has been determined as a function of temperature (6). A calculated diagram (7) provides an estimate of phase relations in the Li_2O-Al_2O_3 binary. Phase relations at low temperatures have been partially studied for the ternary system Li_2O-Al_2O_3-H_2O (8). This leaves the four ternary sides of the system in figure 2, as well as the interior quaternary relations, which are largely unstudied. However, as Table 1 indicates, thermochemical data are available for many of the phases in figure 2.

C. Thermodynamic Analysis

Thermochemical data from the literature have been used to calculate the reactions in Table 2, which have in turn been used to derive the schematic phase relations shown in figure 3. The phases Li_5AlO_4 and $LiAl_5O_8$ have not been included in the calculations due to incomplete data. The compositional extent of melt phases based on LiH and LiOH is unknown. The possibility of ternary melts in the system Li_2O-Al_2O_3-H_2O may be real at pressures approaching 100 atm. Given those limitations, the results in

figure 3 provide only an estimate of the major features of phase compatibility in the system. Information in figure 3 has been combined with the single quaternary reaction in Table 2 to produce figure 4.

From figure 4 it can be seen that the reaction plane in figure 1 is not ternary due to the presence of LiH and Al-rich alloy. Figure 5 indicates the products which would result from reaction of LiAl alloy with H_2O, according to relations in figure 4. Instead of occurring as reaction [3], the actual combustion reaction may occur in two stages:

$$5LiAl(\ell) + 2H_2O(g) \longrightarrow 4LiH(\ell) + 4Al(\ell) + LiAlO_2(c) \quad [4a]$$

$$LiH(\ell) + Al(\ell) + 2H_2O(g) \longrightarrow LiAlO_2(c) + 5/2\ H_2(g) \quad [4b]$$

Many of the substances involved would not be at unit activity; in particular, the molten aluminum would contain some lithium.

In order to make quantitative predictions of the course of reaction in combustors, experimental data must be taken on the thermal stability and compositional extent of liquids, and on the distribution of tie lines in figures 3 to 5. The compound $LiAlO_2$ is central to reactions [3], [4a] and [4b], and so a systematic investigation of the system Li_2O-Al_2O_3 has received top priority. Detailed knowledge of melting relations may, in conjunction with partitioning data for Li-Al-Li_2O-Al_2O_3, reveal possibilities for manipulation of combustion reactions to produce molten products, if desired.

Our experimental approach to the system Li_2O-Al_2O_3 utilizes a combination of methods. We supplement classical quenching methods and powder x-ray diffraction analysis with DTA and with Knudsen cell effusion mass spectrometry. The latter method gives data on enthalpy of vaporization which can be related to the phase equilibrium data via solution models. Figure 6 indicates the phase diagram regions covered by the various experimental and theoretical techniques.

II. Sample Preparation and Materials Handling of Li_2O/Al_2O_3 mixtures

(L. P. Cook)

Depending upon whether compositions were in the Li_2O-$LiAlO_2$ or the $LiAlO_2$-Al_2O_3 portion of the system, the sources of lithia were Li_2O_2 and Li_2CO_3, respectively. The reagent grade carbonate, dried at 160 °C under vacuum and weighed in a dry box, could be used to prepare all compositions in the alumina rich end of the system by mixing with 0.3 μm alpha alumina (Linde A)[1] under acetone, drying, and calcining in a covered Pt crucible at approximately 1000 °C. However, for compositions containing more than 50 mole % Li_2O, decarbonation was incomplete, even under high vacuum. Attempts to use $LiNO_3$ were also unsuccessful, and so a method for synthesizing high purity Li_2O starting material was sought, as lithia proved to be unavailable commercially. Oxidation of powdered lithium metal at 400 °C was attempted, but this was also unsuccessful, apparently due to

---

[1]Certain commercial equipment, instruments, or materials are identified in this paper in order to adequately specify the experimental procedure. Such identification does not imply recommendation or endorsement by the National Bureau of Standards, nor does it imply that the materials or equipment identified are necessarily the best available for the purpose.

a kinetic problem. The procedure outlined in (9) was successfully employed to produce Li_2O_2, which was subsequently decomposed under vacuum at 800 °C. This yielded a highly pure Li_2O, as judged from the x-ray powder pattern and the negligible weight loss under high vacuum up to its melting point, which agreed well with that reported by (9) as 1438 ± 15 °C. Lithia prepared in this way was weighed out with $LiAlO_2$; mixtures of about 1 g were homogenized dry using a mortar and pestle in a dry box.

Nearly all manipulations involving these materials were completed in a dry box under an atmosphere of dry N_2 or Ar purged with a recirculating purifier capable of reducing H_2O and O_2 to less than 1 ppm. This includes weighing of mixtures, loading capsules and cells for quench runs and for DTA or Knudsen effusion experiments, opening sealed quench run capsules, and preparing x-ray slides. X-ray work was completed in a special cell which allowed continuous purging by a stream of dry nitrogen.

III. DTA Experiments in the System Li_2O-$LiAlO_2$ (L. P. Cook)

A. Experimental Method

A Mettler[1] thermoanalyzer was employed for DTA work--this allowed simultaneous monitoring of weight change to better than 0.01 mg during all phases of an experiment. The sample arrangement is illustrated in figure 6. Platinum cells with tight fitting lids were used for unknowns as well as for the alumina reference material (NBS SRM No. 742). Cells were cleaned by boiling in HCl solution and then distilled water prior to insertion of each new composition. Cells were weighed in a dry box on a

precision microbalance before and after addition of 70 to 100 mg of powdered sample, and after fitting of the lid. Loaded cells were then transferred to the thermoanalyzer in a sealed container, quickly inserted and pumped to 10^{-5} torr. Following this process, the system was backfilled with gettered argon, and during the DTA experiments argon was flowed through the system at 5 cc/min. This procedure served to minimize the presence of water vapor.

B. Results

Results of DTA experiments are given in Table 3. These experiments were carried out at a heating rate of 10 °C/min, and in most cases samples were repeatedly cycled through a range of several hundred degrees to observe the reproducibility of the thermal effects. The approximate magnitudes of thermal affects are indicated in Table 3 by noting the amplitude of the differential signal where the events were relatively well defined.

Several choices exist as to the manner in which the temperatures of DTA effects are defined. Selection of the best method depends to a certain extent upon the experimental geometry. For the apparatus employed here, it was found that best results were obtained by defining the temperature of the event as shown in figure 7, using the heating part of the cycle. Using this method, calibration runs were within the experimental error of the accepted values for the melting point of NaCl (800.5 °C). Many of the temperature values in Table 3 have uncertainties associated with them; these are derived from statistical analysis of data gathered during thermal

cycling. Additionally, runs were completed on replicate samples of 60/40, 65/35, 70/30, 75/25 and 80/20 mol % Li_2O/Al_2O_3 to confirm the reality of the thermal effects observed.

C. Interpretation

Results of DTA experiments are also plotted in figure 8. The non-reversible exothermic effects occurring between 450 and 550 °C are thought to correspond to reaction of Li_2O and $LiAlO_2$ to form Li_5AlO_4. The fact that this is observed for all compositions except 55/45 may indicate solid solution of Li_2O in $LiAlO_2$. The irreversible endothermic effect between 775 and 825 °C occurs over a large range of compositions and is probably related to a polymorphic inversion in Li_5AlO_4 (10,11). A very weak, apparently reversible effect occurring near 750 °C and detected for the 80/20, 70/30 and 60/40 compositions, is possibly related to a polymorphic inversion in $LiAlO_2$ (12,13). The endothermic effect at about 1055 °C for compositions between Li_5AlO_4 and $LiAlO_2$ corresponds to the temperature of eutectic melting. Although a run was not made at the Li_5AlO_4 composition, the 80/20 run suggests incongruent melting (see Fig. 9). In general, liquidus temperatures have not been observed using DTA in this system. Therefore the higher temperature peak in figure 9 probably corresponds to the incongruent melting of Li_5AlO_4. However this temperature is not in perfect agreement with those on the Li_2O rich side of Li_5AlO_4, and further experimentation seems advisable.

Due to the tendency of Li_2O-rich melts to extensively wet platinum cells and flow out around the covers, the high temperature portion of the run for the 95/05 composition had to be terminated after one cycle, and no

information on reversibility could be obtained. In this run no indication of the incongruent melting of Li_5AlO_4 was observed. This composition shows a rather gradual melting event suggestive of the melting of a solid solution in close proximity to 95/05 (see Fig. 10). Existence of such a solid solution could explain why the melting of Li_5AlO_4 was not observed. Further interpretation of these and other DTA results must await accummulation and interpretation of detailed x-ray powder diffraction data.

IV. Quench Experiments and Crystallographic Studies in the Li_2O-Al_2O_3 System (R. Roth, M. Zocchi[2] and L. Cook)

This system can be naturally divided into two parts, $LiAlO_2$-Al_2O_3 and Li_2O-$LiAlO_2$. The high Al_2O_3 portion is a refractory system with melting points above 1600°C and with few problems related to hydration by atmospheric moisture. On the other hand, the high Li_2O portion melts beginning near 1050 °C, and the sample must be protected from atmospheric moisture and carbon dioxide at all times.

A. Previous Studies

Hummel et al., (14) reported synthesis studies on the system $LiAlO_2$-Al_2O_3 and noted only the compound $LiAl_5O_8$ occurring between $LiAlO_2$ and Al_2O_3. A partial phase diagram for the system $LiAlO_2$-Al_2O_3 was reported in 1961 by Strickler and Roy (15), in which the melting point of $LiAlO_2$ was indicated as 1700 °C and that of $LiAl_5O_8$ tentatively as 1950 °C.

---

[2]Guest Worker, NBS Reactor Division.

A eutectic between these compounds was tentatively indicated at 1670 °C. More recently the JANAF Tables (16) have adopted the melting point of Strickler and Roy (15) for $LiAlO_2$ after reviewing melting point determinations up to about the year 1979. The compound $LiAlO_2$ crystallizes in at least two forms at one atmosphere, a high temperature tetragonal γ form (12) stable above about 600 °C, and a hexagonal form which may be stable at lower temperatures (13). Additionally Chang and Margrave (17) report a third β form of $LiAlO_2$ at high pressure, with all the aluminium in tetrahedral coordination. Subsequently, Fischer (18) has reported the synthesis of β $LiAlO_2$ at atmospheric pressure. The compound $LiAl_5O_8$ was investigated by Collongues (19), Lejus and Collongues (20) and Datta and Roy (21). The latter authors postulated a first order phase transition at 1295 °C, and there has been some controversy regarding this matter (22,23). Lejus and Collongues (20) postulate substantial high temperature solid solution in $LiAl_5O_8$.

On the high lithia side, La Ginestra et al., (24) reported the existence of both Li_5AlO_4 and Li_3AlO_3, although published powder patterns exist only for the former, which has two polymorphs, both studied by Stewner and Hoppe (10, 11). Guggi et al., (25) report a melting point of 1320 °C for Li_5AlO_4. Byker, et al., (7), who carried out a thermodynamic analysis of the system, and estimated a preliminary phase diagram, conclude that Li_3AlO_3 may have no thermodynamic stability in the system.

B. The High-Alumina Portion of the System

Only one intermediate phase has been found in the subsystem $LiAlO_2$-Al_2O_3, at the composition $Li_2O{\cdot}5Al_2O_3$ ($LiAl_5O_8$). It has a spinel-like x-ray diffraction pattern. Specimens of four compositions were prepared with Li_2O:Al_2O_3 ratios of 1:1, 1:2, 1:4.78 and 1:5. These specimens were prepared by mixing Li_2O with either α-Al_2O_3 or γ-Al_2O_3 and firing at about 700 °C in air for 24 hours. All further heat treatments were made by preparing specimens from these calcines in a dry box and firing in air at various temperatures. The specimens were then transferred to the dry box via a dessicator and prepared for x-ray diffraction under flowing N_2. Results are summarized in Table 4.

Heat treatments above 1600 °C were performed by sealing a small portion of the specimen in a Mo tube in a He atmosphere. These tubes were then heated in the high temperature furnace in $95N_2$:$5H_2$. This furnace employs a W resistance heater and a W-Re thermocouple, calibrated by embedding a small Pt wire in Al_2O_3 in a sealed Mo tube. The specimens were heated at various temperatures near the melting point of Pt (1769 °C) and the thermocouple was found to need no appreciable correction. Although it was not possible to quench specimens from the tungsten furnace, specimens could be cooled to less than 1000 °C in several seconds by turning off the furnace power. Following this the Mo capsules were opened and characterized optically and by x-ray diffraction in a dry atmosphere. The melting point determinations were made by visual observation of the specimen after removal from the Mo tube. Results are summarized in Table 5 and figure 11. The compound $LiAlO_2$ probably melts congruently at about 1750 °C ± 25 °C. The compound $LiAl_5O_8$ also melts at approximately the same temperature but

probably incongruently. Specimens at the 1:2 ratio were observed to melt at considerably lower temperatures than the single phase specimens and the eutectic temperature is about 1630 °C ± 20 °C. We have not yet established whether there is a measurable amount of solid solution in either of these phases. The elements are low in atomic number and x-ray diffraction does not allow identification of a small amount of second phase.

C. Neutron Diffraction Study of $LiAl_5O_8$

Neutron diffraction provides a method for determination of structure in compounds comprised of light elements not having appreciable x-ray scattering power. Analysis of neutron diffraction data can yield detailed structural information without the necessity for single crystal growth and x-ray precession analysis. A large batch of $LiAl_5O_8$ was prepared for neutron diffraction analysis in order to test for Li:Al site order in the spinel structure. The specimen was quickly cooled from about 1600 °C and should represent the high temperature order/disorder state. The neutron diffraction pattern, unlike the corresponding x-ray pattern, showed many peaks which could not be attributed to the phases $LiAl_5O_8$ or Al_2O_3 (Fig. 12). The "spurious" peaks which can be indexed on the basis of a primitive unit cell with α = 8.09 A, were eliminated from the pattern and the structure of $LiAl_5O_8$ was refined by the Rietveld method (See Table 6 and Fig. 13). The results show that the structure is similar to $LiFe_5O_8$ and the structural formula can be written as $Al_8(Li_4Al_{12})O_{32}$ involving a 1:3 ordering of the cations in the octahedral sites. Space group is $P4_332$ or $P4_132$. There is no sign of Li^+ in tetrahedral sites.

D. The High-Lithia Portion of the System

Initially, the subsystem Li_2O-$LiAlO_2$ was investigated using Li_2CO_3 as a starting material. Specimens were contained in Au foil envelopes and inserted into 1 cm diam. Vycor glass tubes under Ar. Each tube was then evacuated and heated in a split, nicrome furnace with a maximum temperature capability of about 900 °C. After most of the CO_2 had evolved at this temperature with the system under roughing pump vacuum, an ion pump was used to complete final CO_2 evolution until the evacuated chamber reached at least 10^{-6} torr. The specimen was then quickly cooled to room temperature by shutting off the furnace. The specimen, evacuated tube and the valve maintaining the vacuum in the tube were taken to the Ar atmosphere dry-box. The specimen was then x-rayed under controlled atmosphere conditions. Results of the x-ray examination are shown in Table 7. Because of incomplete reaction this method was determined to be unsatisfactory for preparation of starting materials and Li_2O, prepared as outlined in Section II, was used for the remainder of the experiments.

Six compositions were prepared in the high Li_2O portion of the system by dry mixing of Li_2O and precalcined $LiAlO_2$. Small portions of these specimens were sealed in Pt tubes and quenched in air from various temperatures between 700° and 1050 °C. However, the results of these heat treatments are inconclusive (see Table 8). Compositions containing 95 and 90 percent Li_2O show only Li_2O and $LiAlO_2$ or melted material. Compositions between 85 and 55 percent Li_2O show inconclusive results for the phase transition between α and β Li_5AlO_4. Apparently this transition cannot be

reproducibly quenched from any given temperature although both phases were never found to exist in the same diffraction pattern. Further work is needed to characterize this transition.

V. Mass Spectrometric Vapor Pressure Measurements in the System Li_2O-Al_2O_3 (E. R. Plante)

This section deals with vapor pressure measurements made over several two-phase regions in the lithium aluminate system. Also, in the course of this work, a literature search of the previous vapor pressure data related to the lithia-alumina system was carried out.

A. Literature Survey

Vapor pressure measurements in the lithia-alumina system have been reported by Hildenbrand et al., (26) and summarized later by Potter et al., (27). These torsion effusion studies provided total vapor pressure data over the $LiAlO_2$-$LiAl_5O_8$ system (26). In addition, mass spectrometric ion current measurements of Li^+ and O_2^+ over the same two-phase system showed that, in this part of the phase diagram, Li and O_2 comprised about 98 percent of the vapor composition. These workers also summarized data obtained over the $LiAl_5O_8$-Al_2O_3 system. From these data they derived values for the heats of the vaporization reactions which can also be used to calculate standard heats of formation of $LiAlO_2$(c) and $LiAl_5O_8$(c) using auxiliary thermodynamic data.

Popkov and Semenov (28) reported Li(g) pressures obtained by mass spectrometry. They described the process in terms of the vaporization of $LiAlO_2$ to form Al_2O_3 even though this does not represent an equilibrium condition.

Guggi, Neubert and Zmbov (29) made mass effusion measurements over $LiAlO_2$ which gave Li pressures higher than those of Popkov and Semenov (28). Because of reduction or reaction of the $LiAlO_2$ with their metallic effusion cells, and the supposition that Pt absorbed Li(g), they concluded that the true pressures of Li must lie between those of (26) and their measured pressures using a Mo cell.

In a second paper, Guggi et al., (25) reported measurements over three, two-phase (condensed) regions in the lithia-alumina system using mass spectrometry. These data include Li pressures over the Li_5AlO_4-$LiAlO_2$, $LiAlO_2$-$LiAl_5O_8$ and $LiAl_5O_8$-Al_2O_3 regions. Ikeda et al., published similar measurements to those of Guggi et al., which can be found in a preliminary report (30) and a final paper (31) which includes additional details of the measurements.

Other auxiliary sources of data are the JANAF (16) thermochemical tables, which give detailed thermochemical data for $LiAlO_2$(c) and $LiAlO_2$(ℓ) as well as auxiliary thermochemical data, and the review paper on the lithia-alumina system by Byker et al., (7).

B. Mass Spectrometer Method

Vapor pressure measurements were made using the classical Knudsen effusion method coupled with a modulated beam, quadrupole mass spectrometer. In the classical Knudsen method the pressure is related to the rate of effusion by the expression,

$$P_i = \frac{m_i}{ca\Delta t}\left[\frac{2\pi RT}{M_i}\right]^{1/2} \qquad [5]$$

where, for species i, P_i is the partial pressure, m_i the mass loss in time period Δt, c the Clausing factor which corrects for flow through a non-ideal orifice, a the orifice area, R the gas constant and T the temperature in Kelvin. With a mass spectrometer species detector, the partial pressure P_i is determined from the positive ion current using the expression

$$P_i = kI_i^+T \qquad [6]$$

where k is a mass spectrometer constant dependent on species identity.

These relationships are based on the condition of molecular effusion which requires that the mean free path be much larger than the orifice diameter. For practical orifice sizes of about 0.5 mm and typical temperatures and molecular weights, these relations are valid to pressures up to about 10^{-4} atm.

Elimination of P_i from equations [5] and [6] gives an expression relating the mass spectrometer constant to known or measured quantities which is,

$$k = [m_i(2\pi R)^{1/2}]/[ca\Delta t\ I_i^+(M_iT)^{1/2}]. \qquad [7]$$

In practice, the sum of mass losses for a number of experiments at different temperatures and time periods are observed and only the most abundant isotope having an atomic abundance ratio A_i is routinely monitored. Thus the mass spectrometer constant becomes,

$$k_i = [A_i \cdot m_i(2\pi R)^{1/2}]/[caM_i^{1/2}\ \textstyle\sum I_i^+\ \Delta t \cdot T^{1/2}]. \qquad [8]$$

This method of determining the mass spectrometer constant has the advantage that the pressure is independent of assumptions concerning ionization cross sections and mass discrimination effects. For the vaporization experiments described here, the vapor contains primarily Li and O_2, which simplifies the use of expression [8].

C. Thermodynamic Treatment

Equilibrium vapor pressure data can be used to obtain thermodynamic functions using the second or third law methods. The third law method uses known or estimated entropy data, together with the measured Gibbs energy changes, to calculate heats of reaction or heats of formation of key products or reactants. One method of application of the third law treatment is to use tabulated free energy functions (Gibbs functions) to calculate a heat of reaction at a reference temperature (usually 298.15 K). This is done using the formula

$$\Delta H°(298.15) = T\left[\sum_{p-r} -(\overset{\circ}{G}_T - \overset{\circ}{H}_{298})/T - R\ln K\right] \qquad [9]$$

where $-(\overset{\circ}{G}_T - \overset{\circ}{H}_{298})/T$ are tabulated Gibbs functions summed over products (p) less reactants (r) and K is the equilibrium constant for the reaction under consideration.

The second law method makes use of the measured Gibbs energy data (in this case the free energy for a vaporization reaction) to evaluate both the heat or enthalpy of reaction and the entropy change of the reaction. In this study we have chosen to evaluate the second law values by use of the expression:

$$\sum_{p-r} - (\overset{\circ}{G}_T - \overset{\circ}{H}_{298})/T - R\ln K = \frac{\Delta H°(298)}{T} + B \qquad [10]$$

in which the known Gibbs functions and measured equilibrium constant on the left hand side are used to determine, by least squares, $\Delta H°(298)$ and B as slope and intercept respectively. It can be shown that B equals $\Delta S°(298,$ 3rd law) - $\Delta S°(298,$ 2nd law) and that $\Delta H°(298)$ evaluated as the slope is an accurately adjusted second law heat.

Whether to select the second or third law heats depends to some extent on how well the Gibb's functions are known. It is widely recognized that second law values are very sensitive to temperature or composition errors. In the case of the lithium aluminates there appear to be other problems which cause unexplained temperature trends in the data and most studies in the literature have given more weight to the third law values.

JANAF (16) lists Gibbs functions for all the gaseous species of interest as well as $Li_2O(c)$ and $LiAlO_2(c)$ and these data are used in this report. However, Gibbs function data are not available for $LiAl_5O_8$ nor for Li_5AlO_4 in the temperature range of interest.

Venero and Westrum (32) have measured the heat content of $LiAl_5O_8$ up to 540 K. Most of the literature studies have assumed that the Gibb's function (fef) of $LiAl_5O_8$ can be set equal to the expression,

$$\text{fef } (LiAl_5O_8) = 0.5 \text{ fef } (Li_2O) + 2.5 \text{ fef } (Al_2O_3). \qquad [11]$$

but Hildenbrand et al., (26) as well as Potter et al., (27) assumed that

$$\text{fef } (LiAl_5O_8) = \text{fef } (LiAlO_2) + 2.0 \text{ fef } (Al_2O_3). \qquad [12]$$

At 500 K, Venero and Westrum (32) obtain a value of $(\mathring{G}_T - \mathring{H}_{298})/T$ equal to 42.674 cal/mol K compared to 41.851 for equation [11] and 44.018 for equation [12]. Byker et al., (7) estimated free energy functions for $LiAl_5O_8$ at higher temperatures. At 1800 K the various estimates are 110.642 from Byker et al., 107.735 from Hildenbrand et al., and 105.750 cal/mol K using summation of Li_2O and Al_2O_3 functions. Probably the most logical choice would be to select the estimates of Hildenbrand since they fall near the mean of the other estimates. However, for the present, we have used the linear combination of Li_2O and Al_2O_3 data for both the $LiAl_5O_8$ and Li_5AlO_4 Gibbs function data.

D. Vaporization of $LiAlO_2$ - $LiAl_5O_8$

The phase diagram indicates that compositions falling in the $LiAlO_2$-$LiAl_5O_8$ two phase area should undergo univariant incongruent vaporization. The vaporization reaction for this region of the phase diagram can be written as

$$5/4\ LiAlO_2(c) = Li(g) + 1/4\ O_2(g) + 1/4\ LiAl_5O_8(c). \qquad [13]$$

Preliminary data were obtained using a Pt effusion cell having an effusion orifice with an effective area of 4.3×10^{-3} cm^2. The results of these experiments appeared to indicate that the rate of effusion was under control of a kinetic rather than thermodynamic process. In retrospect, it appears likely that much of the preliminary data was affected by the inclusion of small impurities such as Li_2CO_3 or Li_2O in the initial sample. The effect of volatile impurities will increase the apparent weight loss and increase the magnitude of the mass spectrometer constant thus making the estimated partial pressures too high. A second experimental sequence, in which a new mass spectrometer constant was determined, gave Li pressures close to those expected for this two phase region.

Further measurements were carried out using an Ir crucible having an effective orifice area of 5.1×10^{-4} cm^2. The sample used in these experiments contained fewer impurities than that used in the preliminary measurements although the CO_2^+ mass spectral ion was observed through the

early stages indicating decomposition of unreacted Li_2CO_3. These data showed less tendency to be time dependent than the preliminary measurements.

There was, however, a reproducible tendency for the pressures to be higher especially at the lower temperatures when temperatures were varied during an experimental sequence in an upward rather than downward direction. This behavior is shown in figure 14 for the results from the 901I and 901D data analyzed in Table 9 and is typical of most of the up versus down temperature sequences.

It is difficult to account for this type of behavior in terms of a thermodynamic process. The most plausible explanation is that the order-disorder transformation of $LiAl_5O_8$ described by Lejus and Collongues (20), which is accompanied by a sizable volume change, disturbs the sample in the Knudsen cell sufficiently to increase the amount of impurities able to evaporate when the temperature is again cycled upward. It was also noted that at the beginning of an upward temperature cycle, higher than expected Li^+ ion currents were observed. These signals were also strongly time dependent. Since at the lower temperatures, the rate of Li loss from the samples is very small, it would not be consistent for the decay in Li^+ signals to be due to composition change. But this observation would be consistent with the uncovering of previously encased impurities which could then evaporate.

Figures 15 and 16 show representative Li partial pressure data for increasing (I) and decreasing (D) temperature run chronology, respectively. A few points below 10^{-7} atm have been omitted to reduce the scale require-

ments of the graphs. Overall, the scatter in the data is about ± 25 percent which is characteristic of a system in which some processes are not under thermodynamic control.

The results of a second and third law analysis of data selected with respect to time and temperature direction are listed in Table 9 in chronological order. For reaction [13] it can be shown that for effusive flow, $P_{Li} = 1.86\ P_{O_2}$, giving an equilibrium constant of $P_{Li}^{5/4}/(1.86)^{1/4}$. The heat and entropy changes for reaction [13] at 298 K as well as the third law heat of reaction, using the sum of $Li_2O(c)$ and $Al_2O_3(c)$ Gibbs functions to estimate the Gibbs function of $LiAl_5O_8$, are tabulated for each experimental run. It is concluded that the most reliable thermodynamic values for the heat of reaction from this treatment is that from run 902D because this experiment gives the most satisfactory agreement between the 2nd and 3rd law heat of reaction. Also, the suspected role of impurities in the evaporation process would tend to increase the apparent Li pressure. It should be noted that in general the 2nd law heat of reaction is significantly lower for increasing, as opposed to decreasing, temperature runs.

Over the course of this experimental series the sample underwent a change in bulk composition from essentially 100 wt. % $LiAlO_2$ to 64 wt% $LiAlO_2$ and 36 wt % $LiAl_5O_8$. Further measurements on a sample in this two phase region would be useful to aid in confirming the role of impurity vaporization.

E. Li and O_2 Pressure Data

As noted previously, it is possible to simultaneously determine both Li and O_2 partial pressures. The value of the mass spectrometer sensitivity constant for O_2 was estimated from that determined by weight loss for Li using the equation

$$k_{O_2} = k_{Li} \ (\sigma_{Li} \cdot \tau_{Li} \cdot A_{Li}) / (\sigma_{O_2} \cdot \tau_{O_2} \cdot A_{O_2}) \qquad [14]$$

where σ_i is the ionization cross section of species i, τ_i the relative transmission factor, and A_i the species isotopic abundance factor. The cross section of Li was based on Mann's maximum cross section and corrected by the ratio of the I^+_{max}/I^+_{30} at the 30 eV ionizing energy used, while the O_2 cross section was taken to be 1.10 based on literature values. Measurements of the transmission factor were made using a rare gas mixture of known composition and component ionization cross sections. For the 901D data the average P_{Li}/P_{O_2} ratio was 1.92 which agrees very well with the theoretical value of 1.86. The Li and O_2 pressures for the 901D data set in figure 17 indicate a constant ratio with temperature, as expected for a well behaved thermodynamic system.

F. Vaporization of $LiAl_5O_8$ - Al_2O_3

The $LiAl_5O_8$ - Al_2O_3 region of the phase diagram is also a two-phase area which should undergo univariant-incongruent evaporation. The vaporization reaction for this region of the phase diagram can be written as,

$$LiAl_5O_8(c) = Li(g) + 1/4\ O_2(g) + 5/2\ Al_2O_3(c). \qquad [15]$$

Vaporization experiments, starting with essentially stoichiometric $LiAl_5O_8$, were carried out in the same fashion as for the $LiAlO_2$-$LiAl_5O_8$ study.

The vaporization behavior in this region of the phase diagram is similar to that in the $LiAlO_2$-$LiAl_5O_8$ region except that there is a greater tendency for a decreased vaporization rate with time. The Li partial pressure data are shown in figure 18 for data taken with temperatures increased from point to point during a series while figure 19 shows data obtained when temperatures were decreased. The scatter in the data is comparable to that for the $LiAlO_2$-$LiAl_5O_8$ region except that for experiments following the 104D series the pressures decreased more rapidly with time.

The results of a second and third law analysis of the data are listed in Table 10. As with the $LiAlO_2$-$LiAl_5O_8$ data there is a tendency for pressures to be higher when temperatures are varied in an experimental run in an upward direction as opposed to varying temperatures in a downward direction. Figure 20 illustrates this effect for data taken in the 912I, the 912D, and the 104I series. Here, for simplicity these data sets are labelled run 1 inc T, run 1 dec T and run 2 inc T. Note that after the run 1, dec T experiment there has been a recovery in the Li pressure giving better agreement with the run 1 inc T data than the run 1 dec T data. It appears that factors other than the usual time dependent effects are present.

There is clearly a relationship between these effects for the $LiAlO_2$-Li_5AlO_8 and Li_5AlO_8-Al_2O_3 phases and it may be related to the phase change in which $LiAl_5O_8$ (ordered spinel) is transformed to $LiAl_5O_8$

(disordered structure). It is also possible that there is a solid solubility range on either or both sides of the $LiAl_5O_8$(c) range and that the reestablishment of equilibrium is fast in one direction but slow in the other.

To select the most reliable results for reaction [15] from the Table 10 data we should note that the decrease in pressure from run to run can be due to (a) evaporation of traces of impurities initially present in the sample such as $LiAlO_2$, or unreacted Li_2CO_3 or Li_2O, as well as (b) surface depletion effects due to formation of Al_2O_3 on the surface of the sample or (c) a solid solution range of $LiAl_5O_8$. Lacking definitive information concerning these possibilities, the most reliable results are considered to be those near the beginning of the experimental series. Also, there is reasonably good agreement between 2nd and 3rd law heats of reaction only for data taken during runs where the temperature was decreased between experimental points. From this argument we believe that the results from experiment 104D are the most reliable for the heat reaction determination.

G. Discussion

The $\Delta H°$ values for the vaporization reactions listed in Table 11 may be used, together with auxiliary data (Table 12), to derive standard heats of formation from the elements for each of the high temperature compounds found in the lithia-alumina system, as shown in Table 13.

Potter et al., (27) used different free energy functions from those used here and their results were adjusted to account for this difference. Also, Ikeda et al., (31) used an unusual method of expressing the vaporiza-

tion reactions and their data were reevaluated using the Li pressures only. As mentioned previously, free energy function data for Li_5AlO_4(c) and $LiAl_5O_8$(c) are not available in the temperature range of the experiments and a linear combination of Li_2O(c) and Al_2O_3(c) data was used to estimate these quantities.

It should be noted that ΔH_f° $LiAl_5O_8$ can be obtained directly from reaction [C]. This quantity can then be used to calculate ΔH_f° $LiAlO_2$ using the ΔH for reaction [B]. However, the calorimetric value of ΔH_f° $LiAlO_2$ is thought to be quite reliable and can be used with reaction [B] to yield a second value of ΔH_f° $LiAl_5O_8$. For these calculations we have used the reference data shown in Table 12 from JANAF (16). Table 13 gives results for ΔH_f° $LiAl_5O_8$ using reactions [B] and [C] and also the calorimetric value of ΔH_f° $LiAlO_2$. It may be noted that the values of ΔH_f° $LiAl_5O_8$ agree better when calculated from reaction [C] than from those using the calorimetric value of ΔH_f° $LiAlO_2$ and reaction [B]. This is due to the addition of deviations for the combined reaction, and the direct observations using reaction [C] are considered more reliable. Values for ΔH_f Li_5AlO_4 have similarly been derived from the results of Guggi et al., (25) and Ikeda et al., (31) using reaction [A] and the calorimetric value of ΔH_f° $LiAlO_2$, as shown in Table 13. At the present time it seems likely that these values cannot be correct because the Li pressures reported by Ikeda et al., (31) and those back calculated from the work of Guggi et al., (25) appear to exceed the vapor pressure of Li over pure Li_2O (c).

To summarize, the vapor pressure data from the present work agree reasonably well with the literature but the behavior of the samples across the composition ranges is more complex than generally assumed. Analysis of the thermodynamic data obtained from the vapor pressure measurements is hampered by the lack of thermodynamic functions for the $LiAl_5O_8$ and Li_5AlO_4 compounds. The extent of solid solubility of $LiAl_5O_8$ appears to be uncertain and may be difficult to determine by many experimental methods because of the order-disorder transition near 1300 °C. Measurement of the Li pressure across a more extensive region of the $LiAlO_2$ - $LiAl_5O_8$ and $LiAl_5O_8$ - Al_2O_3 region is desirable. It seems possible that some of the results observed in the current study are due to impurity effects. We note that a lower pressure than that selected from the data in this study would bring the heats of formation of $LiAl_5O_8$ obtained using equations [13] and [15] closer together. However, a more definitive thermodynamic analysis of the vapor pressure data requires quantification of the following likely effects: (a) evaporation of impurities, (b) solid solution in either $LiAl_5O_8$ or $LiAlO_2$ and (c) surface depletion. Data in the high lithia region, especially the Li_5AlO_4 compound appears unsatisfactory and measurements of at least the solid state should be made on this material using microbalance and/or mass spectrometric techniques.

VI. Solution and Phase Equilibria Models for the Li_2O-Al_2O_3 System

(J. W. Hastie and W. S. Horton[3])

Given the experimental complexity of the phase equilibrium behavior in the Li_2O-Al_2O_3 system, it is desirable to develop a theoretical framework to guide and enhance the experimental program. In a previous attempt to empirically model the phase diagram for Li_2O-Al_2O_3, Byker et al., (7) used the Redlich Kister equations to provide an empirical fit to partially complete phase diagram and related thermodynamic data. The validity of these equations to ceramic systems has never been established and the resulting phase equilibria data are often highly questionable and can seriously disagree with experimental evidence, as discussed by us in detail elsewhere (33).

In previous work on various Na_2O, K_2O, SiO_2, Al_2O_3 mixtures we have shown that a chemically based Ideal Mixing of Complex Components (IMCC) model can correctly predict the solution activity and vaporization properties and, to a lesser accuracy, the liquidus and solidus phase equilibria (34). From this earlier experience we believe that the IMCC approach, should also be applicable to the Li_2O-Al_2O_3 system.

A. Basis of the Model

The rationale and theoretical basis for the mixing model used in this study has been presented elsewhere (33). To summarize, the key features of the model are as follows. We attribute large negative deviations from

---

[3]NBS Consultant

ideal thermodynamic activity behavior to the formation of stable complex liquid (and solid) components such as $LiAlO_2$, $LiAl_5O_8$ and Li_5AlO_4. The terminology of components and complex components refers to the usual reference state oxides, e.g., Li_2O or Al_2O_3 and to their compounds (liquid or solid), e.g., $LiAlO_2$ (i.e., $Li_2O \cdot Al_2O_3$), respectively. The component and complex component oxides formed are assumed to mix ideally, in accordance with Raoult's law. Hence thermodynamic activities and mole fractions are equivalent quantities with this model. It should be noted that alternate definitions of ideality, such as the Temkin model, require structural assumptions that are not necessary in the present treatment. The component liquids considered here are distinctly different from the hypothetical associated species used in other modeling approaches. For the most part, the component liquids are established neutral, stable, thermodynamic compounds, appearing in phase diagrams in equilibrium with congruently melting solids, and also in reference tables of thermodynamic functions. The free energies of formation (ΔG_f) are either known or can be estimated for these complex component liquids (and solids). By minimizing the total system free energy one can calculate the equilibrium composition with respect to these components. Thus, for instance, the mole fraction of Li_2O present (X^*Li_2O) in equilibrium with $LiAlO_2$, and other complex liquids (and solids) containing Li_2O, is known. As we have shown previously for similar oxide systems, the component activities can, to a good approximation, be equated to these mole fraction quantities. Thus physical interactions among the complex components are considered negligible compared with the strong chemical interactions leading to their formation.

From the assumption of Ideal Mixing of Complex Components (IMCC), it also follows that lithium partial pressures can be obtained from their thermodynamic relationship to activities. Thus, for example, in the binary Li_2O-Al_2O_3 system,

$$P_{Li} = (2 \cdot X_{*Li_2O} \cdot K_p)^{0.4} \qquad [16]$$

where K_p is the stoichiometric dissociation constant for reaction of pure Li_2O (liquid or solid) to yield Li and O_2.

In the following discussion we test the model, and its accompanying thermodynamic data base, by comparing predicted P_{Li} data with experimental values. Thermodynamic activities and phase compositions are also calculated using this model. The model is constrained to obey the Gibbs-Duhem activity and Gibbs phase rule relationships.

B. Thermodynamic Data Base

In practice, application of the IMCC model requires a thermodynamic data base for the component and complex solids and liquids. The SOLGASMIX computer program (33) used for calculation of the equilibrium composition, and hence activities, utilizes a data base of the type given in Table 14. The coefficients to the ΔG_f equation were obtained mainly by fitting ΔG_f vs T data available in JANAF (16). In a few instances, the literature thermodynamic data have been re-evaluated within the experimental error limits which typically are 1 to 3 kcal/mol; e.g., see the earlier work of Hastie et al., (34). For cases where no literature data were available for the liquids, we estimated the thermodynamic functions in the manner

described earlier (34). Usually, data available for the corresponding solid phase were converted to liquid functions by estimating the melting enthalpy or entropy.

Application of the IMCC theory to predictions of phase equilibria requires a thermochemical data base for all possible solid, liquid, and vapor components and phases. We have converted all pertinent available literature thermodynamic data for the Li-Al-O system to the form used in the SOLGASMIX computer program for free energy minimization, as shown in Table 14. The Gibbs energies of formation (ΔG_f) corresponding to the coefficients of Table 14 are given in Table 15. The thermodynamic data base as represented in Table 14 should be considered an interim set. We expect to refine these thermodynamic functions in future work to resolve differences between JANAF and the results of more recent workers, including the present work.

C. Results

With the current interim data base of Table 14, we have calculated the likely phase equilibria behavior of the Li_2O-Al_2O_3 mixtures. Representative data are shown in Table 16 and figures 22 and 23. Of particular note in figure 23 is the region between about 1900 and 1920 K where solid $LiAlO_2$ and liquid coexist. Table 17 summarizes the principal reactions for this phase-transition region. The thermodynamic activity of liquid Li_2O increases markedly with increasing temperature over this transition interval, leading to a rapid rise in Li partial pressure (P_{Li}), as shown in figure 23. We believe that the reason for this unusual behavior will be clarified when additional components are included in the theoretical

data-base, and when the thermodynamic functions derived from various sources are refined to provide a single self-consistent set of data-base thermodynamic functions. The comparison between the experimental Li partial pressure curve and the predicted result is considered satisfactory and is within the combined errors of the data-base thermodynamic functions and the experimental work.

Preliminary model results for other compositions are given in figure 22, in comparison with the interim phase boundaries based on the experimental results. Note that the model generally predicts the correct phase behavior.

In future studies we will use this chemical approach to optimize the thermodynamic model data base by application of existing computer methods (35, 36) which couple experimental phase diagram data with solution activities and compound thermodynamic functions.

VII. Needs for Future Research in the Li-Al-O-H System

In this report we have presented data on the phase equilibria and vapor pressures in the system Li_2O-Al_2O_3, with ancillary modeling. From this work a number of problem areas needing further study have been defined including: solid solution of Al_2O_3 in Li_2O; the α/β transition in Li_5AlO_4; solid solution vs. order/disorder in $LiAl_5O_8$; and mass spectrometry of the composition Li_5AlO_4. These problems will be addressed by us in future work. A thermochemically optimized diagram for the system Li_2O-Al_2O_3 will be produced. This diagram will be combined with the known phase diagram for Li-Al to yield, with minimal experimental work, a diagram for the

system Li-Al-Li_2O-Al_2O_3. This system will depict equilibria between metal alloy reactants and oxide products in the stored chemical energy conversion scheme. Additionally, we plan to determine the extent to which molten LiH dissolves LiAl, Li_2O, $LiAlO_2$ and LiOH. Similarly important are solubilities and activities of $LiAlO_2$, Li_2O, and LiH in LiOH melts. The basic data thus derived will allow a second generation of predictions and calculations for the Li-Al-H-Li_2O-Al_2O_3-H_2O subsystem of the quaternary system Li-Al-O-H .

VIII. References Cited

1. Bush, K. L. and Merrill, G. L., SCEPS - An Advanced Thermal Power Plant for Torpedoes, AIAA/SAE/ASME 17th Joint Propulsion Conference, Colorado Springs, Col., (1981)

2. SCEPS II. A New High-energy Undersea Propulsion System, Garrett Pneumatic Systems Division, Report No. 41-3675 (1982).

3. Veleckis, E., Van Deventer, E. H., and Blander, M., J. Phys. Chem. 78 [19], 1933 (1974).

4. McAlister, A. J., Bull. Alloy Ph. Diag. 3 [2] 177 (1982).

5. Wriedt, H. A., Bull. Alloy Ph. Diag. (in press).

6. Yonc, R. M., Maroni, V. A., Strain, J. E., and Devan, J. H., J. Nucl. Mat. 79 [2] 354 (1979).

7. Byker, H. J., Eliezer, N., and Howald, R. A., J. Phys. Chem. 83 [18] 2349 (1979).

8. Kotsupalo, N.P., Pushnyakova, V. A., and Berger, A. S., Zh. Neorg. Khim. 23 [9] 2514 (1978).

9. Ortman, M. S. and Larsen, E. M., J. Amer. Ceram. Soc. 66 [9] 645 (1983).

10. Stewner, F., and Hoppe, R., Z. Anorg. Allgem. Chem. 380 [7] 241 (1971).

11. Stewner, F., and Hoppe, R. Z. Anorg. Allgem. Chem. 381 [4] 149 (1971).

12. Marezio, M. and Remeika, J. P., J. Chem. Phys. 44 [8] 3143 (1966).

13. Marezio, M., Acta Cryst. 19 [3] 396 (1965).

14. Hummel, F. A., Sastry, B. S. R. and Wotring, D., J. Am. Ceram. Soc. 41 [3] 88 (1958).

15. Strickler, D. W. and Roy, R., J. Am Ceram. Soc. 44 [5] 228 (1961).

16. Stull, D. R. and Prophet H., JANAF Thermochemical Tables, Second Ed.: U. S. Govt. Printing Office, Washington, DC, NSRDS-NBS 37, (1971). See also later supplements for 1971-1981 (J. Phys. Chem. Ref. Data)

17. Chang, C. H., and Margrave, J. L., J. Am. Chem. Soc., 90 [8] 2020 (1968).

18. Fischer, A. K., Inorg. Chem. 16 [4] 974 (1977).

19. Collongues, R., Ann. Chim. 8 [7-8] 395 (1963).

20. Lejus, A. M. and Collongues, R., C. R. Acad. Sci. 254 [7] 2005 (1962).

21. Datta, R. K. and Roy, R., J. Am. Ceram. Soc. 46 [8] 388 (1963).

22. Hafner, S. and Laves, F., J. Am. Ceram. Soc. 47 [7] 362 (1964).

23. Roy, R. and Datta, R. K., J. Am. Ceram. Soc. 47 [7] 362 (1964).

24. La Ginestra, A., Lo Jacono, M. and Porta, P., J. Thermal Anal. 4 [1] 5 (1972).

25. Guggi, D., Ihle, H. R. and Neubert, A., Proc 9th Symp. Fusion Tech., Pergamon Press, Oxford, U.K. (1967) pp. 635-644.

26. Hildenbrand, D. L., Theard, L. P., Hall, W. F., Ju, F., Viola, F. S., and Potter, N. D. Ford Motor Company, Aeronutronic Division, Publication No. U-2055, March 15 (1963).

27. Potter, N. D., Boyer, M. H., Ju, F., Hildenbrand, D. L. and Murad, E. AFOSR 70-211TR, 1970, NTIS-715567.

28. Popkov, O. S. and Gemenov, G. A., Russian J. Phys. Chem. 45, [2] 266 (1970).

29. Guggi, D., Neubert, A. and Zmbov, K. F., Proc. 4th Int. Conf. on Chem. Thermodyn., Montpellier, France, Paper III/23, p. 124 (1975).

30. Ikeda, Y., Ito, H., Matsumoto, G. and Hayashi, H., J. Nucl. Sci. and Tech. 17, [8] 650 (1980).

31. Ikeda, Y., Ito, H., Matsumoto, G. and Hayashi, H., J. Nucl. Matls. 97, [1-2] 47 (1981).

32. Venero, A., and Westrum, Jr.,E. F., J. Chem. Thermo. 7, [8] 693 (1975).

33. Hastie, J. W. and Bonnell, D. W., A Predictive Phase Equilibrium Model for Multicomponent Oxide Mixtures. Part II: Oxides of Na-K-Ca-Mg-Al-Si, High Temp. Science, in press (1984).

34. Hastie, J. W., Horton, W. S., Plante, E. R., and Bonnell, D. W. Thermodynamic Models of Alkali Vapor Transport in Silicate Systems, IUPAC Conf., Chemistry of Materials at High Temperature Harwell, U.K., August 1981; High Temp.--High Press. 14 [6], 669 (1982).

35. Lukas, H. L., Weiss, J., Krieg, H., Henig, E. T., and Petzow, G., High Temp--High Press. 14 [5], 607 (1982).

36. Lin, P. L., Pelton, A. D., Bale, C. W., and Thompson, W. T., CALPHAD 4 [2], 47 (1980).

37. Gambill, W. R., Chem. Eng. 66 [3] 123 (1966); 66 [3] 127 (1966); 66 [4] 151 (1966).

38. Brandes, E. A., Ed., Smithell's Metals Reference Book, Sixth Ed.: London, Butterworths (1983).

39. Kendall, J., and Monroe, K. P., J. Am. Chem. Soc. 39 [1] 1 (1917); 39 [3] 787 (1917); 39 [5] 1802 (1917); 43 [1] 115 (1921).

40. Steinour, H. H., Ind. Eng. Chem. 36 [2] 840 (1944); 36 [2] 901 (1944).

IX. Appendix 1. Modeling of Viscosities in Multiphase Mixtures (L. Grabner)

Empirical relations have been applied in the past to model a variety of multiphase systems (37). A literature survey failed to reveal any data on viscosities of lithia-alumina melts; however the viscosities of molten Li and Al are well known (38).

In situations where two liquids mix ideally, then the relation proposed many years ago by Kendall and Monroe (39) applies well:

$$\mu^{1/3} = X_1 \mu_1^{1/3} + X_2 \mu_2^{1/3} \qquad [17]$$

where X_1 and X_2 are the mole fractions of the two components in the mixure and μ_1 and μ_2 are their viscosities. This assumes the absence of strong interactions between components. Viscosity data for pure Li and Al have been plotted in figure 23. At 1200 K, viscosities calculated for Al/Li mixtures using equation [17] are shown in figure 24.

For multiphase systems, most efforts to correlate suspension viscosity have resulted in relatively simple equations giving μ_S, the viscosity of the liquid-solid mixture, in terms of the viscosity of the suspending liquid, μ_L, and the volume fraction of the solid particles, ϕ_S. The relations proposed are many. They are listed in (37). Of these, the relation proposed by Steinour (40):

$$\frac{\mu_s}{\mu_L} = \frac{10^{1.82\phi_s}}{1-\phi_s} \qquad [18]$$

is favored for values of $\phi_s < 0.4$. A graph of equation [18] is given in figure 25.

X. Appendix 2. Literature Search on the System Li-Al-O-H (L. Cook)

A comprehensive computerized literature search was designed with the aid of NBS library staff. Various combinations of the elemental and oxide components of the system Li-Al-O-H were used as descriptors, such as Li-O, Li-Al-O, Li_2O-Al_2O_3, Li_2O-H_2O, Li-Al-H and Li-Al-H-O. Additionally, certain compound names were used in the search, such as lithium aluminate and lithium alumium hydride. No restrictions (other than to avoid duplication) were made on these searches, so that all references, as for example with keywords lithium aluminate and water, would be retrieved regardless of other keywords present.

The data bases searched included Metadex (1966-1983), Chemical Abstracts (1967-1983), DOE Energy (1974-1983) and Compendex (1970-1983). The search generated approximately 2000 references. This large number stems partly from technological interest in the system Li-Al-O-H for applications such as nuclear fusion, advanced batteries, hydrogen storage and metal organic synthesis. The majority of these references were neither of direct nor indirect application to the problem of reaction in the system Li-Al-O-H, and were eliminated, leaving the remainder, which have been loosely grouped below according to chemistry. No attempt has been made to annotate this bibliography, but titles are included for the aid of the interested reader.

(A) The System lithia-alumina

1. Lithium aluminates--crystal chemistry

Abritta, T.; Melamed, N. T.; Neto, J. M.; and Barros, F. de S., 1979, The optical properties of chromium(+3) ion in lithium aluminate ($LiAl_5O_8$) and lithium gallium oxide ($LiGa_5O_8$): J. Lumin, V. 18-19, pt. 1, p. 179-182.

Abritta, T.; Neto, M.; Barros, de S.; and Melamed, N. T., 1983; The fluorescence of chromium(+3) in ordered and disorded lithium aluminum oxide ($LiAl_5O_8$): Inst. Fis., Univ. Rio de Janeiro, Brazil, Report No. UFRJ-IF-07/83, 41 p.

Agarkov, B. N. and Batalova, S. Sh., 1970, Low-induction ferrites of the lithium system: Elektron. Tekh. Nauch.-Tekh. Sb. Ferrit. Tekh., No. 3, p. 14-20.

Aubry, J. and Klein, F., 1970, Lithium aluminate: Chim. Ind., Genie Chim., V. 103, No. 13, p. 1643-4.

Baranov, M. N. and Kustov, E. F., 1973, Optical spectra of iron group ions in aluminum lithium oxide ($LiAl_5O_8$) single crystals: Opt. Spektrosk., V. 34, No. 4, p. 726-8.

Brabers, V. A. M., 1976, Infrared spectra and ionic ordering of the lithium ferrite-aluminate and chromite systems: Spectrochim. Acta, V. 32A, No. 11, p. 1709-11.

Datta, R. K. and Roy, R., 1968, Order-disorder in M magnesium aluminate. The systems: $MgAl_2O_4$-$LiAl_5O_8$, $MgAl_2O_4$-$NiAl_2O_4$ and $NiAl_2O_4$-$ZnAl_2O_4$: Amer. Mineral., V. 53, p. 1456-75.

Doerhoefer, K., 1979, A reindexing of the x-ray powder diffraction pattern of β-lithium aluminate: J. Appl. Crystallogr., V. 12, No. 2, p. 240-1.

Doman, R. C. and McNally, R. N., 1973, Solid solution studies in the magnesium oxide-lithium metaaluminate system: J. Mater. Sci., V. 8, No. 2, p. 189-91.

Famery, R.; Bassoul, P.; Delamarre, C.; Queyroux, F.; and Gilles, J. C., 1982, Precipitation of metastable phases with periodic antiphase structure in lithium aluminum oxide ($LiAl_5O_8$)-alumina system: Philos. Mag., V. 45A, No. 1, p. 63-80.

Famery, R.; Queyroux, F.; Gilles, J. C.; and Herpin, P., 1979, Structural study of the ordered form of lithium aluminum oxide ($LiAl_5O_8$): J. Solid State Chem., V. 30, No. 2, p. 257-63.

Firsov, Yu. P., 1979, Effect of heat treatment conditions on the formation of the defect state in spinel solid solutions: Tr. VNII Khim. Reaktivov i Osobo Chist. Khim., No. 41, p. 154-5.

Follstaedt, D. M. and Biefeld, R. M., 1978, Nuclear-magnetic-resonance study of lithium(+1) motion in lithium aluminates and lithium hydroxide: Phys. Rev. B: Condens. Matter, V. 18, No. 11, p. 5928-37.

Fritzer, H. P.; Sliuc, E.; and Torkar, K., 1973, Spectroscopic studies and phase relations in the system lithium oxide-aluminum oxide-chromium(III) oxide: Monatsh. Chem., V. 104, No. 1, p. 172-81.

Gessner, W. and Mueller, D., 1983, Coordination of aluminum in β-lithium aluminate ($LiAlO_2$): Z. Anorg. Allg. Chem., V. 505, p. 195-200.

Gula, E.; Kolodziejczyk, A.; Obuszko, A.; and Pszczola, J., 1973, Possibility of the existence of iron(+3) ions with lowered magnetic moment in lithium ferrites-aluminates: Acta Phys. Pol. A, V. 43, No. 1, p. 175-6.

Hoppe, R. and Koenig, H., 1977, On the crystal structure of β-lithium aluminate (Li_5AlO_4): Z. Anorg. Allg. Chem., V. 430, p. 211-17.

Ignat'ev, I. S.; Lazarev, A. N.; and Kolesova, V. A., 1976, Normal vibrations of aluminates with tetrahedrally coordinated aluminum atoms: Izv. Akad. Nauk SSSR, Neorg. Mater., V. 12, No. 7, p. 1230-9.

Jarocki, E. and Kubel, W., 1973, Structural investigations and the problem of bisquare exchange in the ferrite-lithium aluminate $Li0.5Fe_{1.7}Al0.8O_4$: Zesz. Nauk. Akad. Gorn.-Hutn., Krakow, Zesz. Spec., V. 43. p. 211-20.

Kolesova, V. A., 1974, Infrared absorption spectrum of lithium ortho-aluminate Li_5AlO_4: Zh. Neorg. Khim., V. 19, No. 10, p. 2898-9.

Malve, A.; Gleitzer, C.; and Aubry, J., 1971, Lithium aluminate-lithium ferrate system. Detection of a $Li_5Al_4/7Fe_3/7O_4$ compound: C. R. Acad. Sci., Ser. C, V. 273, No. 15, p. 888-90.

McNicol, B. D. and Pott, G. T., 1973, G. T., Luminescence of manganese ions in ordered and disordered lithium aluminum oxide: J. Lumin., V. 6, No. 4, p. 320-34.

Melamed, N. T.; Barros, F. de S., Viccaro, P. J.; and Artman, J. O., 1972, Optical properties of Fe^{3+} in ordered and disordered $LiAl_5O_8$: Phys. Rev. B, V. (3)5, No. 9, P. 3377-87.

Melamed, N. T.; Viccaro, P. J.; Artman, J. O.; and Barros, F. de S., 1970, Fluorescence of Fe^{3+} in ordered and disordered phases of $LiAl_5O_8$: Proc. Int. Conf. Lumin., p. 384-67.

Neto, J. M.; Abritta, T.; Barros, F. de S.; and Melamed, N. T., 1981, Comparative study of the optical properties of Fe^{3+} in ordered $LiGa_5O_8$ and $LiAl_5O_8$: J. Lumin., V. 22, No. 2, p. 109-120.

Pakhomova, N. L. and Kozlov, V. A., 1982, Magnetic anisotropy and exchange interactions in lithium-aluminum ferrites: Izv. Vyssh. Uchebn. Zaved., Fiz., V. 25, No. 11, p. 54-7.

Petrov, M. P.; Szymczak, H.; Wadas, R,; and Wardzynski, W., 1971, Crystal field of low symmetry in $LiAl_5O_8$ + Cr^{3+}: Electron Technol., V. 4, No. 1-2, p. 75-90.

Petrov, M. P.; Szymczak, H.; Wadas, R.; and Wardzynski, W., 1971, Low-symmetry crystal field in lithium spinel: J. Phys. (Paris), V. 32, No. 2-3.

Polyakov, V. P., 1971, Magnetic short-range order and Curie temperature of ferrimagnetic spinels containing lithium ions: Elektron. Tekh. Nauch.-Tekh. Sb. Ferrit. Tekh., No. 4, p. 12-17.

Pott, G. T. and McNicol, B. D., 1971, Phosphorescence of Fe^{3+} doped lithium aluminate ($LiAl_5O_8$): Chem. Phys. Lett., V. 12, No. 1, p. 62-4.

Pott, G. T. and McNichol, B. D., 1973, Luminescence of chromium(+3) ions in ordered and disordered lithium aluminum oxide ($LiAl_5O_8$): J. Solid State Chem., V. 7, No. 2, p. 132-7.

Semenov, N. N.; Merkulov, A. G.; and Fomin, A. G., 1967, Low-temperature modification of lithium aluminate: Redk. Shchelochnye Elem., Sb. Dokl. Vses. Soveshch., 2nd, Novosibirsk, (Plyushchev, V. E., Ed.) p. 100-9.

Stel'mashenko, M. A.; Rubal'skaya, E. V.; Perveeve, A. I., Shlyakhina, L. P.; and Nekhoroshev, G. V., 1973, Crystal lattice distortion effect on the magnetic anisotropy of lithium-aluminum ferrites: Izv. Vyssh. Uchev. Zaved., V. 16, No. 5, p. 113-16.

Stewner, F. and Hoppe, R., 1971, Crystal structure of α-lithium aluminate: Z. Anorg. Allg. Chem., V. 380, No. 3, p. 241-3.

Stewner, F. and Hoppe, R., 1971, Crystal structure of β-Li_5AlO_4: Z. Anorg. Allg. Chem., V. 381, No. 2, p. 149-60.

Vicarro, P. J.; Barros, F. de S., and Oosterhius, W. T., 1972, Paramagnetic Fe^{3+} in lithium aluminate. Magnetic field effects in the Moessbauer spectrum: Phys. Rev. B, V. (3)5, No. 11, p. 4257-64.

Wadas, R.; Wardzinski, W.; Petrov, M. P., and Szymczak, H., 1971, Crystalline field in $LiAl_5O_8$:Cr^{3+}: Paramagn. Rezonans 1944-1969, Vses. Yubileinzyz Knof. (Rivkind, A. I., Ed.) p. 60-2.

Waychunas, G. A. and Rossman, G. R., 1983, Spectroscopic standard for tetrahedrally coordinated ferric iron: $Iron^{3+}$-doped γ-lithium aluminate: Phys. Chem. Miner., V. 9, No. 5, p. 212-15.

Zhilyakov, S. M. and Rodinov, S. I., 1973, Temperature of the order-disorder transition in the lithium ferrite-aluminate system: Dokl. Yubilein, Nauchno-Tekh. Konf., Radiofiz. Fa,., Tomsk Univ., No. 3, p. 114-19.

2. Lithium aluminates--vapor pressure and thermodynamic properties

Broers, G. H. J. and Van Ballegoy, H. J. J., 1969, Phase equilibria in Li-Na-K carbonate/aluminate systems: Third international symposium on fuel cells, Brussels, p. 77-86.

Guggi, D.; Ihle, H.; Neubert, A.; and Woelfle, R., 1976, Tritium re-lease from lithium meta-aluminate, its thermal decomposition and phase relationships. γ-lithium meta-aluminate-lithium aluminum oxide ($LiAl_5O_8$). Implications regarding its use as a blanket material in FRT: Radial. Eff. Tritium Technol. Fusion React., Proc. Int. Conf. (Watson, J. S. and Wiffen, F. W., Eds.), V. 3, p. 416-32.

Guggi, D.; Ihle, H. R.; and Neubert, A., 1976, Thermal stability of solid lithium compounds proposed for use in CTR blankets: Comm. Eur. Communities, (Rep.), No. EUR 5602, Proc. 9th Symp. Fusion Technol., p. 635-44.

Guggi, D. J.; Neubert, A.; and Zmbov, K. F., 1975, Vaporization be-havior of γ-lithium metaaluminate: 4th Conf. Int. Thermodyn. Chim., (C. R.) (Rouquerol, J. and Sabbah, R., Eds.), V. 3, p. 124-31.

Ikeda, Y.; Ito, H.; and Matsumoto, G., 1980, Thermal stability of lithium aluminates by high temperature mass spectrometry: J. Nucl. Sci. Technol. (Tokyo, Japan), V. 17, No. 8, p. 650-653.

Ikeda, Y.; Ito, H.; and Matsumoto, G., 1981, Vaporization and thermo-chemical stability of lithium aluminates: J. Nucl. Mater. (Netherlands), V. 97, No. 1-2, p. 47-58.

Iwamoto, N.; Ikeda, Y.; Kamegashira, N.; and Makino, Y., 1979, Vapori-zation behavior in the lithium oxide-aluminum oxide system: Trans. JWRI (Japan) V. 8, No. 2, p. 287-288.

Vasil'ev, V. G.; Borisov, S. R.; Ryazantseva, N. N.; and Vashman, A. A., 1980, Investigation of physicochemical properties of irradiated lithium inorganic compounds: lithium oxide, lithium aluminate and lithium silicates: At. Energ. (USSR), V. 48, No. 6. p. 392-394.

Vasil'ev, V. G.; Shulyatikova, L. G.; Tymonyuk, M. I.; Shiskov, N. V.; Kozlova, N. M.; and Zhmak, V. A., 1980, Synthesis and physicochemical properties of lithium aluminate, titanate, niobate, silicates and oxide: Izv. Akad. Nauk. SSSR Neorg. Mater., V. 16, No. 2, p. 332-334.

Veleckis, E.; Yonco, R. M.; and Maroni, V. A., 1979, Current status of fusion reactor blanket thermodynamics, Argonne Natl. Lab., Report No. ANL-78-109, 34 p.

Venero, A. F., 1976, The thermodynamic properties of the spinels lithium aluminate and lithium ferrite: Diss. Abstr. Int. B, V. 37, No. 7, p. 1277-8.

Venero, A. F. and Westrum, E. F., Jr., 1975, Heat capacities and thermodynamic properties of lithium ferrate ($LiO_{.5}Fe_{2.5}O_4$) and lithium aluminate ($LiO_{.5}Al_{2.5}O_4$) from 5 to 545 K: J. Chem. Thermodyn., V. 7, No. 7, p. 693-702.

Yudin, B. F.; Lapshin, S. A.; Polonskii, Yu. A.; and Mosilenskii, V. I., 1976, Thermodynamics of the processes of reduction of Al_2O_3, Y_2O_3 and Sc_2O_3 in lithium vapor: Izv. Akad. Nauk. SSSR Neorg. Mater., V. 12, No. 11, p. 1985-1990.

3. Lithium aluminates--processing

Arendt, R. H. and Curran, M. J., 1980, Molten salt synthesis of lithium meta-alumina powder (Patent): General Electric Co., Patent No. US 4,201,760.

Bauman, W. C.; Lee, J. M.; and Burba, J. L., III, 1980, Crystalline lithium aluminates (Patent): Dow Chemical Co., Patent No. US 4,384,296 A.

Bauman, W. C. and Lee, J. M., 1980, Crystalline lithium aluminates (Patent): Dow Chemical Co., Patent No. US 4,348,297 A.

Burba, J. L., III, 1980, Crystalline lithium aluminates (Patent): Dow Chemical Co., Patent No. US 4,348,295 A.

Burba, J. L., III, 1980, Lithium aluminates for gas chromatograph columns (Patent): Dow Chemical Co.. Patent No. US 4,321,065 A.

Burmakin, E. I.; Cherei, A. A.; and Stepanov, G. K., 1981, Solid electrolytes in the lithium germanate (Li_4GeO_4)-aluminum oxide system: Izv. Akad. Nauk SSSR, Neorg. Mater., V. 17, No. 10, p. 1837-40.

Cockayne, B. and Lent, B., 1981, The Czochralski growth of single crystal lithium aluminate, $LiAlO_2$: J. Cryst. Growth, V. 54, No. 3, p. 546-50.

Dietrich, W. C., 1968, Determination of lithium in lithium aluminate: U. S. At. Energy Comm., Report No. Y-1601, 22 p.

Dixon, S., Jr., 1975, Nonlinear properties of aluminum-substituted lithium ferrite: AIP Conf. Proc., V. 24, p. 485-6.

Eichinger, G., 1981, Decomposition mechanisms of some lithium ionic conductors: Solid State Ionics, V. 2, No. 4, p. 289-295.

Ermenin, N. I.; Vilyugina, M. D.; and Makarenkov, V. N., 1982, Behavior of lithium in the decomposition of aluminate solutions: Izv. Vyssh. Uchebn, Zaved., Tsvetn. Metall., No. 3, p. 36-9.

Gazza, G. E., 1972, Hot-pressing of $LiAl_5O_8$: J. Amer. Ceram. Soc., V. 55, No. 3, p. 172-3.

Gurwell, W. E., 1966, Characterization of lithium-aluminate powders in J.O. 909 and J.O. 911: DOE Report, No. RL-GEN-1142(W/Del), 19 p.

Johnson, R. T., Jr. and Biefeld, R. M., 1979, Ionic conductivity of lithium aluminum oxide (Li_5AlO_4) and gallium oxide (Li_5GaO_4) in moist air environments: potential humidity sensors: Mater. Res. Bull., V. 14, No. 4, p. 537-42.

Kinoshita, K.; Sim, J. W.; and Ackerman, J. P., 1978, Preparation and characterization of lithium aluminate: Mater. Res. Bull., V. 13, No. 5, p. 445-455.

Kinoshita, K.; Sim, J. W.; and Kucera, G. H., 1979, Synthesis of fine particle size lithium aluminate for application in molten carbonate fuel cells: Mater. Res. Bull., V. 14, No. 10., p. 1357-1368.

Klein, F.; Gleitzer, C.; and Aubry, J., 1979, Some properties of γ-lithium aluminate with regard to its utilization as an electrolyte support for a high temperature fuel cell: Silic. Ind., V. 44, No. 11, p. 257-64.

Kvachkov, R.; Yanakiev, A.; Puliev, Kh.; Balkanov, I.; Yankulov, P. D.; and Budevski, E., 1981, Effect of the starting aluminum oxide and of the method of preparation on the characteristics of lithium-stabilized β-aluminum oxide ceramics: J. Mater. Sci., V. 16, No. 10, p. 2710-16.

Maslova, E. I.; Samsonova, T. I.; and Strukulenko, N. A., 1967, Interaction of oxides in a lithium oxide-aluminum oxide-ferric oxide system at sintering temperatures: Redk. Shchelochnye Elem., Sb. Dokl. Vses. (Plyushchev, V. E., Ed.), p. 230-41.

Mason, D. M. and Van Drunen, J., 1976, Production of β-lithium aluminate ($LiAlO_2$) (Patent): Inst. of Gas Tech., Patent No. US 3,998,939.

Owen, J. H.; Randall, D.; Watson, J. S.; Wiffen, F. W.; Bishop, J. L.; and Breeden, B. K. (Eds.), 1976, Equilibrium and kinetic studies of systems of hydrogen isotopes, lithium hydrides, aluminum and $LiAlO_2$: International conference on radiation effects and tritium technology for fusion reactors (Gatlinburg, TN), DOE Report No. CONF-750989-P3, p. 433-457.

Scott, A. J.; Wessol, D. E.; and Judd, J. L., 1983, Preliminary neutronic calculations for fusion blanket testing in the engineering test reactor: Nucl. Technol. Fusion, V. 3, No. 1, p. 129-136.

Sharabati, H.; Hecker, R.; and Joneja, O. P., 1982, Tritium breeding measurements in a lithium aluminate blanket assembly using thermoluminescent dosimeters: Nucl. Instrum. Methods Phys. Res., V. 201, No. 2-3, p. 445-449.

Sim, J. W.; Singh, R. N.; and Kinoshita, K., 1980, Testing of sintered lithium aluminate structures in molten carbonate fuel cells: J. Electrochem. Soc., V. 127, No. 8, p. 1766-8.

Sinyh, R. N.; Dusek, J. T.; and Sim, J. W., 1981, Fabrication and properties of a porous lithium aluminate electrolyte retainer for molten carbonate fuel cells: Am. Ceram. Soc. Bull., V. 60, No. 6, p. 629-635.

Sooki-Toth, G.; David, P.; Lukacs, J.; Molnar, I.; Horvath, P.; Krajcsovics, F.; Keszler, J.; Gal, S.; Pungor, E.; and Tomor, K., 1974, One-step production of γ-lithium metaaluminate electrolyte of high-temperature fuel cells (Patent): Villamosipari Kutato Intezet-Budapesti Muszaki Egyetem, Patent No. Hungary Teljes HU 9936.

Van der Straten, P. J. M. and Metselaar, R., 1980, Liquid phase epitaxial growth of lithium ferrite aluminate films: J. Cryst. Growth, V. 48, No. 1, p. 114-20.

Youngblood, G. E.; Virkar, A. V.; Cannon, W. R.; and Gordon, R. S., 1977, Sintering processes and heat treatment schedules for conductive, lithia-stabilized β-Al_2O_3 : Am. Ceram. Soc. Bull., V. 56, No. 2, p. 206-210.

Yunker, W., (Ed.), 1976, Extraction of tritium from lithium aluminate: DOE Report No. HEDL-TME-76-81, 79 p.

4. Li_2O-Al_2O_3

Bruening, D.; Guggi, D.; and Ihle, H. R., 1983, The diffusivity of tritium in the system lithium oxide-aluminum oxide: Comm. Eur. Communities, (Rep.), No. EUR 7983, Fusion Technol., 1982, V. 1, p. 543-8.

Byker, H. J.; Eliezer, I.; Eliezer, N.; and Howald, R. A., 1979, Calculation of a phase diagram for the lithium oxide-aluminum oxide ($LiO_{0.5}$-$AlO_{1.5}$) system: J. Phys. Chem., V. 83, No. 18, p. 2349-55.

Efros, M. D.; Oboturov, A. V.; and Ermolenko, N. F., 1969, Effect of lithium oxide additives on the sorption and catalytic properties of aluminum oxide: Vestsi Akad. Navuk Belarus. SSR, Ser. Khim. Navuk, No. 3. p. 98-101.

Eliseev, V. B.; Lyutsareva, L. A.; Pivnik, E. D.; and Fokina, I. I., 1979, Properties of b-alumina doped with lithium oxide: Fiz. Khim. Elektrokhim. Rasplavl. Tverd. Elektrolitov, Tezisy Dokl. Vses. Konf. Fiz. Khim. Ionnykh Rasplavov Tverd. Elektrolitov, V. 3, 41 P.

Eremin, N. I.; Vilyugina, M. D.; and Makarenkov, V. N., 1981, Solubility of lithium oxide in aluminate solutions: Izv. Vyssh. Uchebn. Zaved., Tsvetn. Metall., No. 6, p. 26-9.

Eremin, N. I.; Vilyugina, M. D.; and Makarenkov, V. N., 1981, Solubility of lithium oxide in aluminate solutions (translation): Sov. Non-Ferrous Met. Res., V. 9. No. 6, p. 457-460.

Eremin, N. I.; Vilyugina, M. D.; and Makarenkov, V. N., 1982, The behavior of lithium during decomposition of aluminate solutions: Izv. V.U.Z. Tsvetn. Metall., No. 3, p. 36-39.

Fischer, A. K., 1977, Atmospheric pressure synthesis for β-lithium aluminum oxide: Inorg. Chem., V. 16, No. 4, p. 974.

Fruma, A.; Ciomartan, D.; Brasoveanu, I.; and Nicolescu, I. V., 1973, Structure of lithium- and titanium-doped aluminum oxide: Rev. Roum. Chim., V. 18, No. 5, p. 803-8.

Surdeanu, T.; Stancovschi, V.; Marinescu, A.; and Crisan, D., 1981, Reactivity of some aluminas in the production of ceramic products of lithium oxide-stabilized β-alumina: Mater. Constr. (Bucharest), V. 11, No. 2, p. 98-100.

Torkar, K.; Fritzer, H. P. and Krischner, H., 1965, Reaction behavior of various aluminum oxides with lithium carbonate: Sci. Ceram., V. 2, No. 15, p. 19-32.

Vilyugina, M. D.; Makarenkov, V. N.; and Eremin, N. I., 1983, A study of lithium oxide in aluminate solutions at elevated temperatures: Izv. V. U. Z. Tsvetn. Metall., No. 5, p. 72-74.

5. Li_2O-Al_2O_3 with third component

Abdullaev, G. K.; Rza-Zade, P. F.; and Mamedov, Kh. S., 1983, Lithium oxide-aluminum oxide-boron oxide system: Zh. Neorg. Khim., V. 28, No. 3, p. 759-63.

Aleixandre-Ferrandis, V.; Fernandez-Navarro, J. M.; and Fernandez-Arroyo, G., 1969, Compounds of the phosphorus pentoxide-aluminum oxide-lithium oxide system. I. Identification by x-ray diffraction and dilatometry: Bol. Soc. Espan. Ceram., V. 8, No. 4, p. 435-57.

Aleixandre-Ferrandis, V.; Fernandiz-Navarro, J. M.; and Fernandez-Arroyo, G., 1969, Phases in the phosphorus pentoxide-alumina-lithium oxide system. II. Infrared and DTA study: Bol. Soc. Espan. Ceram., V. 8, No. 5, p. 511-23.

Burmakin, E. I.; Stepanov, G. K.; and Pazdnikova, L. P., 1978, Structure of solid electrolytes in lithium silicate (Li_4SiO_4)-aluminum oxide and lithium silicate (Li_4SiO_4)-aluminum oxide-lithium oxide systems: Tr. In-ta Elektrokhimii Ural'sk. Nauch. Tsentr AN SSSR, No. 27, p. 72-7.

Cismaru, D. and Manolescu, D., 1970, Structure studies of solid solutions in the system Al_2O_3-Cr_2O_3-Li_2O: Rev. Roum. Chim., V. 15, No. 2, p. 291-5.

Efros, M. D.; Oboturov, A. V.; Ermolenko, N. F.; and Kramarenko, F. G., 1971, Effect of lithium oxide on the phase composition, structure and sorption properties of mixed aluminum and zinc oxides: Dokl. Akad. Nauk Beloruss. SSR, V. 15, No. 3, p. 228-31.

Enriquez, J. L.; Quintana, P.; Vazquez, J.; and West, A. R., 1982, Subsolidus phase equilibriums in the systems lithium oxide-sodium oxide-zirconium oxide and lithium oxide-aluminum oxide-zirconium oxide: Trans. J. Br. Ceram. Soc., V. 81, No. 4, p. 118-21.

Ermolenko, N. F.; Efros, M. D.; Kramarenko, F. G.; Lemeshonok, G. S.; and Kuz'mich, E. I., 1970, Effect of lithium oxide on phase transformations in the aluminum oxide-nickel monoxide system: Kinet. Katal., V. 11, No. 6, p. 1577-80.

Ermolenko, N. F.; Oboturov, A. V.; Efros, M. D.; Kramarenko, F. G.; and Yatsevskaya, M. I., 1969, Effect of lithium oxide addition on the phase composition and sorption properties of aluminum-oxide-titanium dioxide system: Vestsi Akad. Navuk Belarus, SSR, Ser. Khim. Navuk, No. 5, p. 5-10.

Fritzer, H. P.; Sliuc, E., and Torkar, K., 1973, Spectroscopic studies and phase relations in the system lithium oxide-aluminum oxide-chromium(III) oxide: Monatsh. Chem., V. 104, No. 1, p. 172-81.

Izquierdo, G. and West, A. R., 1980, Subsolidus equilibriums in the system lithium oxide-aluminum oxide-chromium oxide: J. Am. Ceram. Soc., V. 63, No. 1-2, p. 7-10.

Izquierdo, G. and West, A. R., 1980, Compatibility relations in the system lithium oxide-magnesium oxide-aluminum oxide: J. Am. Ceram. Soc., V. 63, No. 3-4, p. 227.

Jackowska, K. and West, A. R., 1983, Ionic conductivity of lithium silicon oxide (Li_4SiO_4) solid solutions in the system lithium oxide-aluminum oxide-silicon dioxide: J. Mater. Sci., V. 18, No. 8, p. 2380-4.

Maslova, E. I. and Rychazhkova, E. A., 1970, Interaction of oxides in the lithium oxide-aluminum oxide-ferric oxide-calcium oxide system at sintering temperatures: Izv. Sib. Otd. Akad. Nauk SSSR, Ser. Khim. Hauk, No. 6, p. 19-23.

Maslova, E. I.; Samsonova, T. I.; and Strukulenko, N. A., 1967, Interaction of oxides in a lithium oxide-aluminum oxide-ferric oxide system at sintering temperatures: Redk. Shchelochnye Elem., Sb. Dokl. Vses. Soveshch. 2nd, Novosibirsk (Plyushchev, V. E., Ed.), p. 230-41.

Menzheres, L. T.; Kotsupalo, N. P.; and Berger, A. S., 1978, Phase equilibriums in the subsolidus region of the lithium oxide-magnesium oxide system at 1200°: Zh. Neorg. Khim., V. 23, No. 10, p. 2804-9.

Oboturov, A. V.; Ermolenko, N. F.; Kramarenko, F. G.; and Efros, M. D., 1969, Effect of lithium oxide on the phase composition and sorption properties of the aluminum oxide-iron(III) oxide system: Vestsi Akad. Navuk Belarus. SSR, Ser. Khim. Navuk, No. 4, p. 22-6.

Semenov, N. N. and Zabolotskii, T. V., 1967, Physical-chemical studies in a lithium oxide-calcium oxide-aluminum oxide system: Redk. Shchelochnye Elem., Sb. Dokl. Vses. Soveshch., 2nd, Novosibirsk (Plyushchev, V. E., Ed.), p. 242-53.

Zografou, C.; Reynen, P.; and Von Mallinckrodt, D., 1983, Non-stoichiometry and sintering of magnesium oxide and magnesium aluminate ($MgAl_2O_4$): InterCeram., V. 32, No. 2, p. 40-2.

(B) Lithia with water

1. Li_2O-H_2O

Capotosto, A., Jr. and Petrocelli, A. W., 1968, Use of lithium peroxide for atmosphere regeneration: U. S. Clearinghouse Fed. Sci. Tech. Inform., No. AD-678076, 56 p.

Dobrynina, T. A.; Akhapkina, N. A.; and Chuvaev, V. F., 1969, Synthesis and properties of lithium peroxide monoperoxhydrate $Li_2O_2 \cdot H_2O$: Izv. Akad. Nauk SSSR, Ser. Khim., No. 3, p. 493-6.

Johnson, G. D.; Grow, R. T.; and Hubbard, W. N., 1975, Enthalpy of formation of lithium oxide (Li_2O): J. Chem. Thermodyn., V. 7, No. 8, p. 781-6.

Kahara, T.; Horiba, T.; Tamura, K.; and Fujita, M., 1979, Metal oxide cathodes for lithium high energy batteries: Proc. of the Symp. on Power Sources for Biomed. Implantable Appl. and Ambient Temp. Lithium Batteries, Proc Electrochem. Soc., V. 80-4, p. 300-30.

Nemukhin, A. V. and Stepanov, N. F., 1978, Study of the geometric structure of water, lithium oxide, and lithium hydroxide molecules by the method of diatomic fragments in molecules: Zh. Strukt, Khim., V. 19, No. 5, p. 771-8.

Rashavachari, K., 1982, A theoretical study of the reactions surface for the water-lithium oxide system: J. Chem. Phys., V. 76, No. 11, p. 5421-6.

Turutina, N. V.; Il'in, V. G.; and Kurilenko, M. S., 1977, Study of low-temperature hydrothermal crystallization in lithium oxide-silicon dioxide-water, potassium oxide-silicon dioxide-water, and (lithium oxide, sodium oxide, potassium oxide)-silicon dioxide-water systems: Adsorbtsiya Adsorbenty, V. 5, p. 42-50.

2. Li_2O-Al_2O_3-H_2O

Caranoni, C.; Barres, M.; Capella, L., 1971, Radiocrystallographic study of two hydrates of lithium gallate(III): C. R. Acad. Sci., Ser. C, V. 273, No. 15, p. 884-7.

Dement'eva, S. D.; Visloguzova, N. M.; Shabanov, V. F., and Volkovskaya, A. I., 1983, Interaction in the lithium oxide-sodium oxide-aluminum oxide-silicon monoxide-water system at 280°: Ukr. Khim. Zh. (Russ. Ed.), V. 49, No. 8, p. 885-6.

Dudney, N. J.; Bates, J. B., and Wang, J. C., 1981, Diffusion of water in lithium β-alumina: Phys. Rev. B: Condens. Matter, V. 24, No. 12, p. 6831-42.

Epstein, J. A.; Feist, E. M.; Zmora, J.; and Marcus, Y., 1981, Extraction of lithium from the Dead Sea: Hydrometallurgy, V. 6, No. 3-4, p. 269-275.

Evteeva, O. G. and Kotsupalo, N. P., 1969, Reaction of lithiumaluminate hydrate with water: Izv. Sib. Otd. Akad. Nauk SSSR, Ser. Khim. Nauk, No. 6. p. 70-5.

Guseva, I. V., Kotsupalo, N. P.; Lileev, I. S.; Evteeva, O. G.; and Shirokova, P. V., 1967, Separation of lithium aluminate hydrate from solutions: Redk. Shchelochnye Elem., Sb. Dokl. Vses. Soveshch., 2nd Novosibirsk (Plyushchev, V. E., Ed.), p. 8691.

Kalmykov, V. A. and Markaryan, R. L., 1975, Solubility of water in synthetic aluminates melts: Izv. Akad. Nauk SSSR, Met., No. 4, p. 108-12.

Kolesova, V. A.; Sachenko-Sakun, L. K.; and Guseva, I. V., 1967, Hydrated lithium monoaluminate lithium oxide aluminum oxide in water: Zh. Neorg. Khim., V. 12, No. 11, p. 3220-2.

Kotsupalo, N. P. and Evteeva, O. G., 1970, Hightemperature hydrolysis of lithium dialuminate hydrate: Iav. Sib. Otd. Akad. Nauk SSSR, Ser. Khim. Nauk, No. 3, p. 147-50.

Kotsupalo, N. P.; Evteeva, O. G.; Poroshina, I. A.; and Samsonova, T. I., 1971, Lithium oxide-aluminum oxide-water system at 50°: Zh. Neorg. Khim., V. 16, No. 2, p. 483-9.

Kotsupalo, N. P.; Guseva, I. V.; Evteeva, O. G., and Lileev, I. S., 1967, Properties of lithium aluminate hydrate: Redk. Shchelochnye Elem., Sb. Dokl. Vsses. Soveshch., 2nd, Novosibirsk (Plyushchev, V. E., Ed.), p. 92-9.

Kotsupalo, N. P.; Pushnyakova, V. A.; and Berger, A. S., 1978, Lithium oxide-aluminum oxide-water system at 25, 75, 100, and 150 °C: Zh. Neorg. Khim., V. 23, No. 9, p. 2514-19.

Pelly, I., 1978, Recovery of lithium from Dead Sea brines: J. Appl. Chem. Biotechnol., V. 28, No. 7, p. 469-474.

Poroshina, I. A.; Kotsupalo, N. P.; Tatarintseva, M. I., Pushnyakova, V. A.; and Berger, A. S., 1978, Characteristics of the crystallization of solid phases in the lithium oxidealuminum oxidewater system at 25-150°: Zh. Neorg. Khim., V. 23, No. 8, p. 2232-6.

(C) Lithium-aluminum-hydrogen

1. Lithium hydride

Bergstein, A.; Spitz, J.; and Didier, R., 1968, Electrochemical properties of solid lithium hydride: Czech. J. Phys., V. 18, No. 4, p. 538-545.

Ptashnik, V. B.; Dunaeva, T. Y.; Baikov, Y. M., 1982, Influence of hydrogen pressure on the nature of conductivity of solid lithium hydride: Electrokhimiya, V. 18, No. 10, p. 1335-1339.

Roinel, Y., 1980, Neutron diffraction study of nuclear magnetic ordered phases and domains in lithium hydride: J. Phys. Lett., V. 41, No. 5, p. L123-L125.

Roinel, Y.; Bouffard, V.; and Roubeau, P., 1978, Nuclear Antiferromagnetism in lithium hydride: J. Phys., V. 39, No. 10, p. 1097-1103.

Shpil'rain, E. E.; Yakimovich, K. A.; Shereshevskii, V. A.; and Andrianova, V. G., 1978, V. 16, No. 6, p. 1204-1209.

Veleckis, E.; Van Deventer, E. H.; and Blander, M., 1974, Lithium-lithium hydride system: J. Phys. Chem., V. 78, No. 19, p. 1933-1940.

Wenzl, H., 1980, FeTi and lithium hydrides: properties and applications for hydrogen generation and storage: J. Less-Common Met., V. 74, No. 2, p. 351-361.

2. Lithium-aluminum hydride and lithium hydroaluminates

Akabori, S.; Takahashi, K.; Ohtomi, M.; and Sakamoto, Y., 1981, Abnormal lithium tetrahydroaluminate reduction of 4, 4-diphenyl-3-cyano-2-methyl-pyrrolin-5-one: Bull. Chem. Soc. Jpn., No. 12, p. 3867-8.

Ashby, E. C.; De Priest, R. N.; and Pham, T. N., 1983, Concerning the reduction of alkyl halides by lithium tetrahydroaluminate. Evidence that aluminum hydride produced in situ is the one-electron-transfer agent: Tetrahedron Lett., V. 24, No. 28, p. 2825-8.

Ashby, E. C.; Dobbs, F. R.; and Hopkins, H. P., Jr., 1975, Composition of lithium aluminum hydride, lithium borohydride, and their alkoxy derivatives in other solvents as determined by molecular association and conductance studies: J. Am. Chem. Soc., V. 97, No. 11, p. 3158-62.

Bakum, S. I. and Dymov, T. N., 1970, Fusibility diagram of the lithium aluminohydride-tetrahydrofuran system: Izv. Akad. Nauk SSSR, Ser. Khim., No. 8, p. 1890-1.

Bastide, J. P.; Bonnetot, B. M.; Letoffe, J. M.; and Claudy, P., 1983, Structural chemistry of some complex hydrides of alkali metals: Stud. Inorg. Chem., V. 3 (Solid State Chem.), p. 785-8.

Boldyrev, A. I. and Charkin, O. P., 1980, Nonempirical calculation of the structure and stability of a complex lithium tetrahydroaluminate molecule: Zh. Neorg. Khim., V. 25, No. 1, p. 110-16.

Bousquet, J. and Claudy, P., 1968, Lithium hexahydroaluminate (Patent): Patent No. France FR 1,604,706.

Bousquet, J.; Choury, J. J.; and Claudy, P., 1967, Simple and complex aluminum hydrides. III. Formation mechanism of hydrides and structural theory: Bull. Soc. Chem. Fr., No. 10, p. 3855-7.

Breicis, V.; Tarvide, A.; and Liepina, L., 1972, Composition of solutions of partially hydrolyzed lithium tetrahydroaluminate: Latv. PSR Zinat. Akad. Vestis, Kim. Ser., No. 6, p. 747.

Claudy, P.; Bonnetot, B.; Bastide, J. P.; and Letoffe, J. M., 1982, Reactions of lithium and sodium aluminum hydride with sodium or lithium hydride. Preparation of a new aluminohydride of lithium and sodium ($LiNa_2AlH_6$).

Claudy, P.; Bonnetot, B.; Letoffe, J. M.; and Turck, G., 1978, Determination of thermodynamic constants of simple and complex aluminum hydrides. IV. Enthalpy of formation of lithium tetrahydroaluminate and trilithium hexahydroaluminate: Thermochim. Acta, V. 27, No. 1-3, p. 213-21.

Dymova, T. N.; Roshchina, M. S.; Grazuliene, S.; and Kuznetsov, V. A., 1969, Lithium polyhydroaluminates: Dokl. Akad. Nauk SSSR, V. 184, No. 6, p. 1338-41.

Galova, M., 1982, Conductometric study of the composition of aluminum chloridelithium aluminum hydride ($LiAlH_4$) electrolyte in tetrahydrofuran: Chem. Zvesti, V. 36, No. 6, p. 791-7.

Gavrilenko, V. V.; Vinnikova, M. I.; Antonovich, V. A.; and Zakharkin, L. I., 1982, Aluminum-27 NMR study of the products of the exchange reaction of lithium and sodium aluminohydrides with $MAlR_4$-type tetraalkyl complexes: Izv. Akad. Nauk SSSR, Ser. Khim., No. 10, p. 2367-9.

Gorbunov, V. E.; Gavrichev, K. S.; and Bakum S. I., 1981, Thermodynamic properties of lithium tetrahydroaluminate in the 12-320 K range: Zh. Neorg. Khim., V. 26, No. 2, p. 311-13.

Herley, P. J. and Spencer, D. H., 1979, Photolytic decomposition of lithium aluminum hydride powder: J. Phys. Chem., V. 83, No. 13, p. 1701-1707.

Karpovskaya, M. I.; Turova, N. Y.; and Novoselova, A. V., 1977, Thermal decomposition of lithium and sodium alkoxyaluminates: Koord. Khim., V. 3, No. 9, p. 1296-8.

Lileev, I. S.; Sachenko-Sakun, L. K.; and Guseva, I. V., 1968, Interaction of lithium hydrodialuminate with solutions of caustic soda: Zh. Neorg. Khim., V. 13, No. 2, p. 412-16.

Mikheeva, V. I. and Arkhipov, S. M., 1967, Thermal decomposition of lithium aluminum hydride: Zh. Neorg. Khim., V. 12, No. 8, p. 2025-31.

Mikheeva, V. I.; and Troyanovskaya, E. A., 1971, Solubility of lithium tetrahydro aluminate and lithium borohydride in diethyl ether: Izv. Akad. Nauk SSSR, Ser. Khim., No. 12, p. 2627-30.

Mirsaidov, U.; Bakum, S. I.; Dymova, T. M., 1973, Solubility diagram of the lithium tetrahydroaluminatediglyme system and solubility isotherm in the lithium tetrahydroaluminatepotassium tetrahydroaluminate-diglyme system at 25°: Izv. Akad. Nauk SSSR, Ser. Khim., No. 2, p. 259-61.

Mirsaidov, U.; Pulatov, M. S.; Nazarov, P.; and Alikhanova, T. Kh., 1981, Solubility in the lithium tetrahydroaluminate-sodium tetrahydroaluminate-diethyl ether system at 25°: Zh. Neorg. Khim., V. 26, p. 1699-700.

Mukaibo, T. and Ryu, H., 1966, Thermodynamic study of aluminum hydride complexes. I. Heat of formation of lithium aluminum hydride: Kogyo Kagaku Zasshi, V. 69, No. 9, p. 1693-8.

Murphy, D. K.; Alumbaugh, R. L.; and Rickborn, B., 1969, Reduction of epoxides. III. Lithium aluminum hydride and mixed hydride reduction of some secondary-tertiary epoxides: J. Amer. Chem. Soc., V. 91, No. 10, p. 2649-53.

Nametkin, N. S.; Kuz'min, O. V.; Korolev, V. K.; and Chernysheva, T. I., 1972, Reduction of tetrahalides of germanium and tin by lithium tetrahydroaluminate: Izv. Akad. Nauk SSSR, Ser. Khim., No. 4, p. 985.

Noeth, H., 1980, Lithium tetrahydroaluminate in ether: an NMR study: Z. Naturforsch., B: Anorg. Chem., Org. Chem., V. 35B, No. 2, p. 119-24.

Noeth, H.; Rurlaender, R. and Wolfgardt, P., 1981, Solutions of lithium tetrahydroaluminates in ethers: a lithium-7 and aluminum-27 NMR study: Z. Naturforsch., B: Anorg. Chem., Org. Chem., V. 36B, No. 1, p. 31-41.

Novoselova, A. V.; Turova, N. Ya.; and Yanovskaya, M. I., 1975, Lithium alkoxyaluminates and alkoxyhydroaluminates: Tezisy Dokl.-Vses. Chugaevskoe Soveshch. Khim. Kompleksn. Soedin., 12th, V. 3, p. 472-3.

Osipov, G. A.; Belyaeva, M. S.; Klimenko, G. K.; Zakharkin, L. I.; Gavrilenko, V. V., 1970, Thermal decomposition of alkali metal tetrahydroaluminates: Kinet. Catal., V. 11, No. 4. pt. 1, p. 744-50.

Padma, D. K.; Murthy, A. R.; Vasudeva, A. R.; Becher, W.; and Massonne, J., 1973, Reduction of sulfur hexafluoride by lithium aluminum hydride: J. Fluorine Chem., V. 2, No. 1, p. 113-14.

Pizev, J. S., 1977, Synthetic Reagents: Lithium Aluminum Hydride: Chichester, England, Ellis Horwood, Ltd., 234 p.

Sakaliene, A.; Breicis, V.; and Liepina, L., 1970, Nature of the first exothermal effect on a lithium aluminohydride thermogram: Latv. PSR Zinat. Akad. Vestis, Kim. Ser., No. 1, p. 114-15.

Semenenko, K. N.; Il'ina, T. S.; and Surov, V. I., 1971, Enthalpy of lithium tetrahydroaluminate formation: Zh. Neorg. Khim., V. 16, No. 6, p. 1516-20.

Semenenko, K. N.; Lavut, E. A.; and Burlakova, A. G., 1973, Solubility in the lithium tetrahydroaluminatediethyl ethertoluene system: Zh. Neorg. Khim., V. 18, No. 8, p. 225-26.

Shen, P.; Zhang, Y.; Chen, S.; Yuan, H.; Che, R.; Ban, Y.; and Liu, D., 1982, A new route to lithium aluminum hydride ($LiAlH_4$): Gaodeng Xuexiao Huaxue Xuebao, V. 3, No. 2, p. 169-72.

Sklar, N. and Post, B., 1967, Crystal structure of lithium aluminum hydride: Inorg. Chem., V. 6, No. 4, p. 669-71.

Thompson, B. T.; Gallaher, T. N.; and DeVore, T. C., 1983, The reaction of lithium aluminum hydride with carbon dioxide or sodium bicarbonate: Polyhedron, V. 2, No. 7, p. 619-21.

Tranchant, J. and Mayet, J., 1970, Lithium hexahydroaluminate (Patent): Patent No. France FR 2,093,124.

Turova, N. Y.; Karpovskaya, M. I.; Novoselova, A. V.; Kirakosyan, G. A.; Tarasov, V. P.; and Kozlova, N. I., 1977, Alkali metal alkoxy-aluminates: Koord. Khim., V. 3, No. 9, p. 1299-308.

Yoshio, M. and Ishibashi, N., 1973, Highrate plating of aluminum from the bath containing aluminum chloride and lithium aluminum hydride in tetrahydrofuran: J. Appl. Electrochem., V. 3. No. 4, p. 321-325.

Yoshio, M.; Ishibashi, N.; Waki, H.; and Seiyama, T., 1972, Nature of the mixed hydrides between aluminum chloride and lithium aluminum hydride in anhydrous tetrahydrofuran: J. Inorg. Nucl. Chem., V. 34, No. 8, p. 2439-48.

Yoshio, M.; Miura, H.; Ishibashi, N.; and Takeshima, E., 1976, Studies of aluminum mixed hydrides in tetrahydrofuranbenzene solvents: J. Inorg. Nucl. Chem., V. 38, No. 12, p. 2314-15.

3. Li-Al-H

Field, D. J.; Butler, E. P.; and Scamans, G. N., 1980, High-temperature oxidation studies of Al-3wt.%Li, Al-4.2wt.%Mg, and Al-3wt.% Li-2wt.%Mg alloys; p. 325-345, in Lithium-Aluminum-Alloys: Warrendale, PA, TMS/AIME.

Gayle, F. W., 1980, Alloying additions and property modification in aluminum-lithium-x systems; p. 119-139 in Lithium-Aluminum-Alloys: Warrendale, PA, TMS/AIME.

Grushko, O. E.; Danilkin, V. A.; Zasypkin, V. A.; and Talaev, V. S., 1975, Hydrogen in aluminum alloys with lithium: Tekhnol. Legkikh Splavov. Nauch.-Tekhn. Byul. VILSa, No. 3, p. 711.

Hill, D. P. and Williams, D. N., 1982, Relationship between hydrogen content and low ductility in aluminum-lithium alloys: Battelle Columbus Laboratories, Report No. Ad-A121968, 42 p.

Ivanov, V. P., 1971, Effect of small additions of lithium on the gas content and mechanical properties of aluminum: Izv. Vyssh. Ucheb. Zaved., Tsvet. Met., V. 14, No. 3, p. 118-21.

Novikova, N. M.; Redin, V. I.; Dudenko, P. E.; and Plyushkin, S. A., 1979, Reaction of aluminum with water in the presence of activating additives: Zh. Neorg. Khim., V. 24, No. 6, p. 1722-3.

Owen, J. H. and Randall, D., 1976, Equilibrium and kinetic studies of systems of hydrogen isotopes, lithium hydrides, aluminum, and lithium aluminum dioxide: Proc. Int. Conf. Radiat. Eff. Tritium Technol. Fusion React. (Watson, J. S. and Wiffen, F. W., Eds.), V. 3, p. 433-457.

Talbot, J. B., Smith, F. J.; Land, J. F., and Barton, P., 1976, Tritium sorption in lithium-bismuth and lithium-aluminum alloys: J. Less Common Met., V. 50, No. 1, p. 23-28.

Veleckis, E., 1980, Thermodynamic investigation of the lithium-aluminum and lithiumlead systems by the hydrogen titration method: J. Less Common Met., V. 73, No. 1, p. 49-60.

(D) Lithium and/or aluminum with hydrogen and/or oxygen (oxide)

(author unspecified), 1968, Diffusion in simple and complex oxides, their mixtures and solutions: Diffusion data, V. 2, No. 3-4, p. 329-325.

Adams, P. F.; Hubberstey, P.; and Pulham, R. J., 1975, Review of the solubility of nonmetals in liquid lithium: J. Less Common Met., V. 42, No. 1, p. 1-11.

Antipin, V. P.; Danilkin, V. A.; and Grigoreva, A. A., 1981, On the interactions of hydrogen and oxides in aluminum melts: Liteinoe Proizvod., No. 5, p. 11-13.

Cox, B. N.; Bauschlicher, C. W., Jr., 1982, A cluster model of the chemisorption of atomic lithium, atomic oxygen and sodium by the (111) surface of aluminum: Surf. Sci., V. 115, No. 1, p. 15-36.

Csanady, A. and Kurthy, J., 1981, Oxidation behavior of aluminum alloys containing magnesium and lithium: J. Mater. Sci., V. 16, No. 10, p. 2919-2922.

David, D. J.; Froning, M. H.; Wittberg, T. N.; and Moddeman, W. E., 1981, Surface reactions of lithium with the environment: Appl. Surf. Sci., V. 7, No. 3, p. 185-195.

Emlin, B. I., 1973, Thermodynamics of the Al-O and Al-O-C systems: Izvest VUZ Tsvetnaya Met., No. 2, p. 80-86.

Fromm, E.; Jehn, H.; and Goerz, G., 1976, Gases and carbon in metals (thermodynamics, kinetics, and properties). Part I. Alkali metals, alkaline earth metals, light metals (lithium, sodium, potassium, rubidium, cesium; calcium, strontium, barium; beryllium, magnesium, aluminum): Phys. Daten/Phys. Data, No. 5-1, 26 p.

Gabidullin, R. M.; Kolachev, B. A.; and Zhuravlev, L. N., 1975, Relationship between the H solubility isobar in metals and the phase diagram: Izv. VUZ Tsvetn Metall, No. 3, p. 112-117.

Godshall, N. A.; Raistrick, I. D.; and Huggins, R. A., 1984, Relationships among electrochemical, thermodynamic, and oxygen potential quantities in lithium-transition metal-oxygen molten salt cells: J. Electrochem. Soc., V. 131, No. 3, p. 543-549.

Hubberstey, P.; Adams, P. F.; Pulham, R. J.; Down, M. G.; and Thunder, A. E., 1976, Hydrogen in liquid alkali metals: J. Less Common Met., V. 49, p. 253-69.

Khrushchev, M. S., 1969, Thermodynamic study of the Al-O-C system at high temperatures: Izvest Akad. Nauk SSSR Metally, V. 6, p. 46-49.

Koch, G. P., 1967, Aluminum and aluminum alloys: Encycl. Ind. Chem. Anal., V. 5, p. 110-58.

Konovalov, E. E.; Seliverstov, N. I.; Emel'yanov, V. P., 1968, Solubility of oxygen and chlorine in liquid lithium: Izv. Akad. Nauk SSSR, Metal., No. 3, p. 109-12.

Maroni, V. A.; Calaway, W. F.; Veleckis, E.; and Yonco, R. M., 1976, Solution behavior of hydrogen isotopes and other non-metallic elements in liquid lithium: DOE Report No. CONF-760503-5, p. 1-10.

Migge, H., 1980, Thermochemistry in the systems lithium-oxygen-hydrogen, lithium-oxygen-carbon, lithium-nitrogen carbon: Proc. Int. Conf. Liq. Met. Technol. Energy Prod., V. 2, No. 2, p. 18-9 to 18-7.

Migge, H., 1983, Thermodynamic stability of aluminum ceramics in liquid lithium: Comm. Eur. Communities, Report No. EUR 7983, Fusion Technol. V. 1, p. 655-61.

Pavlyuchenko, M. M. and Popova, T. I., 1969, Effect of the gas phase on the thermal stability of lithium peroxide: Dokl. Akad. Nauk Beloruss. SSR, V. 13, No. 2, p. 133-5.

Rohde, L. E.; Choudhury, A.; and Wahlster, M., 1971, New investigations on the Al-O equilibrium in iron melts: Arch Eisenhuttenwesen, V. 42, No. 3, p. 165-174.

Rumbaut, N. A., 1980, Solvation of some nonmetals in liquid lithium and sodium: Cent. Etude Energ. Nucl. Report No. BLG 536, p. 1-19.

Rumbaut, N.; Casteels, F.; and Brabers, M., 1982, Thermodynamic potential of nitrogen, carbon, oxygen and hydrogen in liquid lithim and sodium: Mater. Behav. Phys. Chem. Liq. Met. Syst. (Borgstedt, H. U., Ed.), p. 437-44.

Samsonov, G. V.; Dubovik, T. V.; Trunov, G. V.; Toropov, A. N.; and Sokhovich, E. V., 1983, Resistance of some nonoxygen materials to the effects of lithium and barium: Tugoplavkie Nitridy (Kosolapova, T. Ya., Ed.), p. 110-12.

Smith, J. F. and Moser, Z., 1976, Thermodynamic properties of binary Li systems: J. Nucl. Mater., V. 59, No. 2, p. 158-174.

Sonchik, S. M.; Andrews, L.; and Carlson, K. D., 1983, Matrix reactions of molecular oxygen and ozone with aluminum atoms: J. Phys. Chem., V. 87, No. 11, p. 2004-2011.

Talbot, D. E. J., 1975, Effects of H in Al, Mg, Cu and their alloys: Int. Metall. Rev., V. 20, p. 166-184.

Wenzl, H., 1980, Hydrogen in metals: Outstanding properties and examples of their utilization. I.: Metall., V. 34, No. 5, p. 407-412.

Weston, J. R.; Calaway, W. F.; Yonco, R. M.; Veleckis, E.; and Maroni, V. A., 1978, Experimental studies of processing conditions for liquid lithium and solid lithium alloy fusion blankets: Proc. Top. Meet. Technol. Controlled Nucl. Fusion, V. 3, No. 2, p. 697-705.

Weston, J. R.; Calaway, W. F.; Yonco, R. M.; Veleckis, E.; and Maroni, V. A., 1978, Experimental studies of processing conditions for liquid lithium and solid lithium alloy fusion blankets: DOE Report No. CONF-780508-40, p. 1-10.

Yanagida, H. and Kroger, F. A., 1968, The system Al-O: J. Amer. Ceram. Soc., V. 51, No. 12, p. 700-706.

Yonco, R. M. and Maroni, V. A., 1977, Solubility of lithium oxide in liquid Li: Trans. of the ANS 1977 Annual Meeting Am. Nucl. Soc., Inc., p. 166-167.

Yonco, R. M.; Maroni, V. A.; Strain, J. E. and Devan, J. H., 1979, A determination of the solubility of lithium oxide in liquid lithium by fast neutron activation: J. Nucl. Mater., V. 79, No. 2, p. 354-362.

Table 1. Phases in the System Li-Al-H-Li_2O-Al_2O_3-H_2O

(a) Solids with Published x-ray Powder Diffraction Data[a]

Phase	Thermochemical Data as f(T)[b]	Comments[c]
Li	X	melts 453.7 K
Al	X	melts 933.5 K
Li_3Al_2		melts incongruently 793 K (4)
LiAl	X	melts 973 K (4)
Li_9Al_2		melts incongruently 608 K (4)
LiH	X	melts 961.8 K
$LiAl_4H_{13}$		
$LiAlH_4$	X	decomposes 410 K
Li_3AlH_6		
AlH_3		
Li_2O	X	melts 1711 K (9)
Al_2O_3	X	melts 2327 K
αLi_5AlO_4		
βLi_5AlO_4		
$\alpha LiAlO_2$		
$\beta LiAlO_2$		
$\gamma LiAlO_2$	X	melts 1973 K
$LiAl_5O_8$		
LiOH	X	melts 744.3 K
$LiOH \cdot H_2O$		
$Al(OH)_3$		

Table 1. Phases in the System Li-Al-H-Li_2O-Al_2O_3-H_2O (continued)

(b) Selected Gases and Liquids

Phase	Thermochemical Data as f(T)[b]
Li(ℓ)	X
Al(ℓ)	X
H_2(g)	X
LiH(ℓ)	X
Li_2O(ℓ)	X
Al_2O_3(ℓ)	X
$LiAlO_2$(ℓ)	X
H_2O(g)	X
LiOH(ℓ)	X

[a]Source of x-ray data is Powder Diffraction File, 1983: JCPDS--International Center for Diffraction Data, Swarthmore, PA.

[b]Source of thermochemical data is JANAF Thermochemical Tables: Nat. Stand. Ref. Data Ser., Nat. Bur. Stand., 37 (June 1971; updates from Dow Chemical Company).

[c]Unless otherwise noted, data on melting or decomposition came from footnote 'b' above.

Table 2. Calculated Reactions at 1100K in the System Li-Al-H-Li_2O-Al_2O_3-H_2O*

Subsystem	Conditions (atm)	Reaction	ΔG_R(Kcal)
Li-Al-H	1	1/2-H_2(g) + LiAl(ℓ) → LiH(ℓ)+Al(ℓ)	-0.038
Li-Al-H	10	1/2-H_2(g) + LiAl(ℓ) → LiH(ℓ) + Al(ℓ)	-2.555
Li-Al-H	100	1/2-H_2(g) + LiAl(ℓ) → LiH(ℓ) + Al(ℓ)	-5.071
Li_2O-Al_2O_3-H_2O	1	2LiOH(ℓ) + Al_2O_3(c) → 2$LiAlO_2$(c) + H_2O(g)	-27.101
Li_2O-Al_2O_3-H_2O	10	2LiOH(ℓ) + Al_2O_3(c) → 2$LiAlO_2$(c) + H_2O(g)	-22.071
Li_2O-Al_2O_3-H_2O	100	2LiOH(ℓ) + Al_2O_3(c) → 2$LiAlO_2$(c) + H_2O(g)	-17.070
Li-Al-Li_2O-Al_2O_3	1	4Li(ℓ) + 2Al_2O_3(c) → 3$LiAlO_2$(c) + LiAl(ℓ)	-49.157
Li-Al-Li_2O-Al_2O_3	1	2Li_2O(c) + 4Al(ℓ) → $LiAlO_2$(c) + 3LiAl(ℓ)	-15.687
Li-Al-Li_2O-Al_2O_3	1	2Li_2O(c) + LiAl(ℓ) → 4Li(ℓ) + $LiAlO_2$(c)	-9.627
Li-Al-Li_2O-Al_2O_3	1	3LiAl(ℓ) + 2Al_2O_3(c) → 3$LiAlO_2$(c) + 4Al(ℓ)	-43.097
Li-H-Li_2O-H_2O	1	2Li(ℓ) + H_2O(g) → LiOH(ℓ)+LiH(ℓ)	-34.439
Li-H-Li_2O-H_2O	10	2Li(ℓ) + H_2O(g) → LiOH(ℓ) + LiH(ℓ)	-39.469
Li-H-Li_2O-H_2O	100	2Li(ℓ) + H_2O(g) → LiOH(ℓ) + LiH(ℓ)	-44.470
Li-H-Li_2O-H_2O	1	Li_2O(c) + H_2(g) LiOH(ℓ) + LiH(ℓ)	+29.042
Li-H-Li_2O-H_2O	10	Li_2O(c) + H_2(g) LiOH(ℓ) + LiH(ℓ)	+34.075
Li-H-Li_2O-H_2O	100	Li_2O(c) + H_2(g) → LiOH(ℓ) + LiH(ℓ)	+39.108
Li-H-Li_2O-H_2O	1	Li_2O(c) + LiH(ℓ) → Li(ℓ) + LiOH(ℓ)	+32.148
Li-H-Li_2O-H_2O	10	LiH(ℓ) + H_2O(g) → LiOH(ℓ) + H_2(g)	-31.33
H-Al-H_2O-Al_2O_3	1	3H_2(g) + Al_2O_3(c) → 3H_2O(g) + 2Al(ℓ)	+183.335
Li-Al-H-Li_2O-Al_2O_3 -H_2O	1	$LiAlO_2$(c) + 4LiH(ℓ) → 2Li_2O(c) + LiAl(ℓ) + 2H_2(g)	+15.839
Li-Al-H-Li_2O-Al_2O_3 -H_2O	10	$LiAlO_2$(c) + 4LiH(ℓ) → 2Li_2O(c) + LiAl(ℓ) + 2H_2(g)	+25.905
Li-Al-H-Li_2O-Al_2O_3 -H_2O	100	$LiAlO_2$(c) + 4LiH(ℓ) 2Li_2O(c) + LiAl(ℓ) + 2H_2(g)	+35.971

*Calculated using data in JANAF tables; data for LiAl(ℓ) estimated using ideal solution approximation; hydrogen assumed to behave ideally.

Table 3. DTA effects observed in the Subsystem Li_2O-$LiAlO_2$

Composition (mol%)	Temp. (°C)	Type[a]	Magnitude[b]	Comments
$(Li_2O)_{100}$	1446 ± 3	N	81	
$(Li_2O)_{95}(Al_2O_3)_5$	480	X(H)	4	
$(Li_2O)_{95}(Al_2O_3)_5$	540	X(H)	6	
$(Li_2O)_{95}(Al_2O_3)_5$	790	N(H)	15	
$(Li_2O)_{95}(Al_2O_3)_5$	1210	N	---	Onset of event
$(Li_2O)_{95}(Al_2O_3)_5$	1365	N	15	Estimated termination
$(Li_2O)_{90}(Al_2O_3)_{10}$	465	X(H)	4	
$(Li_2O)_{90}(Al_2O_3)_{10}$	527	X(H)	8	
$(Li_2O)_{90}(Al_2O_3)_{10}$	778	N(H)	18	
$(Li_2O)_{90}(Al_2O_3)_{10}$	1110	N	33	
$(Li_2O)_{90}(Al_2O_3)_{10}$	1300	N	5	
$(Li_2O)_{85}(Al_2O_3)_{15}$	455	X(H)	12	
$(Li_2O)_{85}(Al_2O_3)_{15}$	500	X(H)	8	
$(Li_2O)_{85}(Al_2O_3)_{15}$	775	N(H)	24	
$(Li_2O)_{85}(Al_2O_3)_{15}$	1126 ± 10	N	160	
$(Li_2O)_{80}(Al_2O_3)_{20}$	482	X(H)	8	
$(Li_2O)_{80}(Al_2O_3)_{20}$	525	X(H)	6	
$(Li_2O)_{80}(Al_2O_3)_{20}$	815	N(H)	31	
$(Li_2O)_{80}(Al_2O_3)_{20}$	947 ± 1	N	2	
$(Li_2O)_{80}(Al_2O_3)_{20}$	1057 ± 3	N	90	Two peaks overlap partially
$(Li_2O)_{80}(Al_2O_3)_{20}$	1095 ± 10	N	20	
$(Li_2O)_{75}(Al_2O_3)_{25}$	478	X(H)	16	
$(Li_2O)_{75}(Al_2O_3)_{25}$	520	X(H)	8	

Table 3. DTA effects observed in the Subsystem Li_2O-$LiAlO_2$ (continued)

Composition (mol%)	Temp. (°C)	Type	Magnitude	Comments
$(Li_2O)_{75}(Al_2O_3)_{25}$	810	N(H)	19	
$(Li_2O)_{75}(Al_2O_3)_{25}$	1026 ± 6	N	224	
$(Li_2O)_{70}(Al_2O_3)_{30}$	470	X(H)	12	
$(Li_2O)_{70}(Al_2O_3)_{30}$	521	X(H)	3	
$(Li_2O)_{70}(Al_2O_3)_{30}$	805	N(H)	22	
$(Li_2O)_{70}(Al_2O_3)_{30}$	950	N(H)	1	
$(Li_2O)_{70}(Al_2O_3)_{30}$	1050 ± 2	N	85	
$(Li_2O)_{65}(Al_2O_3)_{35}$	480	X(H)	3	
$(Li_2O)_{65}(Al_2O_3)_{35}$	525	X(H)	4	
$(Li_2O)_{65}(Al_2O_3)_{35}$	815	N(H)	7	
$(Li_2O)_{65}(Al_2O_3)_{35}$	1053	N	49	
$(Li_2O)_{60}(Al_2O_3)_{40}$	480	X(H)	3	
$(Li_2O)_{60}(Al_2O_3)_{40}$	520	X(H)	2	
$(Li_2O)_{60}(Al_2O_3)_{40}$	816	N(H)	8	
$(Li_2O)_{60}(Al_2O_3)_{40}$	956 ± 10	N	1	
$(Li_2O)_{60}(Al_2O_3)_{40}$	1056 ± 4	N	48	
$(Li_2O)_{55}(Al_2O_3)_{45}$	1054 ± 5	N	19	

[a] N = endothermic
X = exothermic
(H) = initial heating cycle only

[b] Approximate amplitude of thermal excursion, in mV

Table 4. Sequential Heat Treatments of High Alumina Compositions[a]

Composition (mole ratio) Li_2CO_3:Al_2O_3	Heat Treatment (°C)	Duration (hr)	X-ray analysis
50:50	500	40	Li_2CO_3 + Al_2O_3 + $LiAlO_2$
50:50	700	16	α-$LiAlO_2$ + γ-$LiAlO_2$ + Al_2O_3 (+tr.Li_2CO_3)
50:50	700	24	α-$LiAlO_2$ + γ-$LiAlO_2$
50:50	800	3	γ-$LiAlO_2$
50:50	850	5	γ-$LiAlO_2$
50:50	1000	60	γ-$LiAlO_2$
50:50	1400	4	γ-$LiAlO_2$
50:50	1500	0.5	γ-$LiAlO_2$
50:50	1600	1	γ-$LiALO_2$ (no melting)
50:50	575	768	α-$LiAlO_2$ (+tr.Al_2O_3 + tr.Li_2CO_3)
33:67	700	20	(not x-rayed)
33:67	1000	72	γ-$LiAlO_2$ + $LiAl_5O_8$
33:67	1000	1	γ-$LiAlO_2$ + $LiAl_5O_8$ (no melting)
(17.3):(82.7)	700	24	$LiAl_5O_8$
(17.3):(82.7)	1000	168	$LiAl_5O_8$
(17.3):(82.7)	1400	16	$LiAl_5O_8$ + unidentified peak
(17.3):(82.7)	1600	1	$LiAl_5O_8$ + unidentified peak
(17.3):(82.7)	1600 (sealed capsule)	12	$LiAl_5O_8$ (unidentified peaks disappeared)
(17.3):(82.7)	1600 (unsealed capsule)	12	$LiAl_5O_8$ (unidentified peaks disappeared)
(16.7):(83.3)	700	24	$LiAl_5O_8$ (no unidentified peaks)
(16.7):(83.3)	1000	168	$LiAl_5O_8$ (no unidentified peaks)
(16.7):(83.3)	1400	16	$LiAl_5O_8$ (no unidentified peaks)
(16.7):(83.3)	1600	1	$LiAl_5O_8$ (no unidentified peaks and no melting)

Table 4 (continued)

---

[a]Unless otherwise noted, these experiments were performed in a rapid-fire muffle furnace using a large smple (up to several grams) in a covered Pt crucible; mechanical homogenization was completed between heatings at lower temperatures for many of the experiments.

Table 5. Experiments in Sealed Mo Tubes, in Tungsten Furnace

Composition (Mole ratio $Li_2O:Al_2O_3$)	Temperature (°C)	Duration (hr)	Observtions
50:50	1725	3	no melt
50:50	1765	3	partial melt
50:50	1805	3	complete melt
33:67	1600	1	no melt
33.67	1725	3	complete melt
33:67	1805	1	complete melt
33:67	1665	1	complete melt
33:67	1630	1	sintered or possible partial melt
17:83	1725	3	no melt
17:83	1765	1	sintered or possible partial melt
17:83	1805	1	partial melt

Table 6. Results of Rietveld Refinement[a] of $LiAl_5O_8$

(a) Summary

Space Group = $P4_332$

Rw = 0.077

a = 7.9036(1) Å

Structural formula = $A_8^{IV}(Li_4Al_{12})^{VI}O_{32}$

(b) Tetrahedral cations[b,c]

8 Al at position 8(c) at (x, x, x); with: x = -0.0014(6)
B = 0.23(6)

(c) Octahedral cations

12 Al at position 12(d) at (1/8, x, 1/4-x); with: x = 0.3689(5)
B = 0.35(8)

4 Li at position 4(b) at (5/8, 5/8, 5/8); with: B = 2.3(4)

(d) Anions

24 O at position 24(e) at (x, y, z); with: x = 0.1145(3)
y = 0.1330(3)
z = 0.3842(2)
B = 0.28(4)

8 O at position 8(c) at (x, x, x); with: x = 0.3854(3)

(e) First coordination distances		D (in Å)
Al in 12(d) to 2 O in 24(e)		1.850(4)
Al in 12(d) to 2 O in 24(e)		1.911(2)
Al in 12(d) to 2 O in 8(c)		1.943(7)
	Average of 6 distances	1.901 ± 0.042
Al in 8(c) to 3 O in 24(e)		1.77(5)
Al in 8(c) to 1 O in 8(c)		1.83(7)
	Average of 4 distances	1.785 ± 0.026
Li in 4(b) to 6 O in 24(e)		2.042(2)

Table 6 (continued)

(f) Second coordination sphere	D(in Å)
Al in 12(d) to 4 Al in 12(d)	2.829(3)
Al in 12(d) to 2 Li in 4(b)	2.761(3)
Al in 12(d) to 2 Al in 8(c)	3.32(3)
Al in 12(d) to 2 Al in 8(c)	3.27(3)
Al in 12(d) to 2 Al in 8(c)	3.23(3)
Li in 4(b) to 6 Al in 12(d)	2.761(3)
Li in 4(b) to 6 Al in 8(c)	3.287(3)
Al in 8(c) to 3 Al in 12(d)	3.23(3)
Al in 8(c) to 3 Al in 12(d)	3.27(3)
Al in 8(c) to 3 Al in 12(d)	3.32(3)
Al in 8(c) to 3 Al in 8(c)	3.409(5)
Al in 8(c) to 1 Al in 8(c)	3.461(5)
Al in 8(c) to 3 Li in 4(b)	3.29(1)

[a]Rietveld, H. M., J. Appl. Crystallogr. 2 [1]65 (1969).

[b]Hahn, T. (Ed.), International Tables for Crystallography. Volume A: Dordrecht, Holland, D. Reidel Publ. Co. (1983), p. 638.

[c]B is isotropic thermal parameter.

Table 7. Results of Calcining High-Lithia Compositions Under Vacuum[a]

Composition (Mole ratio $Li_2O:Al_2O_3$)	Temperature (°C)	Duration (hr)	X-ray Analysis
90:10	900	56	$\gamma LiAlO_2$, βLi_5AlO_4, Li_2O, unidentified phase
83:17	700	6	αLi_5AlO_4, $\beta LiAlO_4$, Li_2O, Li_2CO_3, $\gamma LiAlO_2$
83:17	800	6	Li_2O, $\gamma LiAlO_2$, βLi_5AlO_4
83:17	800	6	αLi_5AlO_4, βLi_5AlO_4, $\gamma LiAlO_2$, Li_2O
83:17	900	23	$\gamma LiAlO_2$, βLi_5AlO_4
75:25	800	15	Li_2O, $\gamma LiAlO_2$, βLi_5AlO_4

[a]Lithium carbonate starting material; final vacuum 5 X 10^{-6} torr.

Table 8. Results of Quenching Experiments in Sealed Pt Tubes

Composition (Mole % Li_2O)	Heat Treatment[a] (°C)	Phases Present in X-ray pattern[b]
95	900	Li_2O + $\gamma LiAlO_2$ (+ tr. LiOH)
95	1000[c]	Li_2O + $\gamma LiAlO_2$ (+ tr. LiOH) + unidentified phase with peak at 23.70°
95	1050[c]	Li_2O + $\gamma LiAlO_2$ (+ tr. LiOH) + unidentified phase with peak at 23.70°
90	900	Li_2O + $\gamma LiAlO_2$ (+ tr. LiOH)
85	700	αLi_5AlO_4 (+ tr. LiOH)
85	750	αLi_5AlO_4 (+ tr. LiOH)
85	800	βLi_5AlO_4 (+ tr. LiOH) + unidentified phase with peak at 22.20°
85	850	αLi_5AlO_4 (+ tr. LiOH)
85	900	βLi_5AlO_4 (+ tr. LiOH)
85	900	βLi_5AlO_4 (+ tr. LiOH)
80	700	βLi_5AlO_4 + $\gamma LiAlO_2$ (+ tr. LiOH)
80	700	αLi_5AlO_4 + $\gamma LiAlO_2$ (+ tr. LiOH)
80	750	αLi_5AlO_4 + $\gamma LiAlO_2$ (+ tr. LiOH)
80	800	βLi_5AlO_4 + $\gamma LiAlO_2$ (+ tr. LiOH)
80	850	αLi_5AlO_4 + $\gamma LiAlO_2$ (+ tr. LiOH)
80	850	βLi_5AlO_4 + $\gamma LiAlO_2$ (+ tr. LiOH)
80	900	βLi_5AlO_4 + $\gamma LiAlO_2$ (+ tr. LiOH)
80	900	βLi_5AlO_4 + $\gamma LiAlO_2$ (+ tr. LiOH)
80	900	αLi_5AlO_4 + $\gamma LiAlO_2$ (+ tr. LiOH)
75	800	βLi_5AlO_4 + $\gamma LiAlO_2$
75	1000	βLi_5AlO_4 + $\gamma LiAlO_2$
60	900	$\gamma LiAlO_2$ (+ tr. LiOH) + undentified phase with peak at 18.60°
55	900	$\gamma LiAlO_2$ + $\beta LiAlO_4$
55	900	$\gamma LiAlO_2$ + $\beta LiAlO_4$

[a]Times of heat treatment were variable, from a few hours to a few days
[b]X-ray work completed using CuKα radiation
[c]runs partially melted

Table 9. Second and Third Law Heats of Reaction and Second Law Entropy of Reaction for Equation (14).

Experiment	ΔH(298) kcal/mol	ΔS(298) Gibbs/mol	ΔH(298) 3rd law kcal/mol
825D	131.4 ± 5.2[a]	48.21 ± 3.30	115.3 ± 0.3
826I	88.1 ± 6.5	22.89 ± 3.95	113.5 ± 0.6
826I2	103.2 ± 1.0	31.29 ± 0.59	115.0 ± 0.3
826D	109.0 ± 0.8	34.28 ± 0.48	115.7 ± 0.2
901I	97.8 ± 1.1	28.93 ± 0.63	113.6 ± 0.4
901D	110.7 ± 1.4	35.75 ± 0.79	115.0 ± 0.1
902I	101.9 ± 1.4	30.21 ± 0.87	115.3 ± 0.3
902D	115.2 ± 0.9	36.97 ± 0.53	117.3 ± 0.1

[a] Uncertainties are standard errors

Table 10. Second and Third Law Heats of Reaction and Second Law Entropy of Reaction for Equation (15).

Experiment	ΔH(298) kcal/mol	ΔS(298) Gibbs/mol	ΔH(298) 3rd law kcal/mol
912I	126.1 ± 9.1[a]	41.62 ± 5.57	124.9 ± 0.3
912I2	108.7 ± 2.7	31.45 ± 1.59	125.0 ± 0.4
912D	127.1 ± 4.1	40.55 ± 2.35	127.6 ± 0.2
104I	110.3 ± 1.9	32.28 ± 1.91	125.6 ± 0.4
104D	130.3 ± 1.6	42.25 ± 0.92	127.8 ± 0.1
105I	124.5 ± 3.0	39.12 ± 1.66	127.6 ± 0.3
105D	131.3 ± 1.5	41.92 ± 0.84	129.3 ± 0.1
1014I	106.3 ± 1.9	27.14 ± 1.11	130.8 ± 0.8
1017I	102.4 ± 3.5	25.16 ± 1.90	131.2 ± 1.0
1017D	124.4 ± 1.0	36.16 ± 0.56	133.2 ± 0.2

[a] Uncertainties are standard errors.

Table 11. Third Law Heats of Reaction (at 298K) from Various Workers.

Reference	Reaction A kcal	Reaction B kcal	Reaction C kcal
Guggi (25)	109.4	119.9	128.3
Ikeda (31)	107.3	118.5	125.3
Potter (27)	-	120.8	131.8
This Work	-	117.3	127.8

Reactions

A. $1/4\ Li_5AlO_4(c) = Li(g) + 1/4\ O_2(g) + 1/4\ LiAlO_2(c)$

B. $5/4\ LiAlO_2(c) = Li(g) + 1/4\ O_2(g) + 1/4\ LiAl_5O_8(c)$

C. $LiAl_5O_8(c) = Li(g) + 1/4\ O_2(g) + 5/2\ Al_2O_3(c)$

Table 12. Reference Thermodynamic Data (8)

Material	ΔH_f° (298.15), kcal/mol
$Al_2O_3(c,\alpha)$	-400.500
Li(g)	38.140
$Li_2O(c)$	-143.100
$LiAlO_2(c)$	-284.100

Table 13. Heats of Formation (at 298K) from Vapor Pressure Data

Reference	$-AH_f^\circ\ LiAl_5O_8$ kcal/mol	$-\Delta H_f^\circ\ LiAlO_2$ kcal/mol	$-\Delta H_f^\circ\ LiAl_5O_4$ kcal/mol
	Reaction C	Reaction B	Reaction B	Reaction A
This work	1090.7	1104.9	281.3	
Potter (27)	1094.7	1090.9	284.9	
Guggi (25)	1094.5	1094.5	283.4	568.9
Ikeda (31)	1088.2	1100.1	281.7	560.7
JANAF (16)			284.1	
Average	1091.2	1097.6	282.8	

Table 14. Gibbs Enegies of Formation for Lithium-Aluminum-Oxygen Compounds (Model 3 Data Base)

SPECIES	COEFFICIENTS					
	A	B	C	D	E	F
LiO(g)	10675810000.	-37459100.	188365.78	6.957826	-0.0003699654	-24305.995
Li_2(g)	21383450000.	-74988600.	377318.64	13.936999	-0.0007411582	-48685.048
Li_2O(g)	21389800000.	-75390800.	377532.05	13.940880	-0.0007412760	-48703.793
$LiAlO_2$(ℓ)	8065290000.	-29502100.	142510.96	5.2464154	-0.0002777273	-18354.51
Al_2O_3(ℓ)	- 510210000.	1189700.	-20394.75	-1.214575	0.0000920599	2825.80
Li_2O(ℓ)	21393580000.	-75813400.	378099.92	13.946336	-0.0007416116	-48758.08
$LiAl_5O_8$(ℓ)	3642360000.	-26913900.	185599.79	12.490429	-0.0010968965	-25659.98
Li_5AlO_4(ℓ)	0.	-2214900.	392.34	0.	0.	0.
$LiAlO_2$(s)	8065290000.	-29590000.	142554.50	5.2464154	-0.0002777273	-18354.51
Al_2O_3(s)	-8530000.	-1652600.	0.	-0.026405	0.0000019218	46.92
$LiAl_5O_8$(s)	3642360000.	-27219500.	185741.93	12.490429	-0.0010968965	-25659.98
Li_2O(s)	16136370000.	-57436400.	285145.82	10.508476	-0.0005588794	-36755.96
Li_5AlO_4(s)	10089950000.	-32299400.	114201.00	2.115251	0.	-13868.31

Coefficients are quoted in joules to yield rounding of ~ 400 J (0.1 kcal) and are for the following equation:

$$\Delta G = A/T + B + CT + DT^2 + ET^3 + FT\ell nT$$

Table 15. Gibbs Energy of Formation (kcal/mol) at Temperatures (K) for Model 3 Data Base

T (K)	1750	1800	1850	1900	1950	2000	2050	2100	2150
LiO(g)	-5.081	-4.747	-4.367	-3.959	-3.538	-3.118	-2.704	-2.293	-1.895
Li_2(g)	8.784	9.709	10.728	11.799	12.893	13.992	15.078	16.153	17.205
Li_2O(g)	-53.073	-51.371	-49.576	-47.727	-45.859	-43.989	-42.126	-40.279	-38.459
$LiAlO_2$(ℓ)	-185.317	-182.020	-178.685	-175.328	-171.960	-168.586	-165.215	-161.846	-158.479
Al_2O_3(ℓ)	-260.909	-257.410	-253.936	-250.486	-247.060	-243.658	-240.280	-236.924	-233.587
Li_2O(ℓ)	-82.036	-78.866	-75.621	-72.337	-69.042	-65.757	-62.497	-59.260	-56.054
$LiAl_5O_8$(ℓ)	-712.641	-703.316	-693.915	-684.463	-674.989	-665.536	-656.143	-646.859	-637.740
Li_5AlO_4(ℓ)	-365.274	-360.585	-355.897	-351.208	-346.519	-341.831	-337.142	-332.454	-327.765
$LiAlO_2$(s)	-188.115	-184.297	-180.443	-176.565	-172.677	-168.782	-164.891	-161.002	-157.115
Al_2O_3(s)	-266.466	-262.581	-258.702	-254.827	-250.958	-247.094	-243.235	-239.381	-235.532
$LiAl_5O_8$(s)	-726.229	-715.206	-704.106	-692.955	-681.784	-670.632	-659.540	-648.556	-637.739
Li_2O(s)	-82.852	-79.279	-75.650	-71.993	-68.331	-64.681	-61.054	-57.446	-53.870
Li_5AlO_4(s)	-342.659	-332.112	-321.572	-311.078	-300.660	-290.335	-280.119	-270.017	-260.032

Table 16. Representative Computer Model Output for the Equimolar Li_2O-Al_2O_3 Mixture

T = 1915 K
P = 1.0 atm

	X*/MOL	Y/MOL	P/ATM	ACTIVITY	$\Delta G_f(T)$, kcals	log Kp
Ar(g)	1.00000+000	1.00000+000	9.99899-001	9.99899-001	.000	.000
Li(g)	1.00000+001	7.52367-005	7.52291-005	7.52291-005	.000	.000
LiO(g)	.00000	8.88093-007	8.88003-007	8.88003-007	-3.833	.437
Li_2(g)	.00000	2.33881-010	2.33858-010	2.33858-010	12.125	-1.384
Li_2O(g)	.00000	5.89545-006	5.89485-006	5.89485-006	-47.169	5.383
O_2(g)	1.00000+001	1.85873-005	1.85854-005	1.85854-005	.000	.000
			MOLE FRACTION			
$LiAlO_2$(ℓ)	.00000	1.81706-004	7.52811-001	7.52811-001	-174.318	19.894
Al_2O_3(ℓ)	.00000	2.68847-005	1.11384-001	1.11384-001	-249.454	28.469
Li_2O(ℓ)	.00000	8.18210-007	3.38986-003	3.38986-003	-71.350	8.143
$LiAl_5O_8$(ℓ)	.00000	2.04535-005	8.47391-002	8.47391-002	-681.619	77.790
Li_5AlO_4(ℓ)	.00000	1.15077-005	4.76765-002	4.76765-002	-349.800	39.921
$LiAlO_2$(s)	.00000	9.99965+000		1.00000+000	-175.39870	20.01741
Al_2O_3(s)	.00000	.00000		3.36814-001	-253.66504	28.94958
$LiAl_5O_8$(s)	.00000	.00000		6.90510-001	-689.60182	78.70096
Li_2O(s)	.00000	.00000		3.00815-003	-70.89531	8.09094
Li_5AlO_4(s)	.00000	.00000		7.96765-007	-307.94272	35.14403
Al(ℓ)	1.00000+001	.00000		6.87113-012	.00000	.00000

ALLIO-HI/22 computer run

Computer notation used for exponents, eg. 1.00000+001 = 10

Table 17. Reactions in the Region of 50% Li_2O-50% Al_2O_3 (model 3 data base)

Temperature	Reaction (mole fraction/partial pressure, atm)
1905 K	(a) $5LiAlO_2(s) = LiAl_5O_8(s) + 4Li(g) + O_2(g)$
	(1.0) (1.0) (6.1×10^{-5}) (1.5×10^{-6})
1915 K	(b) $LiAlO_2(s) = "LiAlO_2(\ell)" + Li(g) + O_2(g)$
	(1.0) (0.99) (7.5×10^{-5}) (1.9×10^{-5})
	where $"LiAlO_2(\ell)" = LiAlO_2(\ell) + Li_2O(\ell) + Al_2O_3(\ell) + LiAl_5O_8(\ell) + Li_5AlO_4(\ell)$
	(0.75) (3.4×10^{-3}) (0.11) (8.5×10^{-2}) (4.8×10^{-2})
1920 K	(c) $LiAlO_2(\ell) = Li_5AlO_4(\ell) + Li_2O(\ell) + Al_2O_3(\ell) + LiAl_5O_8(\ell) + Li(g) + O_2(g)$
	(0.76) (0.095) (0.0045) (0.087) (0.053) (8.9×10^{-5}) (2.3×10^{-5})

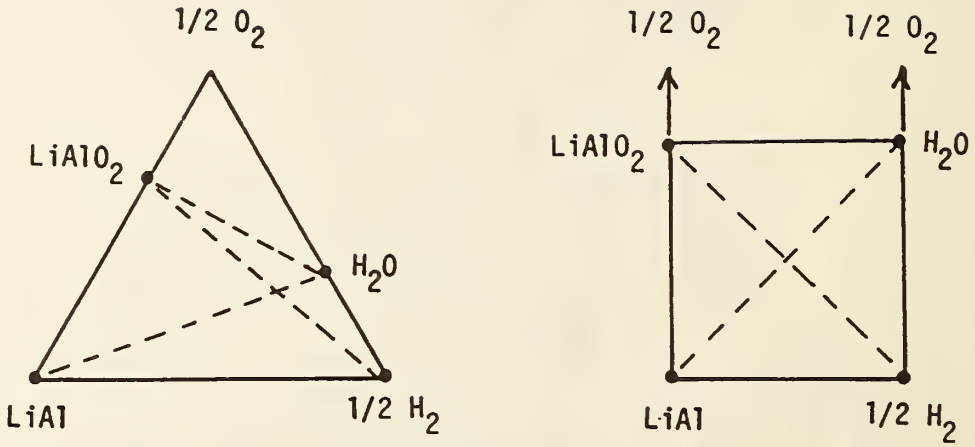

(a) (b)

Figure 1

Alternative representations of Phases in the (Li, Al) alloy reaction system.

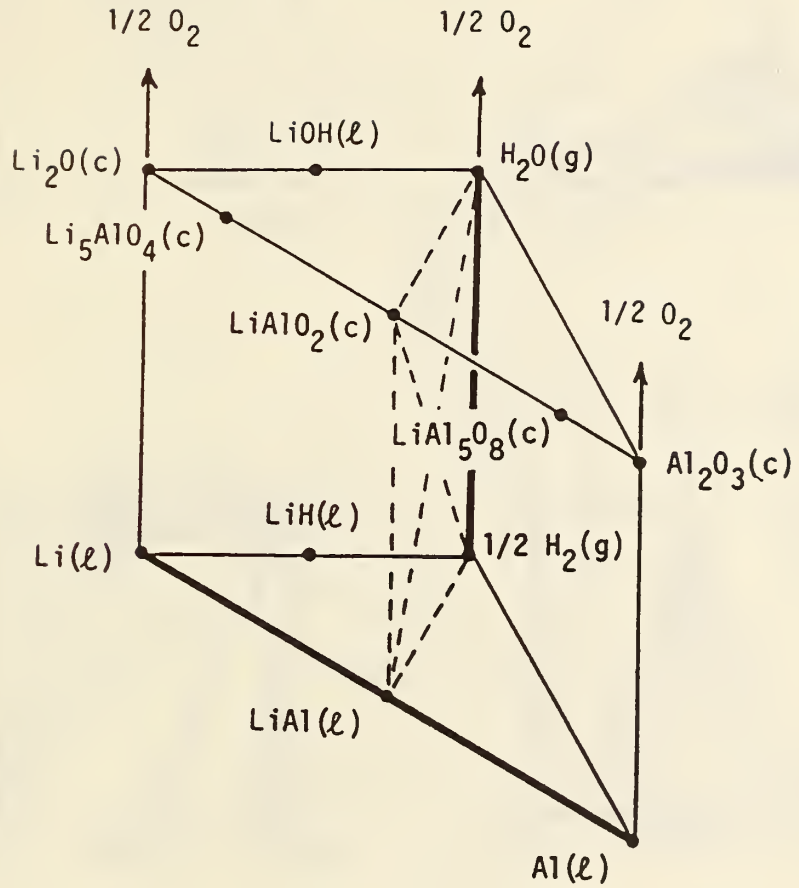

Figure 2

Representation of important phases in the Li-Al-H-Li_2O-Al_2O-H_2O portion of the system Li-Al-O-H.

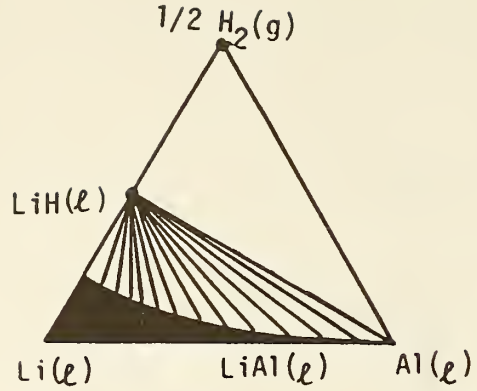

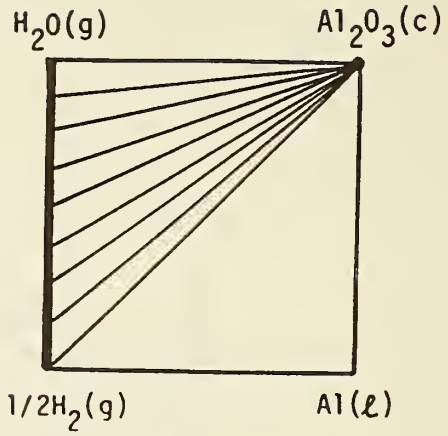

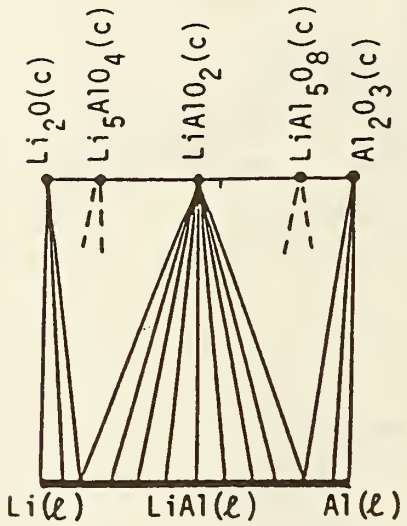

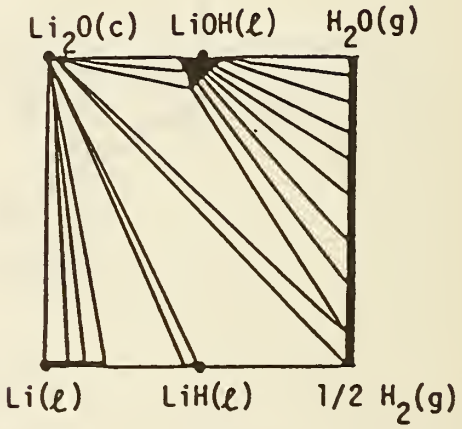

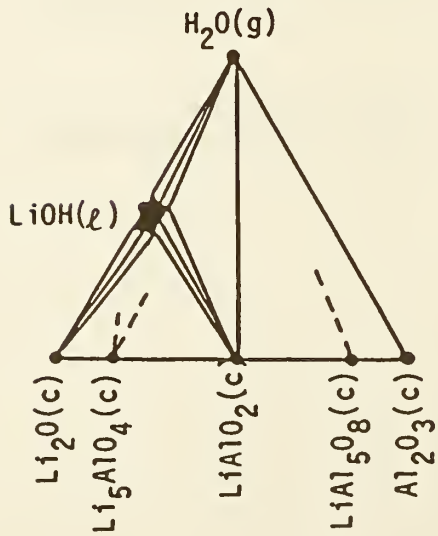

Figure 3

Schematic 1100 K phase diagrams for the ternary boundary systems of figure 2 (based upon calculations in Table 2).

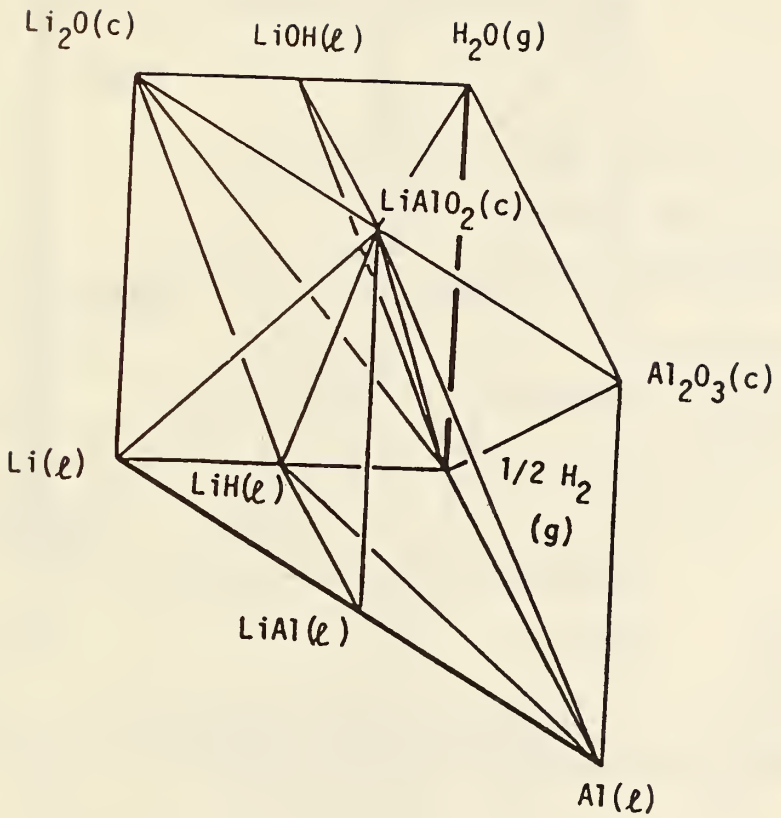

Figure 4

Major features of phase compatibility in the system Li-Al-H-Li_2O-Al_2O_3-H_2O at 1100 K: extent of solutions is not indicated.

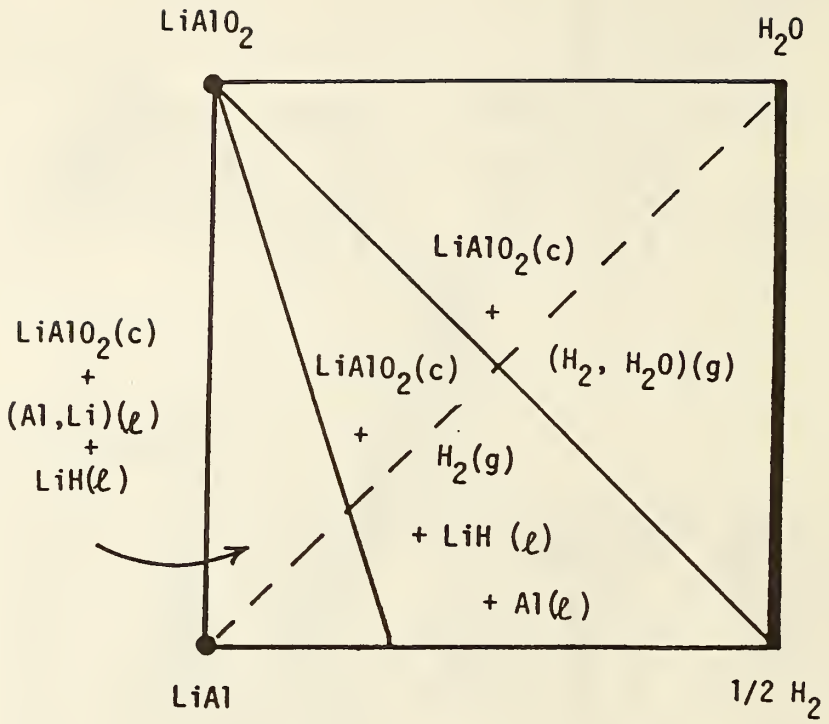

Figure 5

Predicted products of the equilibrium reaction of (LiAl) alloy with water at 1100 K.

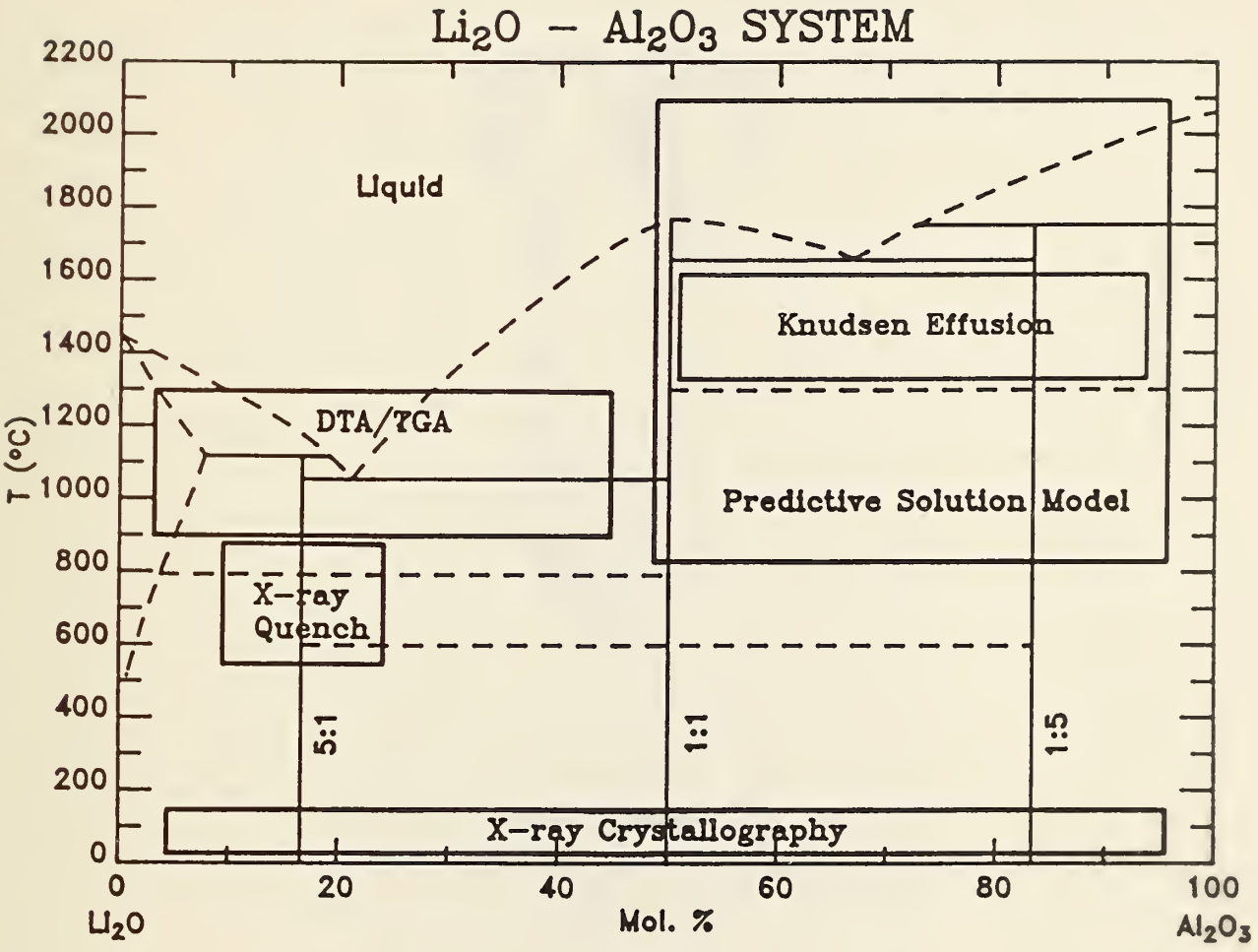

Figure 6

Interim phase diagram based on the approaches used in investigating various portions of the phase diagram (indicated in the boxed areas).

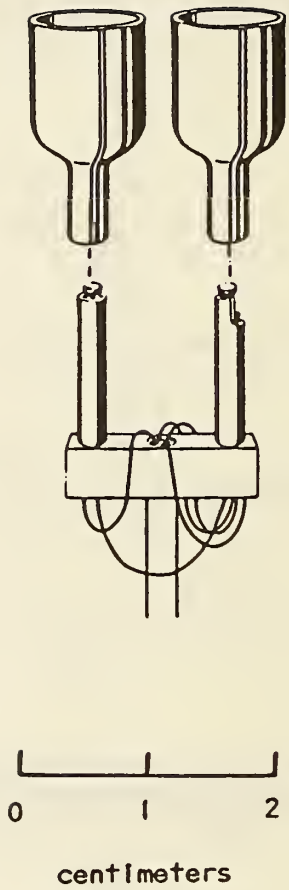

Figure 7

Experimental geometry for DTA measurements showing Pt Cells, Pt-10% Rh thermocouples, and the alumina support structure.

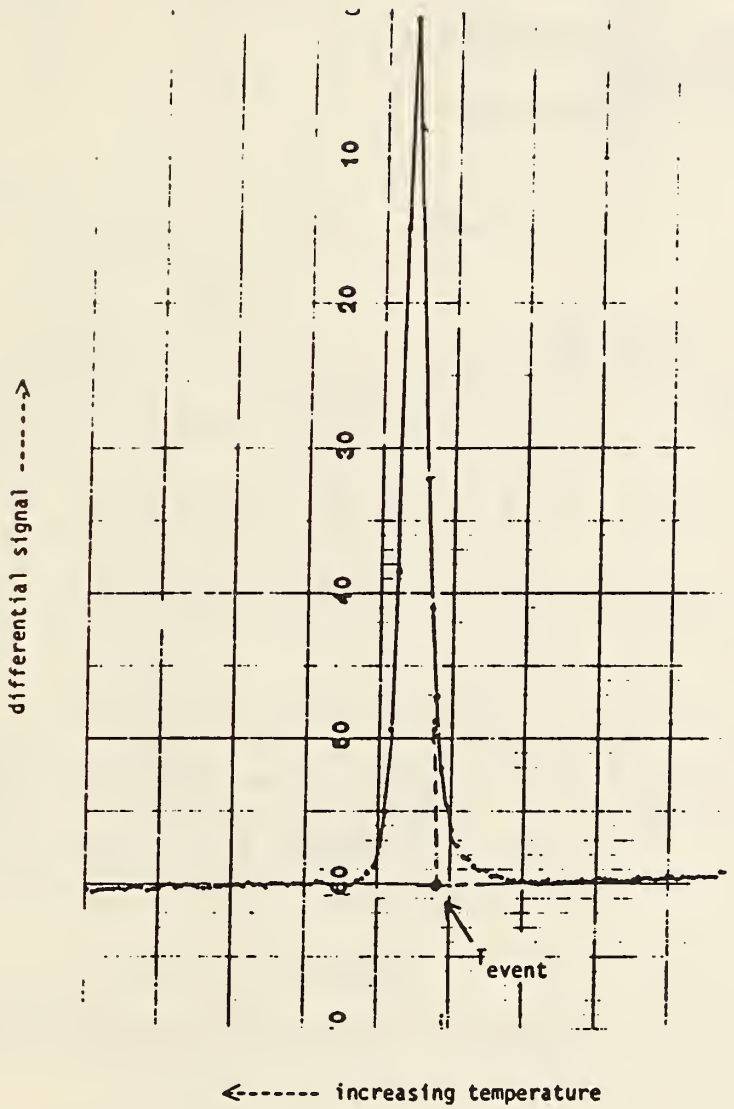

Figure 8

Method used in defining temperature of thermal affects.

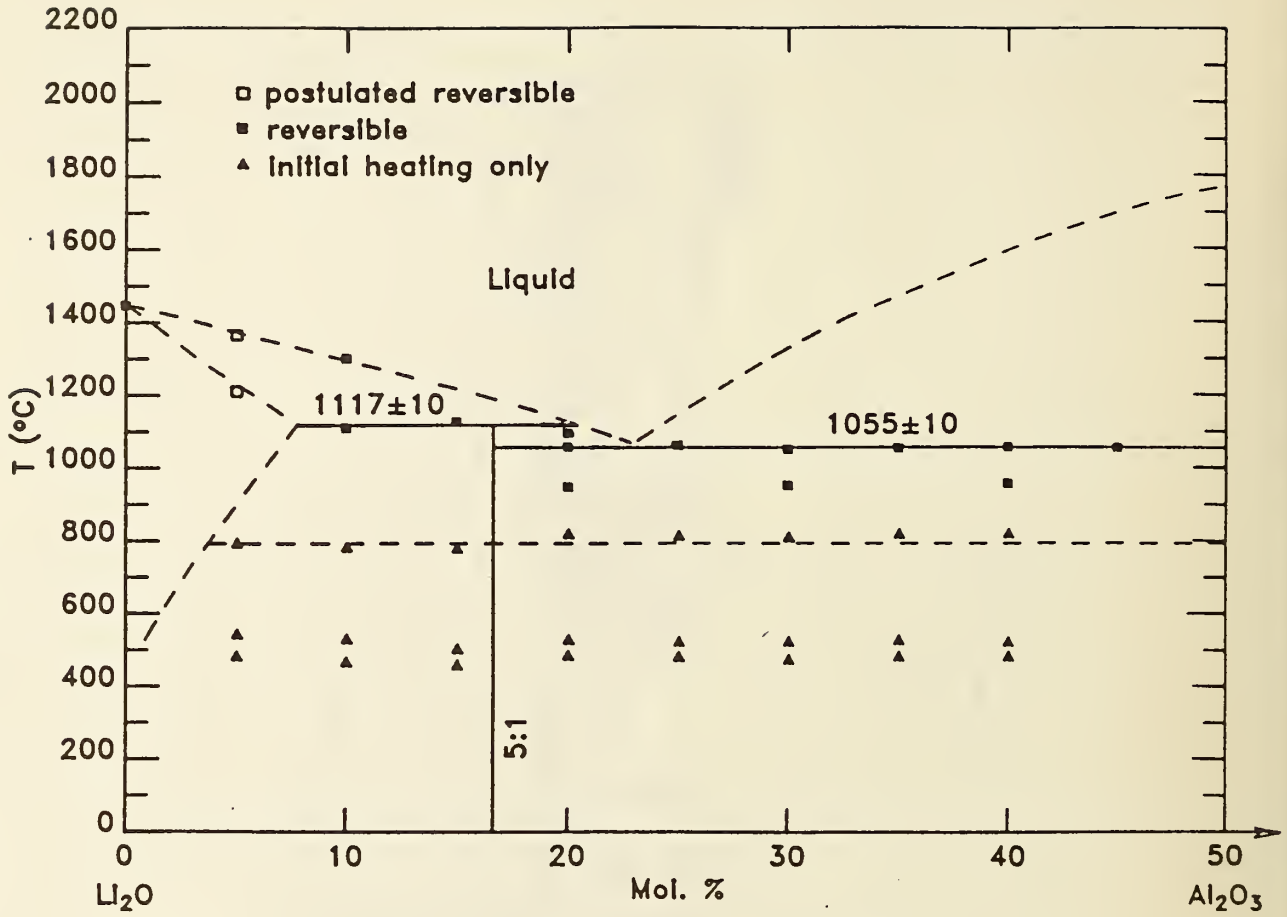

Figure 9

Plot of DTA effects, with tentative interpretation.

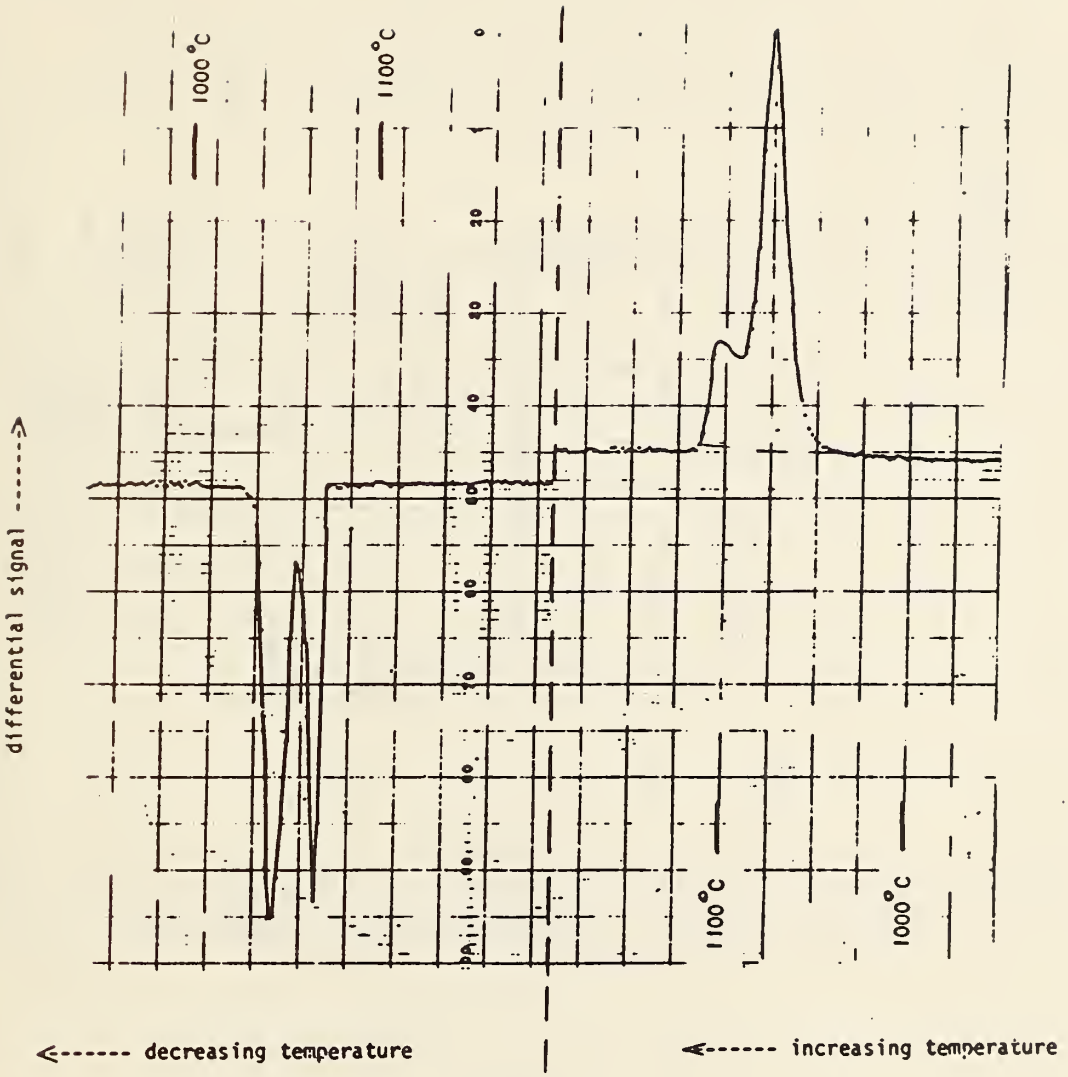

Figure 10

DTA analysis of $(Li_{20})_{80}$ $(Al_2O_3)_{20}$ composition.

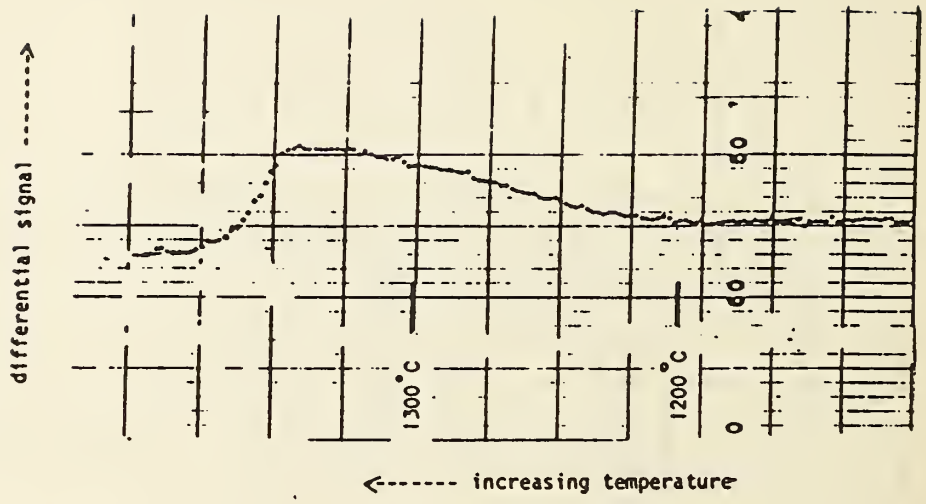

Figure 11

DTA analysis of $(Li_2O)_{95}$ $(Al_2O_3)_5$ composition.

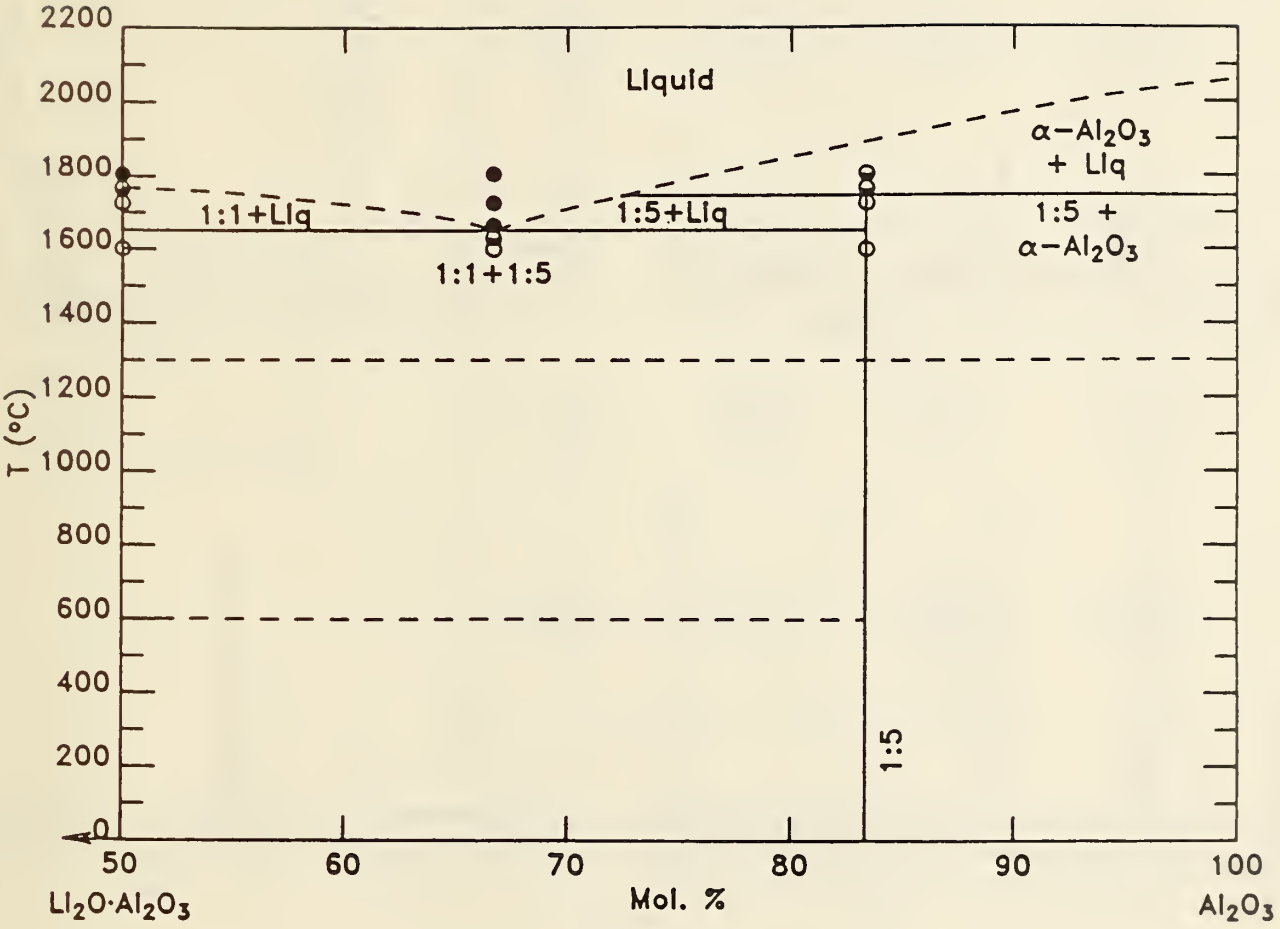

Figure 12

Results of high temperature experiments in sealed capsules for alumina-rich compositions. Solid, half-filled and empty circles represent, respectively, complete, partial and no melting.

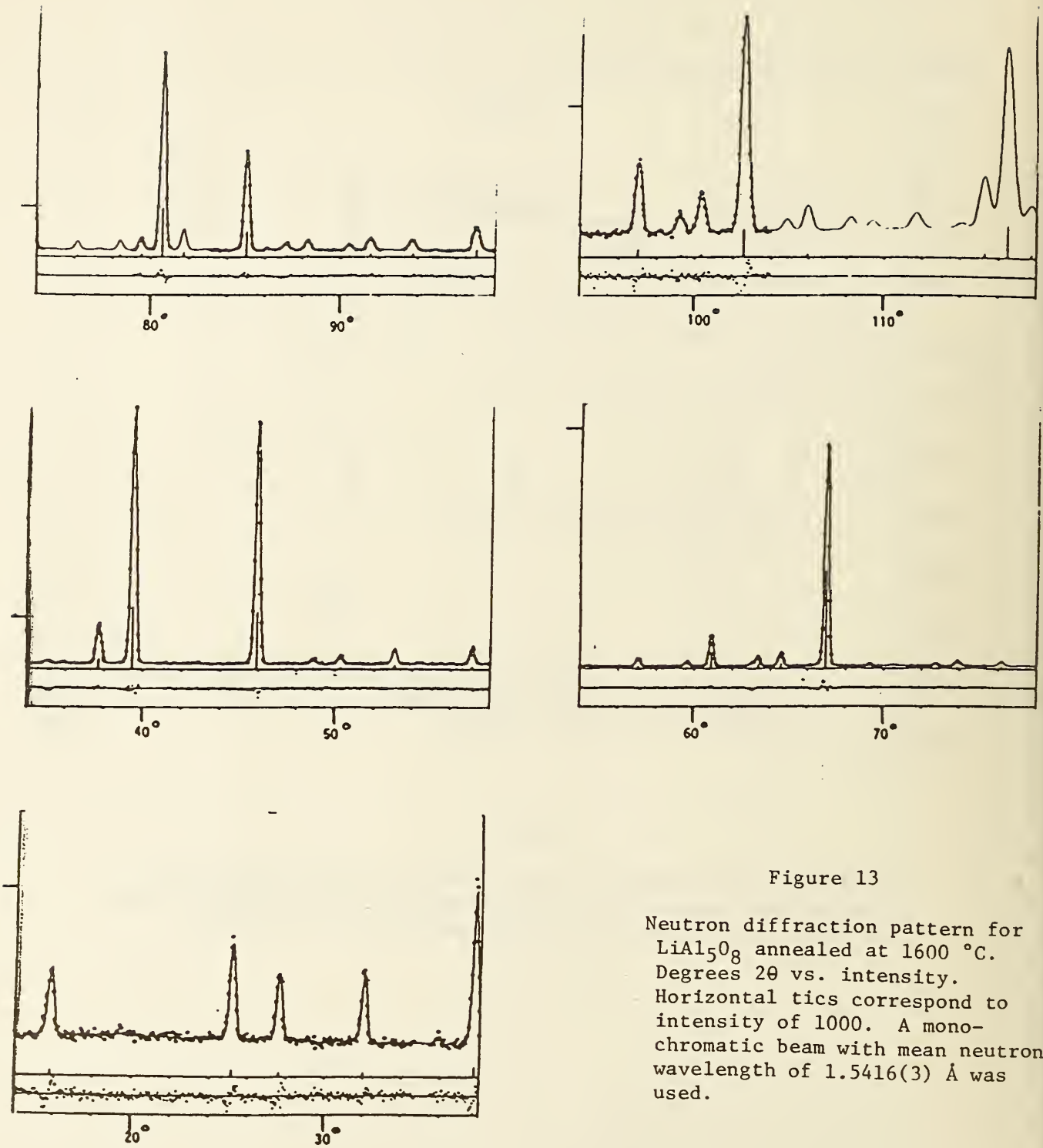

Figure 13

Neutron diffraction pattern for $LiAl_5O_8$ annealed at 1600 °C. Degrees 2θ vs. intensity. Horizontal tics correspond to intensity of 1000. A monochromatic beam with mean neutron wavelength of 1.5416(3) Å was used.

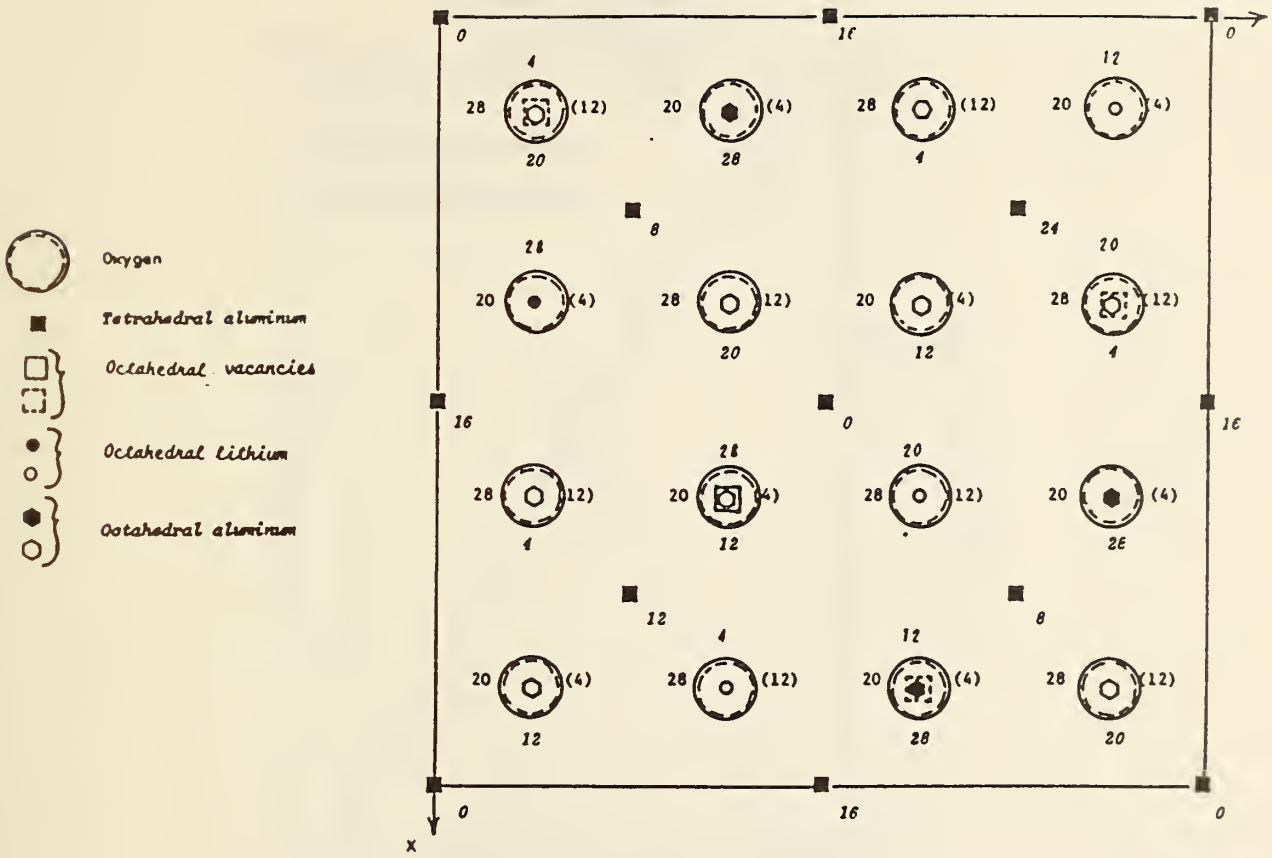

Figure 14

Projected structure of $LiAl_5O_8$, from Rietveld refinement (see Fig. 13 and Table 6). Numbers indicate "Z" coordinates in thirty-seconds. Oxygen coordinates are at left and right of atom positions, octahedral vacancies and octahedral lithium are at top, and octahedral aluminum is at bottom. Open or dashed symbols indicate atoms beneath oxygen.

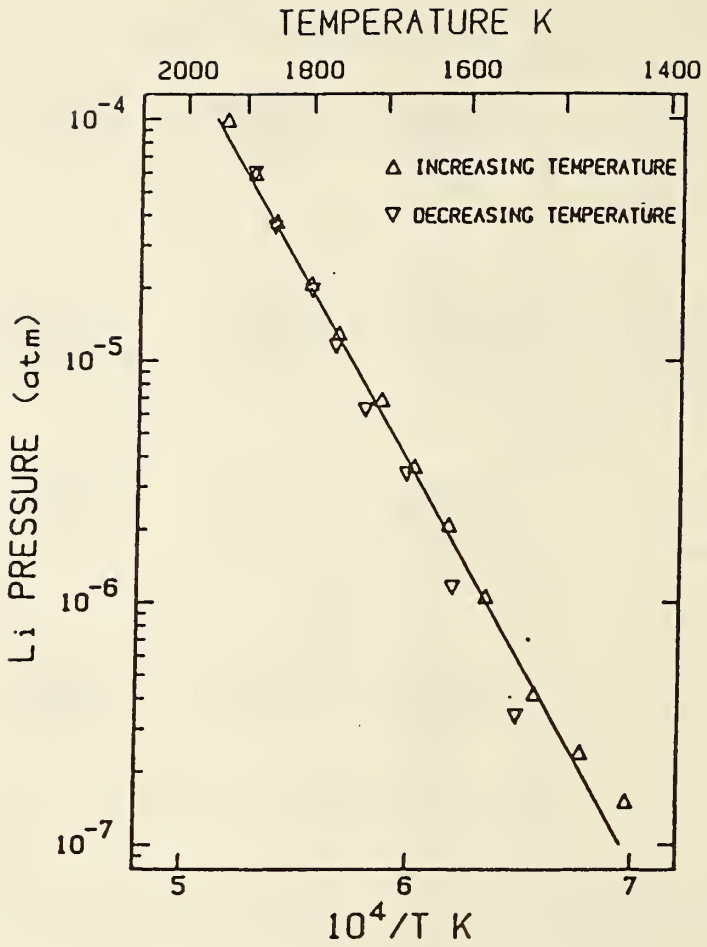

Figure 15

Li pressure versus $10^4/T$ for increasing and decreasing temperature series, 901I and 901D, showing non-reproducibility in Li pressure with increasing or decreasing temperature run chronology.

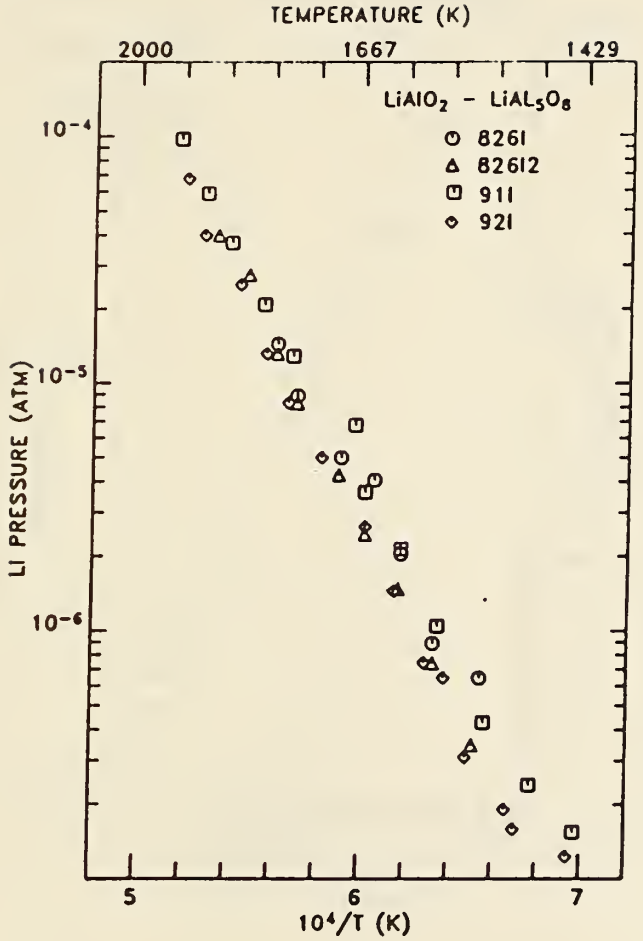

Figure 16

Li pressure versus $10^4/T$ over $LiAlO_2$ - $LiAl_5O_8$ for series of data taken with increasing temperature increments between data points.

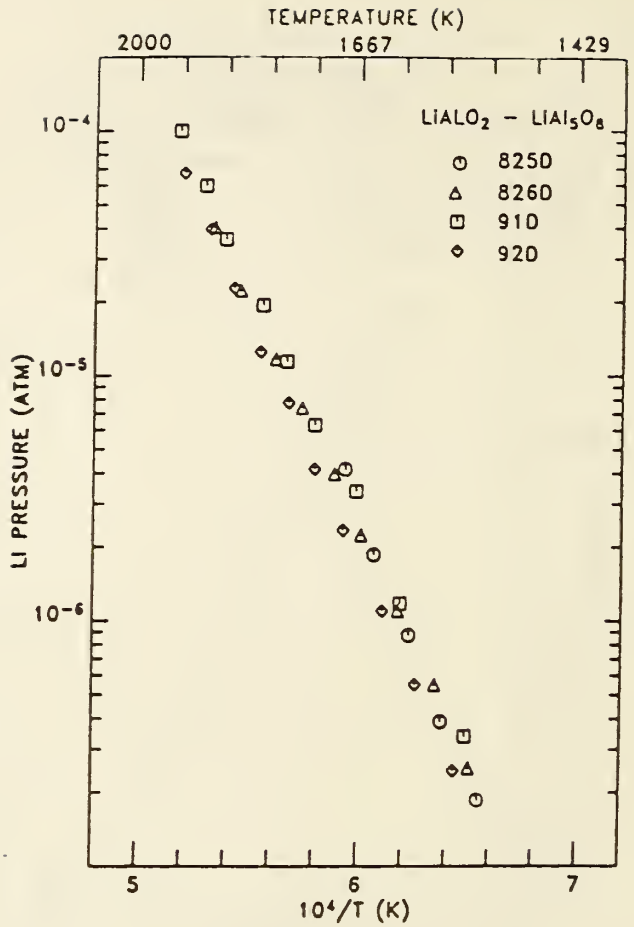

Figure 17

Li pressure versus $10^4/T$ over $LiAlO_2$ - $LiAl_5O_8$ for series taken with decreasing temperature between data points.

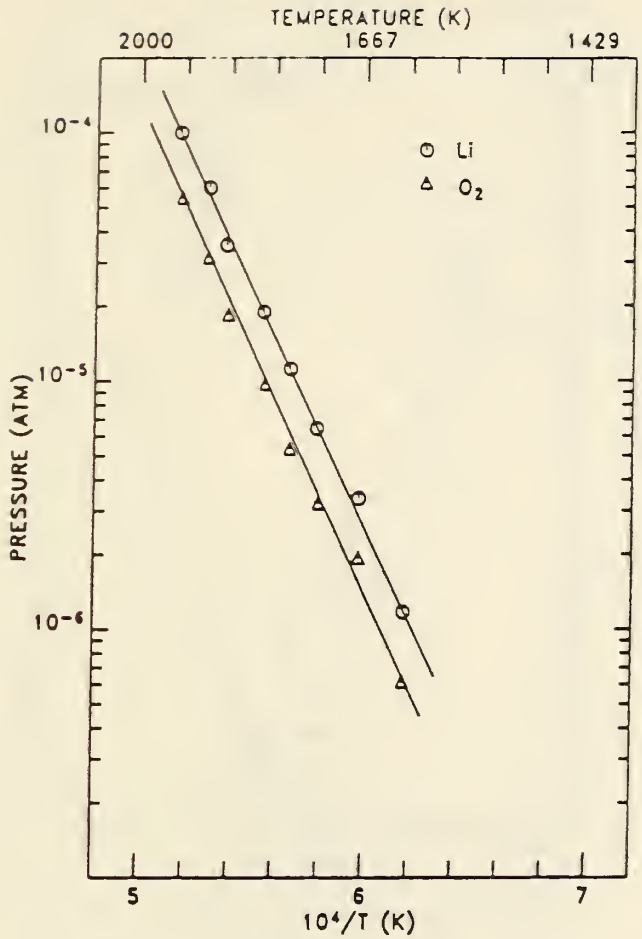

Figure 18

Plot of Li and O_2 pressure versus $10^4/T$ from the 901D data obtained over $LiAlO_2$ -$LiAl_5O_8$ demonstrating constant ratio of Li/O2 pressures.

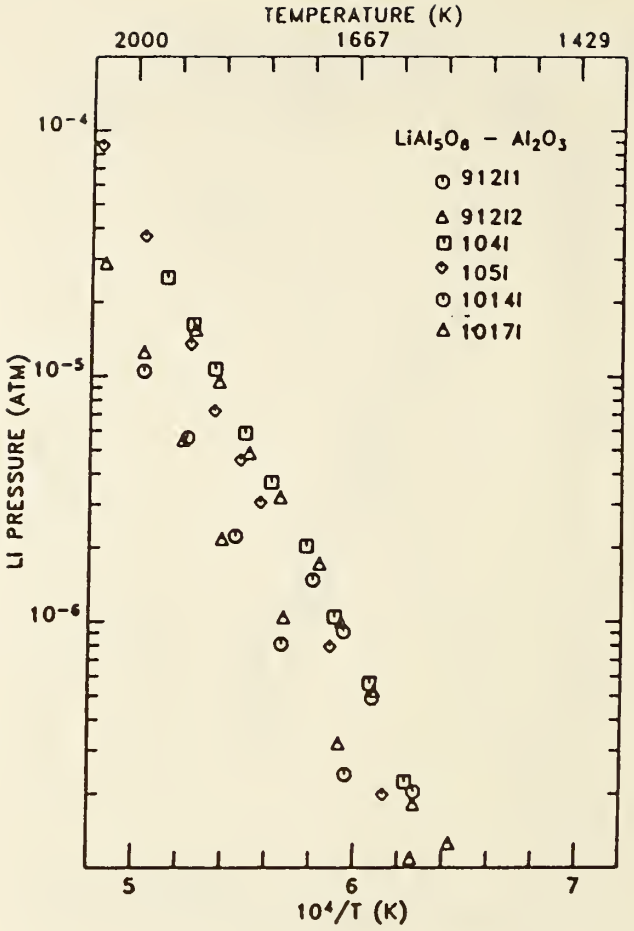

Figure 19

Li pressure versus $10^4/T$ for increasing temperature series observed over $LiAl_5O_8$ - Al_2O_3.

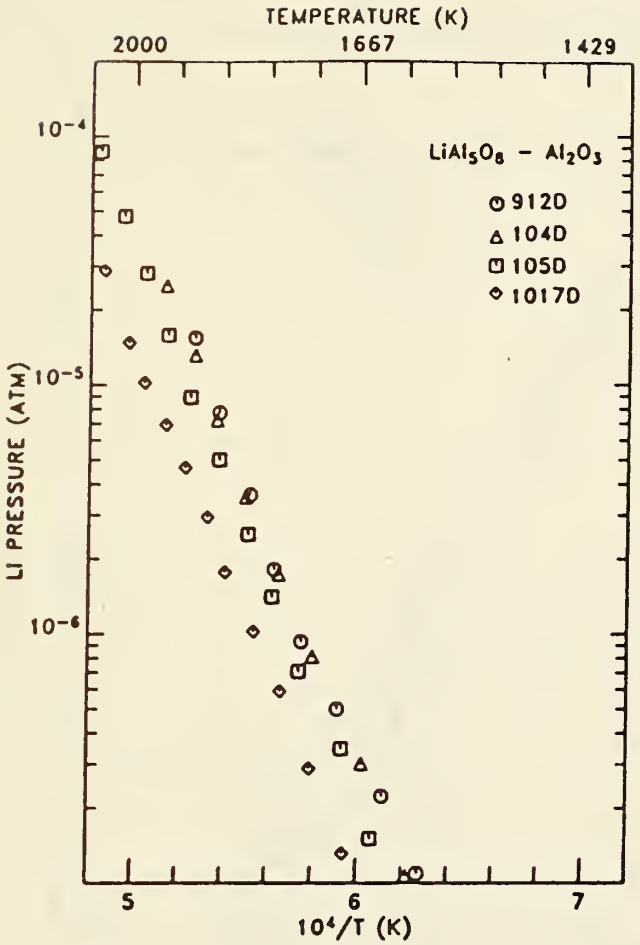

Figure 20

Li pressure versus $10^4/T$ for decreasing temperature series over $LiAl_5O_8$ - Al_2O_3.

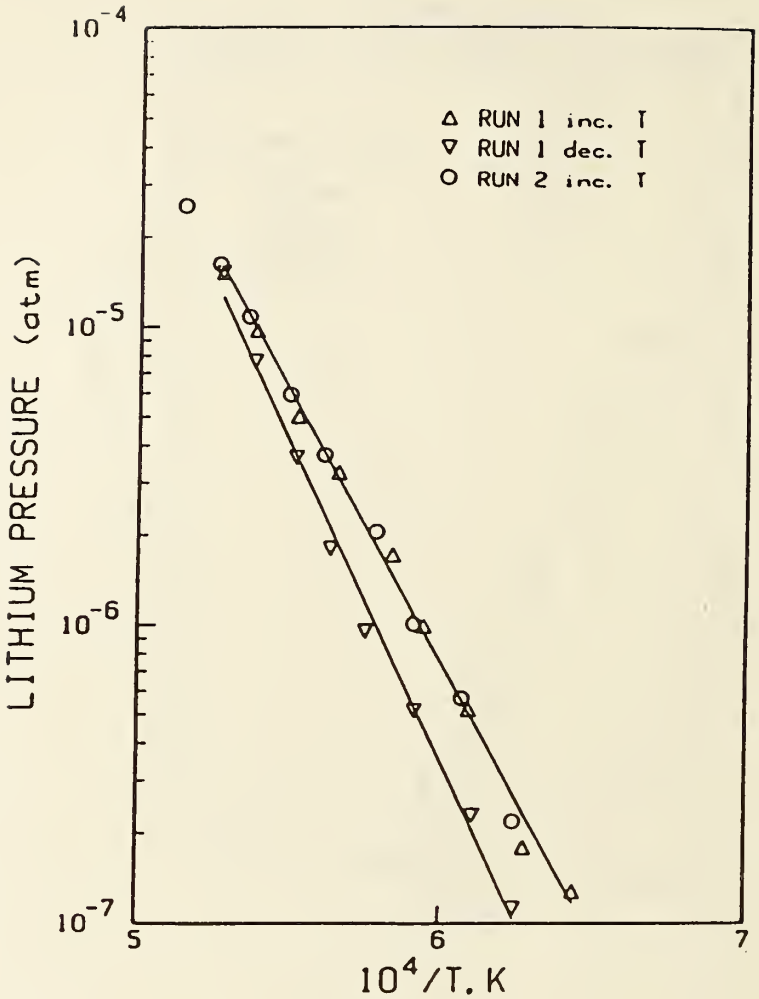

Figure 21

Li pressure versus $10^4/T$ showing effect of temperature variation on experimental slope in the $LiAl_5O_8$ - Al_2O_3 phase region. See text for identification of run 1 and 2 in terms of Table 15 notation.

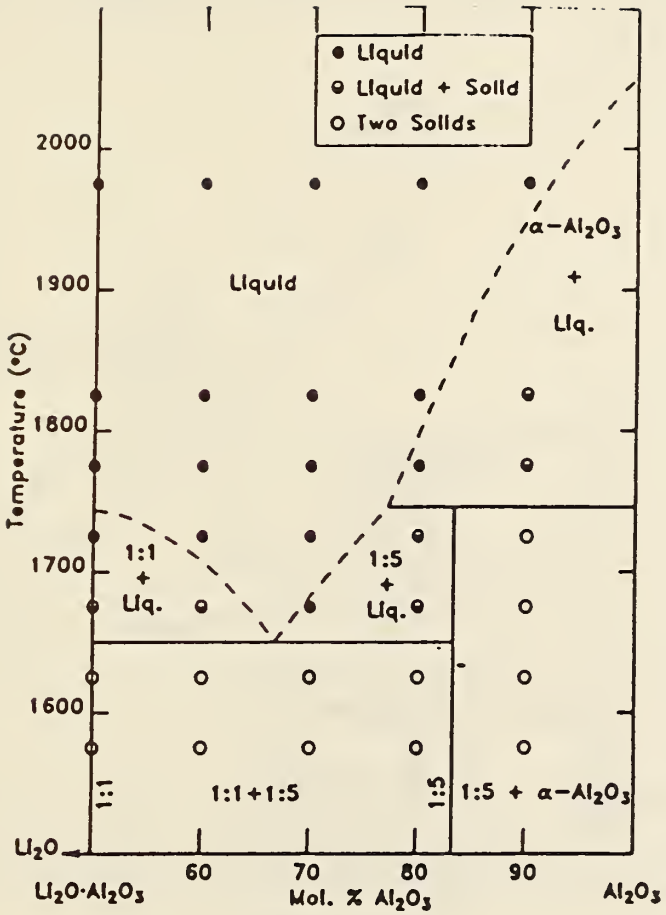

Figure 22

Comparison of model prediction (data points) and experimental phase diagram data (lines) for Li_2O Al_2O_3 - Al_2O_3 mixtures. The ratio 1:1 and 1:5 refer to compound phases of $Li_2O{\cdot}Al_2O_3$ and $Li_2O{\cdot}5Al_2O_3$, respectively.

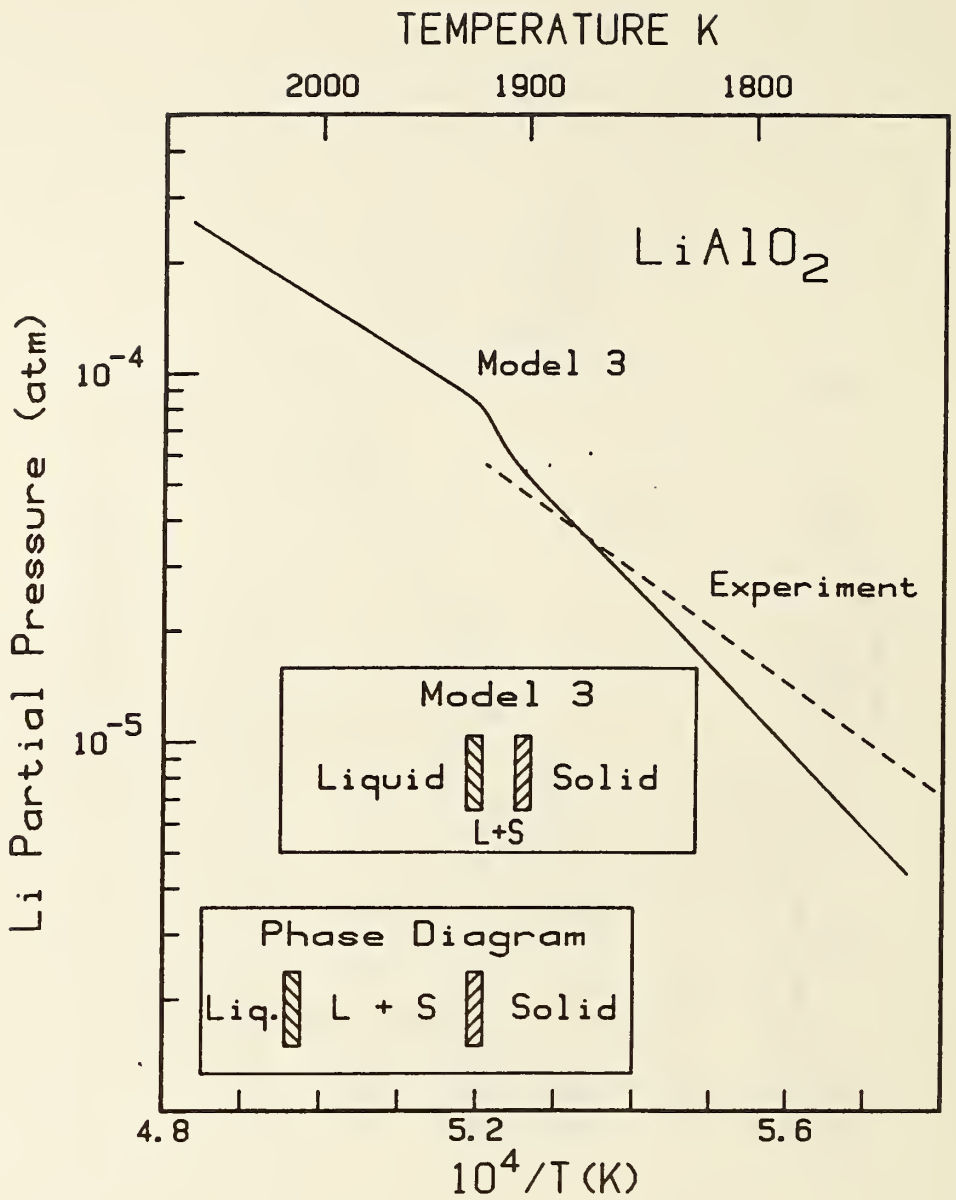

Figure 23

Comparison of predicted (Model 3) and experimental (Knudsen effusion mass spectrometric) Li partial pressures and phase boundaries for the equimoloar Li_2O-Al_2O_3 mixture.

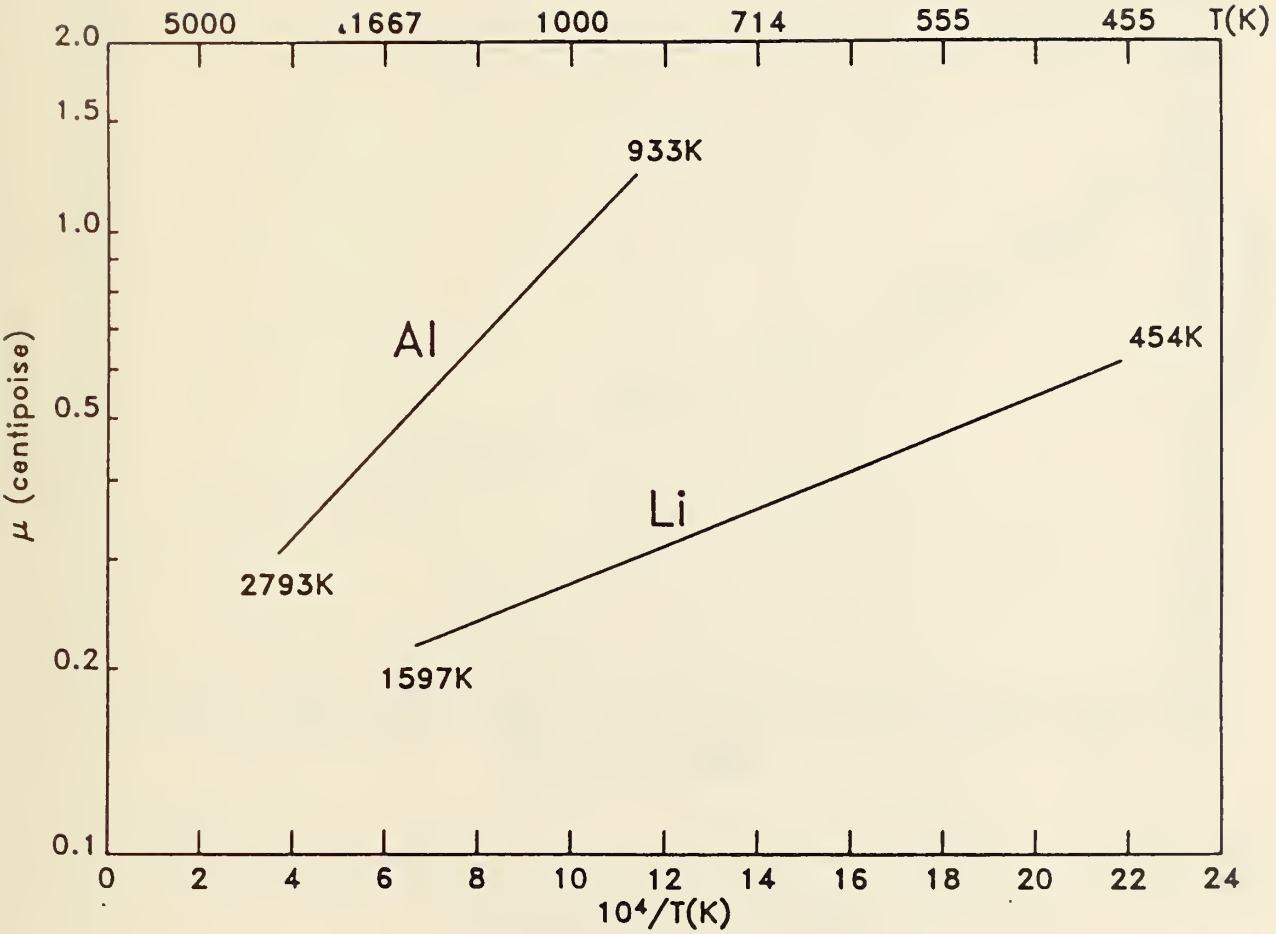

Figure 24

Effect of temperature on the viscosities of Li and Al melts.

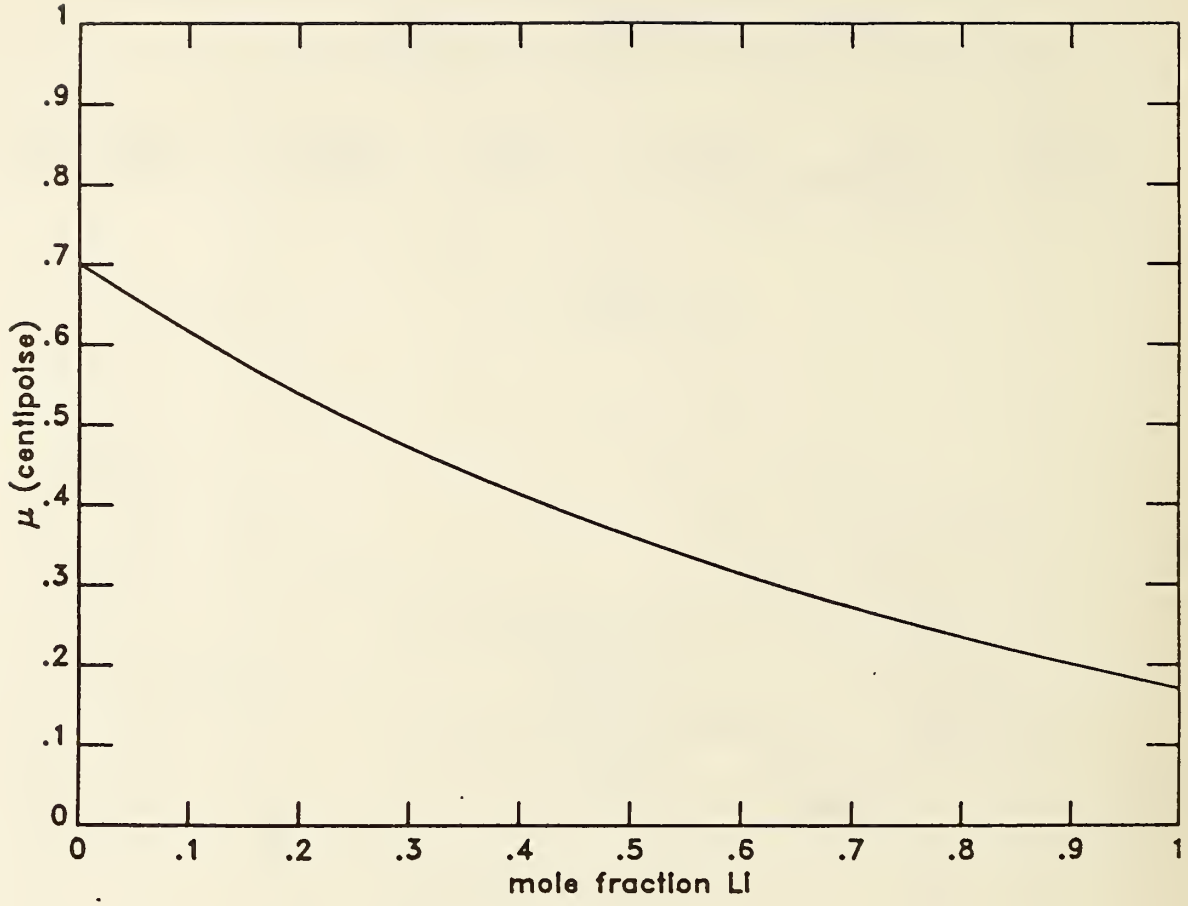

Figure 25

Calculated viscosities of Al/Li liquid mixtures at 1200 K.

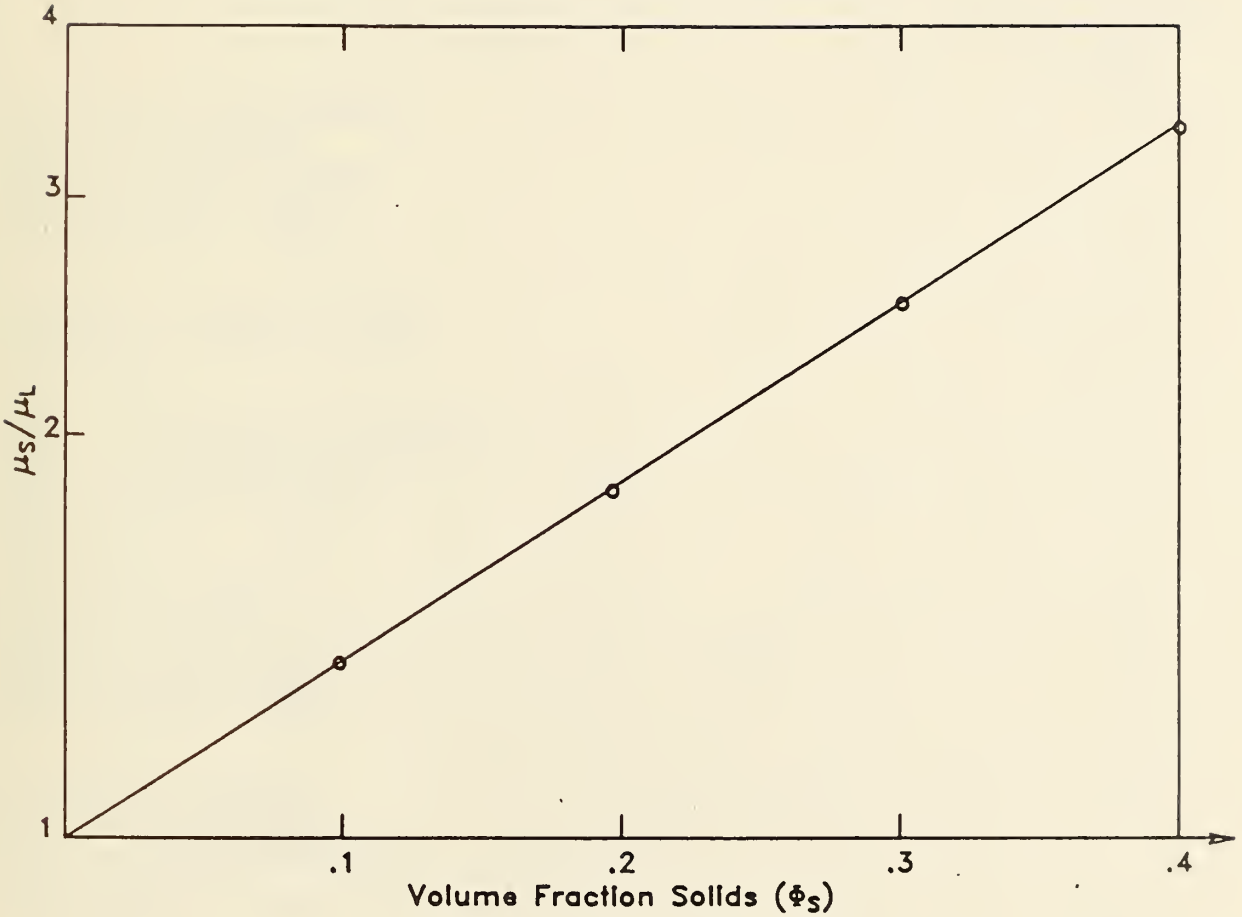

Figure 26

Effect of volume fraction of solids on viscosity of a liquid suspension.

DL/432/84/316

ONR REPORT DISTRIBUTION LIST

CLOSED, LIQUID METAL COMBUSTION

	One copy except as noted
Mr. M. Keith Ellingsworth Mechanics Division Office of Naval Research 800 N. Quincy Street Arlington, VA. 22217	2
Defense Documentation Center Building 5, Cameron Station Alexandria, VA. 22314	12
Technical Information Division Naval Research Laboratory 4555 Overlook Avenue SW Washington, DC 20375	6
Dr. Jerry A. Smith Chemistry Division Office of Naval Research 800 N. Quincy Street Arlington, VA. 22217	
Mr. David S. Siegel Materials Technology Office of Naval Research 800 N. Quincy St. Arlington, VA. 22217	
Dr. H.W. Carhart Combustion & Fuels Naval Research Laboratory Washington, DC 20375	
Professor Allen Fuhs Department of Aeronautics Naval Post Graduate School Monterey, California 93943	
Division Director Engineering and Weapons US Naval Academy Annapolis, Maryland 21402	
Mr. Francis J. Romano Code 63R3 Naval Sea Systems Command Washington, DC 20363	

Dr. Edward G. Liszka
Code PMS406B
Advanced Lightweight Torpedo Project
Naval Sea Systems Command
Washington, DC 20362

Mr. Robert Tompkins
Code 36621, Bldg 126T
Naval Underwater Systems Center
Newport, Rhode Island 02841

Mr. Maurice F. Murphy
Code R33, Room 4-1711
Naval Surface Weapons, White Oak
Silver Spring, Maryland 20910

Dr. Kurt Mueller
Code R10
Energetic Materials Division
Naval Surface Weapons Center, White Oak
Silver Spring, Maryland 20910

Mr. Robert Godfredson
Code 614
Naval Ocean Systems Center
San Diego, California 92152

Mr. James H. Green
Hydromechanics Division, Code 634
Naval Ocean Systems Division
San Diego, California 92152

Mr. John P. Bott
Code 611, Torpedo Propulsion Branch
Naval Ocean Systems Center
San Diego, California 92152

Dr. Herman B. Urbach
Code 272.1
David Taylor Naval Ship
Research and Development Center
Annapolis, MD 21402

Mr. Richard Bloomquist
Code 2752
David Taylor Naval Ship R&D Center
Annapolis, Maryland 21402

Dr. Lawrence P. Cook
High Temperature Processes Group
National Bureau of Standards
Washington, DC 20234

DL/432/84/316

One copy except
as noted

Mr. Norman D. Hubele
Fluidic Systems, MS 1301-RR
Garrett Pneumatic Systems Division
2801 East Washington St.
Phoenix, Arizona 85034

Dr. Hugh H. Darsie
Advanced Technology Group
Sunstrand Energy Systems
4747 Harrison Avenue
Rockford, Illinois 61101

Professor Gerard M. Faeth
Department of Mechanical Engineering
208 Mechanical Engineering Building
The Pennsylvania State University
University Park, Pennsylvania 16802

Dr. Dan H. Kiely
Power & Energy Group
The Pennsylvania State University
Applied Research Laboratory
P.O. Box 30
State College, Pennsylvania 16801

Professor Darryl E. Metzger
Chairman, Department of Mechanical &
Aerospace Engineering
Arizona State University
Tempe, Arizona 85281

Dr. Dae H. Cho
Reactor Analysis & Safety Division
Argonne National Laboratory
Argonne, Illinois 60439

Professor S.H. Chan
Department of Mechanical Engineering
The University of Wisconsin-Milwaukee
P.O. Box 784
Milwaukee, Wisconsin 53201

Professor George A. Brown
Department of Mechanical Engineering
and Applied Mechanics
University of Rhode Island
Kingston, Rhode Island 02881

DL/432/84/316

One copy except
as noted

Dr. David Mann
Associate Director for Engineering Sciences
US Army Research Office
P.O. Box 12211
Research Triangle Park
North Carolina 27709

Dr. Julian Tishkoff
Air Force Office Scientific Research/NA
Bolling Air Force Base
Washington, DC 22032

Dr. F. Dee Stevenson
Chemical Engineering Science Program
Chemical Sciences Division
Department of Energy
Washington, DC 20545

NBS-114A (REV. 2-8C)

U.S. DEPT. OF COMM. BIBLIOGRAPHIC DATA SHEET (See Instructions)	1. PUBLICATION OR REPORT NO. NBSIR 84-2940	2. Performing Organ. Report No.	3. Publication Date September 1984

4. TITLE AND SUBTITLE

PHASE EQUILIBRIA OF STORED CHEMICAL ENERGY REACTANTS
Annual Report

5. AUTHOR(S)
L. P. Cook, E. R. Plante, R. S. Roth, and J. W. Hastie

6. PERFORMING ORGANIZATION (If joint or other than NBS, see instructions)

NATIONAL BUREAU OF STANDARDS
DEPARTMENT OF COMMERCE
WASHINGTON, D.C. 20234

7. Contract/Grant No.
N00014-83-F-0117

8. Type of Report & Period Covered
Annual Report

9. SPONSORING ORGANIZATION NAME AND COMPLETE ADDRESS (Street, City, State, ZIP)

Department of the Navy, Office of Naval Research, Arlington, VA 22217

10. SUPPLEMENTARY NOTES

☐ Document describes a computer program; SF-185, FIPS Software Summary, is attached.

11. ABSTRACT (A 200-word or less factual summary of most significant information. If document includes a significant bibliography or literature survey, mention it here) The reaction of lithium aluminum alloy with water at high temperature is discussed in terms of phase equilibria in the system Li-Al-O-H. A thermodynamic analysis of the system reveals the potential importance of lithium hydride as a reaction product. Major needs for experimental phase equilibria data are outlined, and a determination of the Li_2O-Al_2O_3 phase diagram is given top priority.

DTA investigation of the system Li_2O-AlO_2 has yielded information of equilibrium melting behavior, and the lower limit of melting in the system appears to be 1055° ± 10 °C, with the eutectic located near $(Li_2O)_{75}$ $(Al_2O_3)_{25}$ (mole%). DTA data suggest appreciable solid solution of alumina in Li_2O.

On the high alumina end of the system Li_2O-Al_2O_3, experiments in sealed Mo capsules have shown that the eutectic temperature is near 1650 °C, that $LiAlO_2$ melts congruently near 1750 °C, and that $LiAl_5O_8$ melts incongruently near 1750 °C. Neutron diffraction analysis of $LiAl_5O_8$ cooled rapidly from 1600° shows a 1:3 ordering of Li:Al in the octahedral sites, with extra peaks of undetermined origin.

Mass Spectrometrically determined vapor pressure data are reported for Li_2O, and mixtures of $LiAlO_2$-$LiAl_5O_8$ and $LiAl_5O_8$-Al_2O_3. A thermodynamic model for fitting and prediction of vapor pressure and phase equilibrium data is described.

Appendices are given for the modeling of viscosities in multiphase mixtures, and describing results of a computerized literature search on the system Li-Al-O-H.

12. KEY WORDS (Six to twelve entries; alphabetical order; capitalize only proper names; and separate key words by semicolons)

activities; $LiAlO_2$; $LiAl_5O_8$; Li_2O-Al_2O_3; mass spectrometry; phase diagram; x-ray crystallography

13. AVAILABILITY

☒ Unlimited
☐ For Official Distribution. Do Not Release to NTIS
☐ Order From Superintendent of Documents, U.S. Government Printing Office, Washington, D.C. 20402.
☒ Order From National Technical Information Service (NTIS), Springfield, VA. 22161

14. NO. OF PRINTED PAGES
112

15. Price
$13.00